Using phase-space localized basis functions to obtain vibrational energies of molecules

by

James Brown

A thesis submitted to the
Department of Physics, Engineering Physics & Astronomy
in conformity with the requirements for
the degree of Doctor of Philosophy

Queen's University
Kingston, Ontario, Canada
September 2016

Copyright © James Brown, 2016

Abstract

For decades scientists have attempted to use ideas of classical mechanics to choose basis functions for calculating spectra. The hope is that a classically-motivated basis set will be small because it covers only the dynamically important part of phase space. One popular idea is to use phase space localized (PSL) basis functions. This thesis improves on previous efforts to use PSL functions and examines the usefulness of these improvements. Because the overlap matrix, in the matrix eigenvalue problem obtained by using PSL functions with the variational method, is not an identity, it is costly to use iterative methods to solve the matrix eigenvalue problem. We show that it is possible to circumvent the orthogonality (overlap) problem and use iterative eigensolvers. We also present an altered method of calculating the matrix elements that improves the performance of the PSL basis functions, and also a new method which more efficiently chooses which PSL functions to include. These improvements are applied to a variety of single well molecules. We conclude that for single minimum molecules, the PSL functions are inferior to other basis functions. However, the ideas developed here can be applied to other types of basis functions, and PSL functions may be useful for multi-well systems.

Acknowledgements

First and foremost, I would like to thank my supervisor Tucker Carrington Jr. for his guidance and patience the past six years. Special thanks also goes to Xiao-gang Wang and Gustavo Avila for the fruitful discussions and technical support.

I would also like to acknowledge the moral support provided from my friends and family especially my Mother, Father, Paul, Mary, and Rober. Lastly, I would not be who or where I am today without my wife Katie.

Table of Contents

List of Tables

List of Figures

Nomenclature

BF	Body-Fixed
BO	Born-Oppenheimer
DVR	Discrete Variable Representation
FBR	Finite Basis Representation
FGH	Fourier Grid Hamiltonian
HP	Halverson and Poirier
KEO	Kinetic Energy Operator
LF	Laboratory-Fixed
PES	Potential Energy Surface
PODVR	Potential Optimized Discrete Variable Representation
PSL	phase-space localized
pvb	periodic von Neumann with biorthogonal exchange
pvN	Periodic von Neumann

SD	Simultaneous Diagonalization
SG	symmetrized Gaussian
SOP	sum of products
ST	Shimshovitz and Tannor
TISE	Time Independent Schrödinger Equation
VBR	Variational Basis Representation
vN	von Neumann

Chapter 1

General Introduction

1.1 Purpose

The study of vibrational and rovibrational states is fundamentally important to predicting and understanding spectra. Vibrational states play a key role in phenomena such as how molecules respond to the presence of light. The improved knowledge of vibrational states at a fundamental level is important to a wide array of applications, from pharmaceutical drug delivery to fuel cell technology.

However, difficulty arises when attempting to calculate these vibrational states in that the matrix representation (in a set of basis functions) of the Hamiltonian grows exponentially with the number of degrees of freedom. Therefore, one must develop new ideas to attenuate this exponential growth. Phase-based localized basis functions are a possible path to studying larger systems.

1.2 Organization of thesis

This thesis is in the manuscript format. The thesis will start by outlining the basics of quantum chemistry and nuclear motion theory, as well as a background in the history of classically motivated basis functions in Chapter 2. There will then be a series of 3 published manuscripts Chapter 3 published as Ref. 1, Chapter 4 published as Ref. 2 and Chapter 5 published as Ref. 3. It will then end with some concluding remarks.

For all manuscripts included, I was the first author and Tucker Carrington Jr. was the second author. The development of the ideas, and the writing of the papers was done collaboratively. All implementation of the ideas and calculations were done by myself. The main text of Chapters 3, 4, and 5 are identical to that of the published manuscripts with the exception of a few minor explanations and modifications suggested by my committee members.

Chapter 2

Background

2.1 Brief history of quantum chemistry

One of the main sources for understanding chemical phenomenon is atomic and molecular spectroscopy. In order to better understand (at least in a qualitative manner) the experimental results, quantum mechanics was applied to molecular systems[4]. Initially, the approach to understanding experiments was that of the Born-Oppenheimer[5] (BO) approximation, in that the electrons were moving in the potential generated from immobile classical nuclei. The BO approach was (and still is) very successful in qualitatively describing equilibrium structures, transition states and molecular orbitals. The concept of potential energy surfaces (PES)[6] also stems from the BO approximation and is central to the work presented in this thesis. Richards[7] and Schaefer[8] first described the history of quantum chemistry in three *ages*. The first *age* of quantum chemistry was very crude and the expectation was only an agreement to experiment within an order of magnitude. With the advent and availability of computers, it was possible to obtain calculations in much closer agreement with experiment. The main numerical techniques being developed were *Ab initio* in nature, and based

on molecular orbital wave functions. Although closer to experiment than the first *age* of quantum chemistry, the results could still only be trusted as semi-quantitative and applied only where experiments could not be performed[7]. An example of where experiments could not be performed is unstable molecules. As early as 1970[4], theoretical predictions were being made that were comparable in accuracy to contemporary experiments through electronic structure calculations. This marked the beginning of the third *age* of quantum chemistry. At this point, theoretical quantum chemistry could legitimately make predictions that could call into question the experimental results, or provide new information that could push for the design of new experimental apparatuses. With the development of experimental techniques that could provide more accurate results, it was becoming obvious that keeping the nuclei fixed was not sufficient[4]. Nuclei being fixed classical particles at the bottom of local minima in a PES ignored inherent quantum mechanical properties of the nuclei themselves such as Zero-Point Energy (ZPE) of vibrations[9] or "tunnelling" of nuclei[10]. One of the most famous examples of tunnelling is the inversion of ammonia[11]. Classically and in quantum mechanics, the two wells have equivalent potential energy. The classical states in either well also have the same energy. However, quantum tunnelling causes energy splitting to occur with the even state having a lower energy than the odd state.

Using only electronic structure can be quite successful in obtaining equilibrium quantities which although related to experiments, are not equivalent. It was therefore imperative to enter the fourth *age* of quantum chemistry by including electronic structure and nuclear motion[4]. This could in theory be done by completely including the nuclear motion from the beginning but the BO approximation has produced remarkably good results.

2.2 Overview of vibrational calculations

In order to quantitatively describe vibrations of molecules, an important idea is that of the nuclei moving on a PES. A PES is generated by calculating the electronic structure energy at various positions of the nuclei. In general, a fit of these energies with some set of basis functions is performed in order to generate the full surface from which approximate energies can be found quickly for any nuclear configuration[6]. This nuclei moving on PES framework makes apparent the description of ZPE and tunnelling of nuclei. Using the BO approximation with a PES produces quite accurate rovibrational energies. There are various techniques that are used to calculate rovibrational energies including time-dependent and perturbational methods. In the next section, only time-independent variational methods will be discussed.

2.2.1 Nuclear Motion Theory

The fundamental equation used in calculating states of molecules is of course the time-independent Schrödinger equation,

$$\hat{H}\Psi = \left(-\sum_{i=1}^{N} \frac{1}{2m_i}\nabla^2 + V \right) \Psi = E\Psi, \tag{2.1}$$

where $\hat{H}$ is the Hamiltonian, N is the number of nuclei in the molecule, ∇^2 is the Laplace operator, m_i is the mass of nucleus i (with the BO approximation) and V is the PES. Atomic units are used so $\hbar = 1$ is omitted. The coordinates here are space-fixed. Spin statistics are not explicitly accounted for in Eq. (2.1), however this can be handled with some post-processing of the resultant energies.

Although any set of coordinates could be used to perform rovibrational calculations, the

problem's size can be reduced by using internal coordinates only. In general, the PES is generated using internal coordinates, which assumes the system is isolated. Internal coordinates reduces the dimensionality of the problem by six for vibrational calculations. Three of the dimensions are removed because the Hamiltonian is translationally invariant and the motion of the centre-of-mass of the molecule is separable. Another three dimensions are removed from the rotation of the molecule about this centre-of-mass. To add back rotation to perform rovibrational calculations, a set of three variables is used to describe the orientation of the body-fixed (BF) frame attached to the molecule, relative to the space-fixed (SP) frame. After the BF frame is embedded, it is left to decide how the remaining $3N-6$ internal coordinates are defined. Three coordinates are used to relate the BF frame to the SP frame for the rotational portion of the calculation.

When a choice of internal coordinates is made, it is necessary to convert the time-independent Schrödinger equation of Eq. (2.1) to one defined in internal coordinates. The PES is generally defined in terms of some internal coordinate. If the PES is defined in different coordinates than are chosen for the rovibrational calculations, a transformation T can be used to obtain the values of the potential at the points in the chosen coordinates, given the values in a different set of coordinates. This process is outlined in Eq. (2.2) for a transformation between a PES given in coordinate r_a for the calculation in coordinate r_b.

$$V\left(\bar{r_b}\right) = V\left(\bar{r_b}\left(\bar{r_a}\right)\right), \tag{2.2}$$

The kinetic energy operator (KEO) in the new coordinates is slightly more difficult to obtain. It can be found in one of two ways. The first is to apply chain rule to the original KEO. The second is to write down the classical Hamiltonian in the internal coordinates and use the correspondence principle of Podolsky[12] to obtain the quantum KEO. There are two

types of coordinates that are used most in rovibrational calculations. The first is that of the Eckart-Watson Hamiltonian and the second is general polar coordinates with both types being used in this thesis although a greater focus is on a simplified version of the former.

Eckart-Watson Hamiltonian

A full description of the Eckart-Watson Hamiltonian can be found in the influential paper by Watson of Ref. 13. The coordinates used for this Hamiltonian are defined with respect to a reference structure using the Eckart conditions[14]. The Eckart-Watson KEO (K_{EW}) in atomic units, coordinates q_i and D degrees of freedom is given as[15]

$$K_{EW} = -\frac{1}{2}\sum_{d=1}^{D}\frac{\partial^2}{\partial q_d^2} + \frac{1}{2}\sum_{\alpha,\beta}(J_\alpha - \pi_\alpha)\,\mu_{\alpha\beta}\,(J_\beta - \pi_\beta) - \frac{1}{8}\sum_{\alpha}\mu_{\alpha\alpha} \tag{2.3}$$

where

$$\mu_{\alpha\beta} = \left(\mathbf{I}'^{-1}\right)_{\alpha\beta}; \quad \mathbf{I}'_{\alpha\beta} = \mathbf{I}_{\alpha\beta} + \sum_{k,l,m}\zeta_{km}^{\alpha}\zeta_{lm}^{\beta}q_k q_l$$

and where $\mathbf{I}_{\alpha\beta}$ is the inertia tensor, ζ_{ij}^{α} are Coriolis parameters defined for example in Ref. 13, and

$$\pi_\alpha = -i\sum_{k,l}\zeta_{ij}^{\alpha}q_k\frac{\partial}{\partial q_l}.$$

The second two terms ($\pi^{\mathbf{t}}\mu\pi$ and $\frac{1}{8}\sum_\alpha \mu_{\alpha\alpha}$) of Eq. (2.3) make relatively small contributions to the vibrational energy levels compared to the first term. They are often ignored in $J = 0$ calculations.

The Eckart-Watson Hamiltonian has been applied to a variety of molecules including CO-Cu(100)[16], H_2CN and H_2CS[17], and CH_4[18]. A calculation without the $\pi^{\mathbf{t}}\mu\pi$ and $\frac{1}{8}\sum_\alpha \mu_{\alpha\alpha}$ terms was used to determine $J = 0$ levels of CH_3CN[19]. The program

MULTIMODE[17] uses the full Eckart-Watson Hamiltonian.

Although successful for many molecules, there are a few well-known issues that arise when using the Eckart-Watson Hamiltonian. The first is that the Hamiltonian is singular in certain instances[15]. An example of when this occurs is when a non-linear molecule is in a linear configuration. If a non-linear molecule approaches linearity, the vibrational calculations can be significantly affected. This was shown to occur for highly excited states of H_2O[20] with deviations ranging from 0.3cm^{-1} to 200cm^{-1}. Another issue is that normal coordinates do not describe large amplitude motions well[15]. This is partly due to the fact that the coordinates used are defined with respect to a single reference geometry. However, accurate tunnelling splittings can be obtained by making the reference geometry, the saddle point, as was done for NH_3[21].

General polar coordinates

A simple and general way to generate a KEO is to start with polar coordinates associated with any set of N vectors that specifies the shape and orientation of the molecule. These coordinates can be chosen to simplify the KEO, and are guaranteed to have a one-to-one correspondence with the geometry of the molecule. The coordinates can also be chosen to minimize coupling. If one uses "orthogonal" vectors, the KEO is much simpler. "Orthogonal" in this case, refers to having an *orthogonal* transformation between the mass-weighted nuclear position vectors and the internal mass-weighted Cartesian vectors.

The KEO can be obtained by applying the chain-rule to the quantum mechanically KEO in LF coordinates given by,

$$\hat{T}_N = -\frac{1}{2}\sum_{i=1}^{N}\frac{1}{m_i}\left(\frac{\partial^2}{\partial X_i^2}+\frac{\partial^2}{\partial Y_i^2}+\frac{\partial^2}{\partial Z_i^2}\right). \tag{2.4}$$

There are three steps involved to obtain the KEO in the new polar coordinates. The first step is to convert to mass-weighted coordinates ($\bar{X}_i = m_i^{1/2} X_i$). The second is to introduce the $N \times N$ transformation U that linearly relates $\bar{X}_i$ to $\bar{P}_\alpha$. The third step introduces arbitrary masses μ_α to convert the polar coordinates to mass-unweighted coordinates ($P_\alpha = \mu_i^{-1/2} \bar{P}_\alpha$). This is succinctly described by the transformation $\mathbf{J}$,

$$\mathbf{J} = \mu^{-1/2} U M^{1/2}, \tag{2.5}$$

where μ and M are diagonal matrices of the arbitrary masses and nuclear masses respectively.

The most natural choice of coordinates for describing the shape of the molecule is having r_{N-1} describing the centre of mass of the nuclei, $N-1$ vectors $r_0, r_2, ..., r_{N-2}$ for the remaining vectors, N-2 polar angles θ_α between r_{N-1} and r_0, and N-3 dihedral angles ϕ_β defined between the planes, $r_0 \times r_1$ and $r_0 \times r_\beta$. Using these coordinates results in the KEO defined conveniently as,

$$T = T_s + T_{br} + T_{cor}, \quad \text{where} \quad T_{br} = T_{br,diag} + T_{br,off}, \tag{2.6}$$

with

$$\begin{aligned}
T_s &= -\sum_{k=0}^{N-2} \frac{1}{2\mu_k} \frac{\partial^2}{\partial r_k^2} \\
T_{br,diag} &= \left[B_0\left(r_0\right) + B_1\left(r_1\right)\right] \left[-\frac{1}{\sin\theta_1} \frac{\partial}{\partial\theta_1} \sin\Theta_1 \frac{\partial}{\partial\theta_1} + \frac{1}{\sin^2\theta_1} \left(J_z - L_z\right)^2\right] \\
&\quad + \sum_{k=2}^{N-2} \left[B_0\left(r_0\right) + B_k\left(r_k\right)\right] l_k^2 \\
&\quad + B_0\left(r_0\right) \left[J^2 - 2\left(J_z - L_z\right)^2 - 2J_z\left(L_z\right) + 2 \sum_{k\neq k'=1}^{N-1} l_{kz} l_{k'z}\right] \\
T_{br,off} &= B_0\left(r_0\right) \left[\left(L_+\right) a_2^- + \left(L_-\right) a_2^+ + \sum_{k\neq k'=3}^{N-1} \left(l_{k+} l_{k'-} + l_{k-} l_{k'+}\right)\right] \\
T_{cor} &= -B_0\left(r_1\right) \left[J_- \left(a_2^+ L_+\right) + J_+ \left(a_2^- + L_-\right)\right]
\end{aligned} \tag{2.7}$$

where

$$B_i\left(r_i\right) = \frac{1}{2\mu_i r_i^2} \tag{2.8}$$

$$L_z = \sum_{k=3}^{N-1} l_{kz} \tag{2.9}$$

$$L_\pm - = \sum_{k=3}^{N-1} l_{k\pm} \tag{2.10}$$

$$l_\pm = l_{ix} \pm i l_{iy} \quad (i = 2, ..., N-2) \tag{2.11}$$

$$J_\pm = J_x \pm i J_y \tag{2.12}$$

$$a_2^\pm = \pm \frac{\partial}{\partial\theta_2} - \cot\theta_2 \left(J_z - L_z\right), \tag{2.13}$$

where l_{kx}, l_{ky}, l_{kz}, l_k^2 are the usual angular momentum operators. The terms are grouped

such that T_s is the stretch part, T_{br} is the bend-rotation part, and T_{cor} is the Coriolis portion of the KEO. The J_x, J_y, and J_z are components of the total angular momentum.

The KEO of Eq. (2.6) is Hermitian and valid for any choice of orthogonal vectors. The only difference between KEOs in different orthogonal coordinates is the definition of the arbitrary masses.

The main disadvantage of the KEO of Eq. (2.6) is the lack of flexibility as one must place the BF z-axis along one of the r_i vectors and one must choose polyspherical coordinates from the N-1 r_i vectors as the vibrational coordinates. In Ref. 22, a procedure is outlined to transform Eq. (2.6) when the z-axis is not taken to be the one of the r_i vectors. This is important if rovibrational coupling can be reduced or to exploit symmetry in the molecule.

2.3 Solving the Schrödinger equation

The most popular way to solve the Schrödinger equation (Eq. (2.1)) is to expand the wavefunction in terms of some known basis functions $B_i(\bar{r})$,

$$\Psi(\bar{r}) = \sum_k c_k B_k(\bar{r}), \tag{2.14}$$

where c_i are unknown coefficients and $\bar{r}$ are the full set of coordinates used. In theory, if an infinite number of basis functions were used, the exact wavefunction could be found. However, in practice, it is necessary to restrict the number of basis functions. Although it is possible to attempt to represent the operators directly, with an example being the use of finite-difference for derivatives, the solutions of the Hamiltonian $\hat{H}$ generally resemble some basis set from which acceptable solutions can be found with a smaller matrix representation. Starting from Eq. (2.14), two methods can be used to obtain solutions with the first being

the collocation method.

2.3.1 Collocation Method

The collocation method[23] is a method where the residue function,

$$|R\rangle = (H - E)\,|\Psi\rangle \tag{2.15}$$

is evaluated at collocation points $|r_i\rangle$ which results in the collocation equations,

$$\begin{aligned} \langle r_i|\, R\rangle &= \langle r_i|\,(H-E)\,|\Psi\rangle = 0, \quad i = 1, 2, ..., N_p \\ &= \sum_{k=1}^{N_b} \langle r_i|\,(H-E)\,|B_k\rangle\, c_k = 0, \quad i = 1, 2, ..., N_p \quad , \end{aligned} \tag{2.16}$$

where N_p is the number of collocation points, and N_b is the number of basis functions. Although it is possible to use this method with $N_b \neq N_p$[24], it is generally performed with $N_p = N_b = N$ so the subscripts will no longer be used and the assumption is that the number of basis functions and points is equivalent. The problem can now be rewritten as solving the $N \times N$ generalized eigenvalue problem as,

$$(\mathbf{G} + \mathbf{VR})\mathbf{c} = \mathbf{ERc} \tag{2.17}$$

with asymmetric matrices $\mathbf{R}_{ij} = B_i(r_j)$, $\mathbf{G}_{ij} = TB_i(r_j)$ with T the KEO, $\mathbf{V}_{ij} = V(r_i)\delta_{ij}$. $\mathbf{E}$ is the diagonal matrix of eigenvalues and c is the eigenvectors. If the basis functions have the property that $\mathbf{R}_{ij} = \delta_{ij}$, such that the basis functions are zero at all collocation points except for one, the right matrix becomes the identity and the problem is reduced to the "normal" asymmetric eigenvalue problem.

2.3.2 Raleigh-Ritz Variational Principle

The second method that can be used to find solutions of Eq. (2.1) is the Raleigh-Ritz variational principle. The starting point is the functional $\langle\Psi|\,\hat{H}\,|\Psi\rangle$ which results in the well-known equation,

$$\sum_{k=1}^{N}\langle B_i|\,(H-E)\,|B_k\rangle\,c_k=0,\quad i=1,2,...,N\quad , \tag{2.18}$$

where the generalized eigenvalue problem is now $\mathbf{Hc}=\mathbf{ScE}$, where $\mathbf{H}_{ij}=\int B_i^\dagger(T+V)B_j$ and $\mathbf{S}_{ij}=\int B_i^\dagger B_j$ are Hermitian matrices. The integrals are performed over all of coordinate space. Usually, the basis functions are taken to be orthogonal which reduces the overlap matrix $\mathbf{S}$ to the identity and the problem is the "normal" Hermitian eigenvalue problem. Although the problem is now Hermitian, it now necessitates many integrals to be performed as opposed to collocation where the functions (and the Hamiltonian acting on functions) are evaluated at points. These integrals are generally performed using quadrature but the choice of bases can simplify the problem.

2.4 Basis Sets

The choice of the basis set is very important to how accurate and fast the rovibrational calculations are. The coordinates chosen determine largely what basis functions are appropriate to represent the wavefunctions but a few reformulations have been used.

Variational/Finite Basis Representation

Performing the integrals of Eq. (2.18) exactly is referred to in literature as Variational Basis Representation (VBR)[25]. The errors from VBR are only due to the truncation of the

basis. If the potential matrix elements are performed by quadrature then it is known as Finite Basis Representation FBR. The use of Gauss quadrature has the major advantage that the integral,

$$\int_a^b w(x) f(x) \tag{2.19}$$

can be computed exactly by summing $f(x)$ at N quadrature points x_α multiplied by weights w_α for the function $f(x)$ with polynomial degree up to $2N+1$. With this knowledge, a standard (and enlightening) basis set used in FBR calculations is that of the well-known orthogonal polynomials with the square root of the corresponding weight function. By definition, these polynomials satisfy the relation,

$$\int_a^b w(x) p_n(x) p_m(x) = \delta_{nm} \tag{2.20}$$

where $w(x)$ is the weight function with corresponding orthogonal polynomials $p_i(x)$ of the i^{th} degree over the range a to b. If the one-dimensional basis functions are defined as

$$b_n(x) = A_n \sqrt{w(x)} p_n(x), \quad n = 0, 1, ..., N-1 \quad , \tag{2.21}$$

with A_n being a normalization constant, the relationship of Eq. (2.20) can be computed exactly assuming the N quadrature points are used. In fact, the integral is also exact for $\int_a^b b_m^*(x) x b_n(x) dx$ which is relevant in the development of Discrete Variable Representation (DVR).[25] The choice of the basis functions is generally done as to be eigenfunctions of a significant portion $\hat{H}_0$ of the full Hamiltonian $\hat{H} = \hat{H}_0 + V_{res}$ where V_{res} is known as the residual potential. These eigenfunctions can often be taken as the orthogonal polynomials with the square root of the weight function, with an example being the solutions to the 1D harmonic potential. Included in $\hat{H}_0$ is the kinetic energy operator K and possibly some

portion V_0 of the full PES.

2.4.1 Discrete Variable Representation

The integral relationship of Eq. (2.20) can now be written in a square matrix form with $N+1$ quadrature points (and basis functions $b_0(x), ..., b_N(x)$) as,

$$T_{j\alpha} = A_j \sqrt{w_\alpha} p_j(x_\alpha), \tag{2.22}$$

where $\mathbf{T}^\dagger \mathbf{T} = \mathbf{I}$ as the matrix is orthonormal. Likewise, the matrix X can be written as

$$X = \mathbf{T} \mathbf{X}^{\mathbf{DVR}} \mathbf{T}^\dagger, \tag{2.23}$$

with $\mathbf{X}^{\mathbf{DVR}}$ being a diagonal matrix of the quadrature points x_α. From Eq. (2.23), it can be seen that the diagonalization of the X representation in any basis generates as its eigenvalues, the DVR points, and its eigenvectors as the DVR-FBR transformation. An important property of these DVR functions is that each function is sinc-type. A DVR function is non-zero at the point in which it is localized but zero at the remaining DVR points.

The DVR points (and functions) can either be found by directly calculating the X representation of the chosen basis and diagonalizing, or if using orthogonal polynomials, by diagonalizing the three-term relation matrix. The only care that needs to be taken in the latter case is that the functions need to have the appropriate normalization in order to make the transformation matrix orthonormal under the appropriate weight function.

2.4.2 Potential Optimized Discrete Variable Representation

One popular method to obtain good DVR points is to generate Potential Optimized Discrete Variable Representation (PODVR) basis functions[26, 27]. This is done by choosing some model potential that makes up a substantial portion of the full potential and calculating N eigenfunctions. To do this may require much more than N basis functions. The X representation of these eigenfunctions is then diagonalized to obtain the PODVR points and the FBR-DVR transformation. In multidimensional problems, it is possible to greatly reduce the number of DVR points required to obtain accurate results by generating a PODVR for each coordinate. This technique is most accurate when the coupling between the different dimensions is small.

These PODVRs are similar to the Gaussian quadrature type DVRs in that the FBR-DVR transformation matrix is orthogonal. However, the DVR functions are not exactly sinc-type and therefore the accuracy of the results is determined by the minimization of the residual potential.

2.4.3 The curse of dimensionality

For a molecule with D vibrational coordinates, a wavefunction is often represented in a direct product basis,

$$\psi(\mathbf{x}) = \sum_{n_1=1}^{N_1} \sum_{n_2=1}^{N_2} ... \sum_{n_D=1}^{N_D} c_{n_1,n_2,...,n_D} \ {}^1\theta_{n_1}(x_1) \ {}^2\theta_{n_2}(x_2) ... {}^D\theta_{n_D}(x_D) \ , \tag{2.24}$$

where ${}^c\theta(x_c)$ is a 1D basis function for coordinate c, with maximum indices $N_1, N_2, ..., N_D$. The coefficients are components of eigenvectors of a matrix that represents the Hamiltonian operator in the same basis. A direct product basis is convenient because it enables one

to evaluate the matrix-vector products required to use an iterative eigensolver to compute eigenvalues and eigenvectors of the Hamiltonian matrix at a cost that scales as N^{D+1}, where N is a representative value of N_c , $c = 1, \cdots D$.[25, 28, 29, 30] The N^{D+1} scaling relation is most obvious if the Hamiltonian is a sum of products (SOP) but can also be achieved for a general potential by using quadrature.[25] A SOP potential energy surface (PES) also has the advantage that it permits one to calculate all matrix elements from products of 1D integrals.[31]

Despite the advantages of a direct product basis, the cost of using a direct product basis to compute the spectrum of a molecule with more than five atoms is prohibitive. Most important is the memory cost which scales as N^D, with $D = 3A - 6$, where A is the number of atoms, for a $J = 0$ calculation.

If one wishes to use a direct method to obtaining eigenvalues, the memory costs become prohibitive for anything larger than a three atom molecule. In order to store a full Hamiltonian matrix with 10 basis functions per degree of freedom, the memory requirements to store the full Hamiltonian matrix would be $\approx 7TB$. This is computationally infeasible. A great improvement can be made if one obviates the need to store the full Hamiltonian matrix and uses an iterative eigensolver such as Lanczos[32] or Arnoldi[33]. In this case, one only needs to store a small number of vectors instead of the full Hamiltonian matrix. Using iterative methods permits the calculation of four atom molecules easily while five atom molecules become problematic. For a five atom molecule, one double precision eigenvector of coefficients with 10 basis functions per degree of freedom requires $\approx$ 8GB of RAM.

It is therefore advantageous to reduce the size of the basis to solve the Schrödinger equation for molecules, especially when there are more than four atoms.[15] There are two established ways to reduce the basis size: 1) contract direct product bases for sub-problems

by computing eigenfunctions of reduced-dimension Hamiltonians;[34, 35, 36, 37, 38] 2) prune a direct product basis by discarding some basis functions.[39, 16, 40, 41, 42] Contraction can be used with a general, i.e. not a SOP, PES. Pruning can be used with a general PES, if it is combined with a nondirect product quadrature or collocation.[43, 44, 45, 46]

In this thesis, we use a basis each of whose functions is a product of phase-space localized 1D functions. Conceptually, the basis we use can be thought of being obtained from a direct product basis by pruning, but in practice the direct product basis is never built.

2.5 Review of methods with PSL basis functions

This section focuses on the developments in phase-space localized basis functions prior to 2014, where any relevant developments after this point are included in subsequent chapters. Historically, there are two closely related methods that have been used to reduce the number of needed basis functions by using localized functions. The first is the Distributed Gaussian Basis (DBG) started in 1986 by Ref. 47, while the second is the grid in phase space approach started in 1979 by Ref. 48. Both have been applied to simple 1D systems (like the Morse potential), while DGB has calculated the vibration (without rotation) of H_2O and the neon/argon trimer[49].

2.5.1 Distributed Gaussian Basis

The basic premise of the DGB method is to place a number of Gaussian functions where the potential is lowest. Gaussian functions have the property that they are localized in both coordinate and momentum space.

Basis Functions

The basis functions used for DGB are of the form[47]

$$\phi_i = \left(\frac{2A_i}{\pi}\right)^{(1/4)} \exp\left[-A_i\left(x - x_i\right)^2\right], \tag{2.25}$$

where A_i is the width parameter of a Gaussian function located at x_i. Since a set of Gaussian functions is not orthogonal, the use of the FBR will require one to solve a generalized eigenvalue problem of the form

$$\mathbf{HU} = \mathbf{SUE}, \tag{2.26}$$

where $\mathbf{H}$ is the Hamiltonian you are solving and $\mathbf{S}$ is the overlap matrix. $\mathbf{U}$ are the eigenvectors with eigenvalues on the diagonal of $\mathbf{E}$. Both $\mathbf{H}$ and $\mathbf{S}$ are real symmetric matrices. Generally, the Hamiltonian can be decomposed into a kinetic energy portion $\mathbf{K}$ and the potential (PES) $\mathbf{V}$. This results in,

$$\left(\mathbf{K} + \mathbf{V}\right)\mathbf{U} = \mathbf{SUE}, \tag{2.27}$$

where for the matrix $\mathbf{K}$, the integrals are evaluated exactly, while the potential integrals are most commonly evaluated using quadrature. If the simplified Watson Hamiltonian[13] (without the "π-π" term) is used with a potential in Taylor expanded form (and therefore the Hamiltonian is SOP), the matrix elements can be evaluated analytically. If one wants to use iterative methods, a sum of products potential is definitely advantageous. However, for direct methods, there is not a huge advantage to producing the $\mathbf{V}$ matrix analytically since the product of two exponentials is also an exponential. So integrals can be performed with few gauss-quadrature points. This basis has a trade off between using large and small

A_i. A small A_i leads to large kinetic energy matrix elements but lower conditions numbers. Large A_i leads to smaller kinetic energy matrix elements but large condition numbers in the matrix[49]. The condition number of a matrix gives a bound on how inaccurate a solution to a matrix equation can be. The general rule is that an order of magnitude increase in the condition number may result in an order of magnitude increase in the resulting solution. In previous work[50], this is the exact relationship found.

In the original outline of the Method in Ref. 47, two choices of the centres x_i for the DGB were given. The first was equal spacing and the second using a semi-classical approximation.

Choosing the points semi-classically

Choosing the points semi-classically begins by noting that the nth exact bound state wave function has $n-1$ nodes. When you look at the system semi-classically, the distance between two nodes x_i and x_{i+1} is,

$$\Delta J_n = \int_{x_i}^{x_{i+1}} p\left(x\right) dx, \tag{2.28}$$

where $p\left(x\right)$ is the classical momentum $\sqrt{2m\left(E_n - V\left(x\right)\right)}$. Once you choose an energy E_n, you can determine the classical turning points x_{min} and x_{max}. The number of levels at energy at or below E_n labelled $R_L = n + 1$ can be defined as

$$R_l = \frac{1}{\pi} \int_{x_{min}}^{x_{max}} p\left(x\right) dx + 1/2 = M + 1. \tag{2.29}$$

This is a fairly accurate equation for quantum problems, E_{23} of the Morse potential defined in Ref. 47 was found to have an R_L value of 24. If you happen to want one Gaussian between

each node, then the points can be found using,

$$\int_{x_{min}}^{x_1} p\left(x\right) dx = \pi/4; \quad \int_{x_{i-1}}^{x_i} p\left(x\right) dx = \pi, \tag{2.30}$$

where x_{min} is the classical turning point.

If greater or fewer points are wanted, the transformation

$$\pi \rightarrow \pi \frac{R_l - 1/2}{M - 1/2} \tag{2.31}$$

results in the appropriate semiclassical spacing using Eq. (2.30) with the M desired basis functions. The next set of parameters that need to be chosen is the DGB widths A_i. In Ref. 47, the widths were chosen as

$$A_1 = c^2/\left(x_2 - x_1\right)^2, \; A_i = 4c^2/\left(x_{i+1} - x_{i-1}\right)^2, \; A_N = c^2/\left(x_N - x_{N-1}\right)^2, \tag{2.32}$$

where c is a free parameter that is chosen depending on the system analysed. The reasoning for the dependence on the distance between nearby functions was to ensure that the A_i values remained large enough as to not cause the basis functions to be linearly dependent. The justification for the $1/\left(x_{i+1} - x_i\right)^2$ dependence comes from analysis of the overlap matrix $\mathbf{S}$. It's found that in the large M limit, the $\mathbf{S}$ matrix becomes diagonal insinuating that the DGB becomes a series of δ functions, or not formally overcomplete. Overcompleteness results in many eigenvalues near zero and numerically instability (large condition number). Interestingly, even with the $\mathbf{S}$ matrix having a condition number on the order of 10^{10}, the precision of the computed eigenvalues is not effected until about the 10th digit.

This choice of basis functions does not generalize well to higher dimensions, but one can

see that the basis functions where the potential is lower will be more densely packed and have higher curvature (or momentum).

In a 2001 paper by Garashchuk and Light[49], it was shown that choosing the centres of the DGB quasirandomly could be quite successful. In the spirit of the semiclassical spacing given above, they suggested that the density of the basis functions should be proportional to

$$p\left(x_i\right) = E_{cut} - V\left(x_i\right) + \Delta, \tag{2.33}$$

where p is the probability, E_{cut} is some cut-off energy that you would like to find the eigenvalues below and $V\left(x_i\right)$ is the potential at point x_i. The x_i values only range from the classical turning points x_{min} and x_{max}. Thus the parameter Δ determines the sensitivity of the Gaussian centres to the potential. In the large Δ limit, the distribution $p\left(x_i\right)$ approaches uniform and the spacing between the Gaussians is uniform. In a similar fashion, the A_i values are chosen to be

$$A_i = cm_i\left(E_{cut} - V\left(x_i\right) + \Delta\right), \tag{2.34}$$

where c is once again a free parameter and m_i is the mass in the kinetic energy operator $p^2/2m_i$ for dimension i. Garashchuk and Light found that choosing c such that the condition number on the order of $10^6 - 10^{14}$ produced the most accurate results.

2.5.2 Phase Space Method

The phase space approach to localizing basis functions began in 1979 with a paper by Davis and Heller[48]. The basis set suggested was

$$g_{i,j} = \left(\frac{2\alpha}{\pi}\right)^{1/4} \exp\left[-\alpha\left(x - x_i\right)^2 + ip_j x\right] \tag{2.35}$$

for all real x_i, p_j. The exponential factor α may have an imaginary part but for the purposes of this discussion and for all later uses is taken to be real. x_i, p_j are taken to mean the average position and momentum of the basis functions $g_{i,j}$. This is most evident when you take the Wigner transform,

$$\frac{1}{\pi\hbar}\int_{-\infty}^{\infty} g^*\left(x+y\right) g\left(x-y\right) e^{2ipy/\hbar} \mathrm{d}y, \tag{2.36}$$

of Eq (2.35), which results in the Wigner distribution,

$$\Gamma\left(q,p\right) = \frac{1}{\pi}\exp\left[-\frac{1}{2\alpha}\left(4\alpha^2\left(x-x_i\right)^2 + \left(p-p_j\right)^2\right)\right]. \tag{2.37}$$

The Wigner distribution was introduced in 1928[51] by Eugene Wigner to study quantum wavefunctions as a probability distribution in phase space. As can be seen in Eq. (2.37), the vN functions in phase space are a product of Gaussians in the x and p directions.

Although Davis and Heller have a lengthy discussion about choosing the parameters α, x_i, p_j, the only method that is used in calculations recently involve a classical phase space grid[52, 53] where each square occupies $2\pi\hbar$ area. A proof of why this choice of grid spacing forms a complete basis can be found in Ref. 54. The grid is shown pictorially in Figure 2.1 for the case in which a Morse potential $V\left(x\right) = D\left(1 - e^{-\beta x}\right)^2$ is used, with

$D = 12$, $\beta = 6$, $\hbar = 1$ and the mass $m = 6$. The basis functions are either accepted or rejected depending on whether they are in the classical phase space below some energy cutoff E_{cut}. E_{cut} is generally chosen as the energy from which you would like to obtain all eigenvalues below[52].

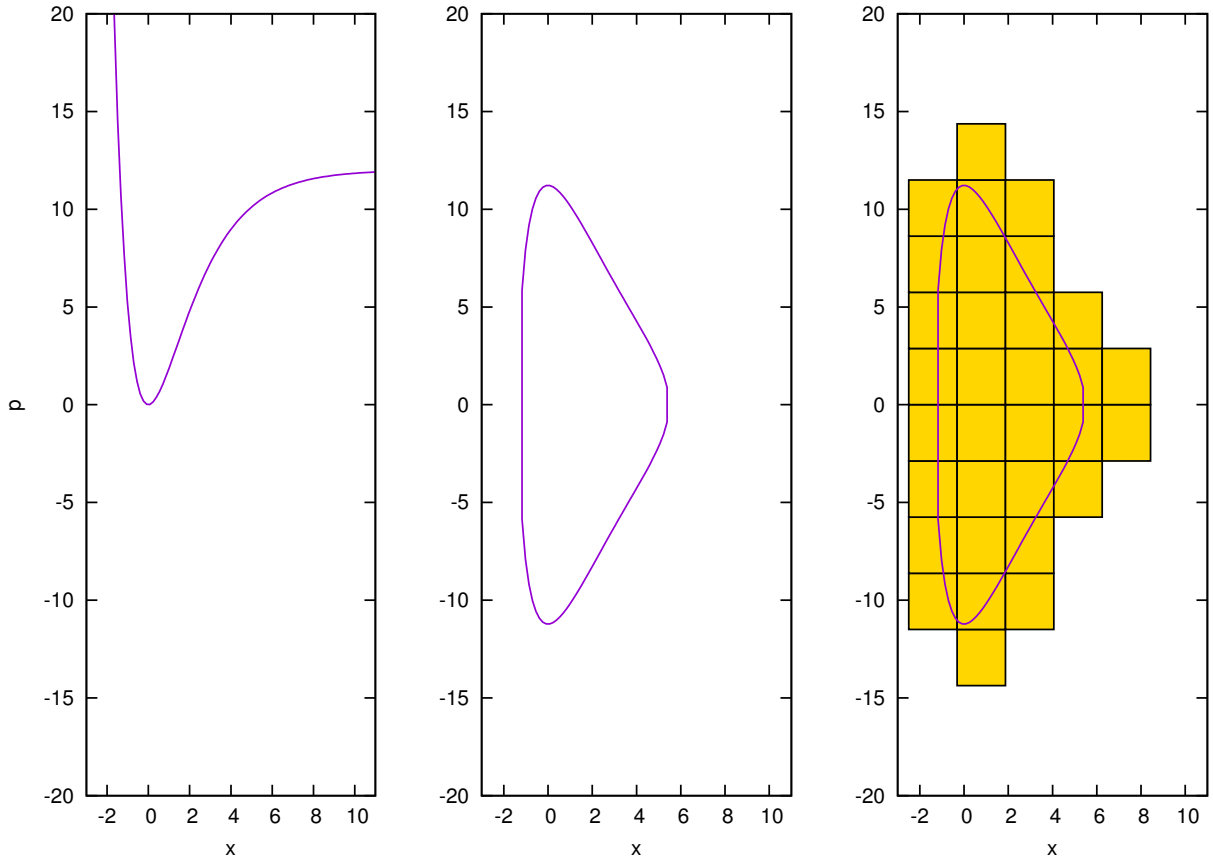

Figure 2.1: Left) Morse potential with parameters D=12,m=6,$\beta = 0.5$. Center) The classically allowed region of a Morse potential. Right) The phase space grid of functions, $g_{i,j}$ are placed at the middle of squares with area 2π.

The method employed by Ref. 52 is to form a basis using the Von Neumann lattice shown pictorially in Fig 2.1. However, instead of each square occupying a area of size $2\pi\hbar$, you begin with a lattice that has square size $\pi\hbar$ and then take only symmetric combinations of $\pm p_i$ functions on the grid. If Ref. 52 left the basis as a complete $\pi\hbar$ grid, it would have been

overcomplete and numerically unstable. The reason to start with this doubly dense lattice is that the critically dense lattice (namely $\Delta x \Delta p = 2\pi\hbar$) is not localized once the basis functions are orthogonalized[55]. The necessity of localization is discussed in more detail in Chapter 5.

Obtaining eigenvalues from a generalized eigenproblem generally requires orthogonalization. This is often performed by Löwdin orthogonalization. In this case, diagonalization of the overlap matrix $S_{i,j,i',j'} = \int g_{i,j}(x)\, g_{i',j'}$ is performed which results in the diagonal matrix of eigenvalues $\mathbf{s}$ and eigenvector matrix $\mathbf{T}$. One can then obtain the inverse square root of $\mathbf{S}$ as $\mathbf{S}^{-1/2} = \mathbf{T}\mathbf{s}^{-1/2}\mathbf{T}^{\dagger}$, The eigenvalues of the Hamiltonian can be found by diagonalizing $\mathbf{S}^{-1/2}\mathbf{H}\mathbf{S}^{-1/2}$. If you set up a vector $\vec{g}$ which has elements $g_{i,j}(x)$ then the vector of orthogonalized basis functions are $\mathbf{S}^{-1/2}\vec{g}$. When using the critically dense vN basis, these orthogonalized functions turn out to only have inverse decay at critical density even though the individual $g_{i,j}(x)$ have Gaussian decay. This was the motivation for starting with the doubly dense basis functions which are

$$g_{i,j} = \exp\left[-A_i\left(x - x_{n_x}\right)^2\right] \cos\left[p_{n_p}\left(x - x_{n_x} - \frac{dx}{2}\right)\right], \tag{2.38}$$

where due to relationships in grid spacing and A_i, the phase factor $\dfrac{dx}{2}$ can also be written as $\sqrt{\dfrac{\pi}{4A_i}}$. The doubly dense functions have exponential decay which is somewhat less localized than the than the Gaussian decay of the $g_{i,j}(x)$.

A second successful use of of Von Neumann lattice basis sets was proposed by Shimshovitz and Tannor in 2012[53]. This begins with the basis set of Eq. (2.37) but instead of applying the Hamiltonian to Gaussians themselves, the initial Hamiltonian matrix is set up using the

Fourier Grid Hamiltonian. The Fourier Grid Hamiltonian (FGH) basis is

$$\phi_n(x) = \sum_{j=-N/2+1}^{N/2} \frac{1}{\sqrt{LN}} \exp\left[\frac{i2\pi j}{L}(x - x_n)\right], \tag{2.39}$$

where x_n are equally spaced points in the domain $[0, L]$. This is commonly referred to as the sinc discrete variable representation which Ref. 53 claims covers approximately the same area phase space as N $g_{i,j}(x)$ basis functions with position space centres in $[0, L]$ and momentum space centres in $[-P, P]$ where $P = Ndp/2$. This correspondence between the FGH and Von Neumann bases is shown for the use of 9 sinc functions and a 3 grid in phasespace. The sinc functions are centred on the grid on the bottom while the Von Neumann basis functions are centred in the middle of the squares.

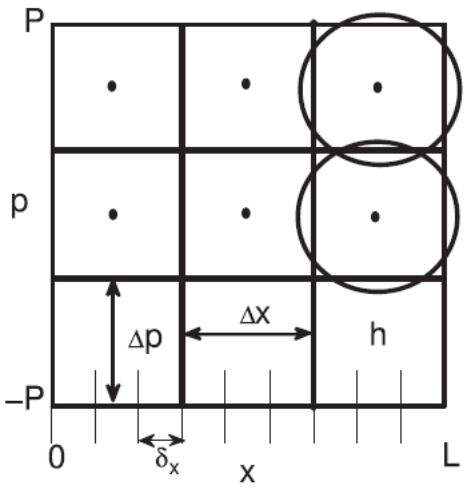

Figure 2.2: 9 sinc and 3 Von Neumann basis functions. The sinc functions are centred on the dashed lines on the bottom while the Von Neumann basis functions are centred in the middle of the squares. Figure taken from Ref. 53

From this, the basis functions are taken to be

$$\tilde{g}_{i,j}(x) = \sum_{n=1}^{N} \phi_n(x_n)\, g_{i,j}(x_n). \tag{2.40}$$

If a G matrix is defined with elements $G_{k,l} = g_l(x_k)$, where l runs over all i, j values, than Eq. (2.40) can be rewritten as $\tilde{G} = \Phi G$. Since $\int \phi_m(x)\,\phi_n(x)$ is diagonal, the matrix representation is

$$H_{i,j,i',j'}U = \sum_{m=1}^{N}\sum_{n=1}^{N} g_{i,j}(x_m)\left(\int \phi_m(x)\, H\phi_n(x)\right) g_{i',j'}(x_n)\, U = SU \tag{2.41}$$

This basis turns out to not be conducive to pruning in that every basis function removed decreases the accuracy of the eigenvalues. If you instead use basis functions $b_k((x) = \sum_{l=1}^{N} \tilde{g}_l \left(S^{-1}\right)_{l,k}$ then it results in the matrix representation

$$H_{k,l}U = .\sum_{m=1}^{N}\sum_{n=1}^{N} b_l(x_m)\left(\int \phi_m(x)\, H\phi_n(x)\right) b_k(x_n)\, U = S^{-1}U \tag{2.42}$$

which can be pruned without decreasing the accuracy.

Chapter 3

Comment on "Phase-Space Approach to Solving the Time-Independent Schrödinger Equation"

3.1 Introduction

When reproducing the results of the ST paper of Ref. 53, it was determined that certain inaccurate conclusions were drawn. A brief review of Ref. 53 is outlined in section 2.5.2 from which is manuscript is a comment on. However, readers are encouraged to have Ref. 53 nearby.

The following content of this chapter is the paper published as Ref. 1.

3.2 Content of Chapter

Shimshovitz and Tannor (ST) [53] introduced a periodic von Neumann (vN) basis for solving the Schrödinger equation. Their contribution is important because it outlines ideas that make it possible to prune a vN basis. We point out that, contrary to statements of ST, neither their biorthogonal pvb basis nor the periodicity of the underlying sinc functions are required to make a pruneable basis with which results of similar quality are obtained. The first attempt to use a vN basis [48] was unsuccessful. Other approaches to exploiting the phase-space locality of vN functions are those of Refs. 40, 52.

ST use vN Gaussians to contract a Fourier grid Hamiltonian (FGH) discrete variable representation (DVR) basis. The simultaneous diagonalization basis of Refs. 41, 42 was used in a similar fashion to contract a harmonic basis. ST begin with a pvN basis,

$$\tilde{g}_m(x) = \sum_{n=1}^{N} \phi_n(x)\, g_m(x_n) \tag{3.1}$$

where $g_m(x)$ are vN Gaussians and $\phi_n(x)$ are periodic sinc functions centered at equally spaced points x_n and transform the time-independent Schrödinger equation (TISE) in the FGH basis, $\mathbf{HU} = \mathbf{UE}$,

to obtain

$$\mathbf{G}^{\dagger}\mathbf{HGV} = \mathbf{SVE}\ , \tag{3.2}$$

where $G_{ij} = g_j(x_i)$, $\mathbf{S} = \mathbf{G}^{\dagger}\mathbf{G}$ and $\mathbf{U} = \mathbf{GV}$. ST propose transforming to a pvb basis,

$$\mathbf{S^{-1}G}^{\dagger}\mathbf{HGS^{-1}Z} = \mathbf{S^{-1}ZE}\ , \tag{3.3}$$

where $\mathbf{Z} = \mathbf{SV}$. Both Eq. (3.2) and Eq. (3.3) are generalized eigenvalue problems of the form

$$\mathbf{AY} = \mathbf{BYL} \ . \tag{3.4}$$

The pruned pvN eigenvalue problem is $\mathbf{C}^\dagger\mathbf{G}^\dagger\mathbf{HGCV} = \mathbf{C}^\dagger\mathbf{SCV}\tilde{\mathbf{E}}$, where $\mathbf{C}$ has n_k diagonal elements equal to one and $n_d = N - n_k$ elements equal to zero. Matrices playing the role of *both* $\mathbf{A}$ and $\mathbf{B}$, in Eq. (3.4) are chopped. Pruning the pvN basis significantly degrades the accuracy of the energies. The pruned pvb eigenvalue problem is

$$\mathbf{C}^\dagger\mathbf{S}^{-1}\mathbf{G}^\dagger\mathbf{HGS}^{-1}\mathbf{CU} = \mathbf{C}^\dagger\mathbf{S}^{-1}\mathbf{CU}\tilde{\mathbf{E}}, \tag{3.5}$$

and in this basis, it *is* possible to prune and maintain accuracy! Again, the matrices playing the role of *both* $\mathbf{A}$ and $\mathbf{B}$ are chopped.

There is, however, no need to introduce the pvb basis. Starting with Eq. (3.2), moving $\mathbf{S}^{-1}$ to the left and *then* pruning, one obtains the nonsymmetric eigenvalue problem

$$\mathbf{C}^\dagger\mathbf{S}^{-1}\mathbf{G}^\dagger\mathbf{H}^{\mathbf{DVR}}\mathbf{GCV} = \mathbf{V}\bar{\mathbf{E}}. \tag{3.6}$$

It is easier to solve Eq (3.6) than Eq. (3.5) with iterative eigenvalue solvers because it is not a generalized eigenvalue problem (therefore larger systems are accessible). For the 1D Morse potential of Ref. 53, we compare eigenvalues computed with Eq. (3.6) and Eq. (3.5), using $N = 196$ initial basis functions. In both cases, the error does not decrease until about $n_k = 98$.

According to ST, the accuracy of the Eq. (3.5) levels is due in part to the periodicity of the sinc DVR. We have confirmed that with Eq. (3.6), energies obtained with non-periodic

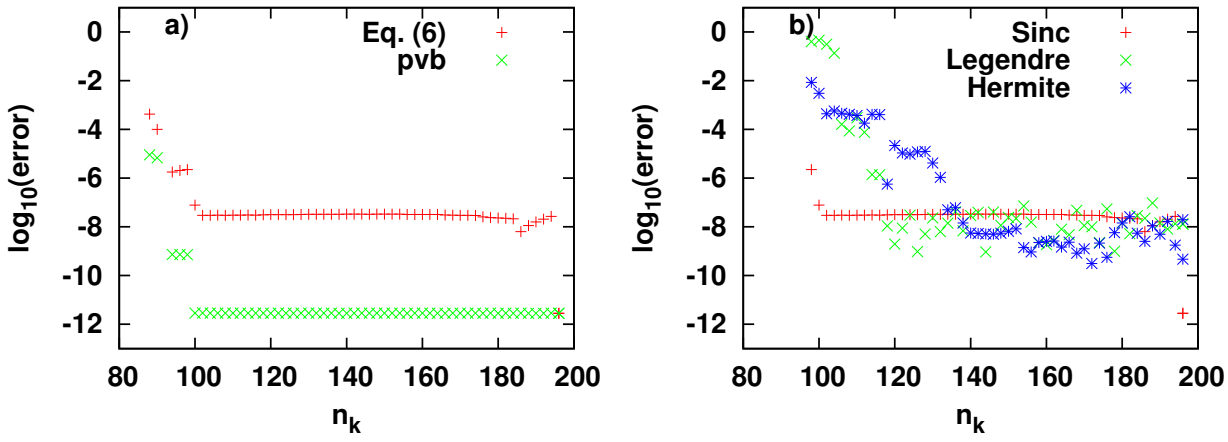

Figure 3.1: The error of the 22nd eigenvalue of the Morse oscillator a) Comparison of ST's pvb with the FGH and Eq. (3.6) with the Colbert and Miller (CM)[56] Sinc DVRs. b) Comparison of Hermite ($H_n(x)$) and Legendre ($P_n(x)$) DVRs using Eq. (3.6) and ST's pvb.

DVRs [25] are also accurate; see Fig. 3.1b for the Morse oscillator of ST. Fig. 3.1b is generated with vN functions at $\sqrt{N}$ position values x_i that are a subset of the DVR points. After sending this comment to ST, we learned that they had done pvb calculations with other DVRs. [57] The fact that both Eq. (3.6) and the ST approach work with other DVRs is clearly incompatible with the assertion that periodicity is important. Knowing that the ST idea of contracting with Gaussians can be applied to other DVRs opens the door to using it to solve many problems for which sinc DVRs are not ideal.

In summary, it is not necessary to think in terms of the pvb basis ST introduce if the pvN eigenproblem is truncated as in Eq. (3.6), and the contraction idea ST use enables one to use Gaussians to contract any DVR basis.

Chapter 4

Using an iterative eigensolver to compute vibrational energies with phase-spaced localized basis functions

4.1 Introduction

This chapter applies the knowledge obtained from manuscript 1 of the previous chapter to the H_2O molecule. It also discusses in detail the theoretical understanding of why the ST method works.

The following content of this chapter is the manuscript published as Ref. 2.

4.2 Abstract

Although phase-space localized Gaussians are themselves poor basis functions, they can be used to effectively contract a discrete variable representation basis (A. Shimshovitz and D.

J. Tannor, Phys. Rev. Lett. 109, 070402 (2012)) This works despite the fact that elements of the Hamiltonian and overlap matrices labelled by discarded Gaussians are not small. By formulating the matrix problem as a regular (i.e. not a generalized) matrix eigenvalue problem we show that it is possible to use an iterative eigensolver to compute vibrational energy levels in the Gaussian basis.

4.3 Introduction

The most general and systematic way to solve the Schrödinger equation is to represent wavefunctions in a basis and use methods of numerical linear algebra to determine coefficients. For example, to solve a 1D time-independent Schrödinger equation (TISE), one uses a basis $\theta_k(x)$

$$\psi(x) = \sum_k c_k \theta_k(x) \tag{4.1}$$

and solves for the c_k. Frequently, the c_k are determined by multiplying on the left by $\theta_j^*(x)$ and integrating to obtain a matrix eigenvalue equation.[39, 58, 59, 34, 15] It is often difficult to implement this procedure to compute solutions of the Schrödinger equation, from which vibrational spectra, photodissociation cross sections, rate constants etc, are calculated because the size of common basis sets scales exponentially with the number of coordinates ($3N-6$, where N is the number of atoms, for a $J=0$ calculation).

The basis is huge in part because quantum mechanics is non-local. However, it is clear that standard direct product basis sets, although they may facilitate calculations, are much larger than they need to be. One way to make a smaller basis that is adequate for the purpose of computing vibrational spectra is to use products of eigenfunctions of reduced-dimension Hamiltonians. This contraction idea is sometimes used with adiabatic-like functions.[34,

36, 60, 61, 62, 63, 64] In this case, a set of basis functions for one group of coordinates is calculated for each of many values of the other coordinates. Contraction can also be done with "simply contracted functions"[35, 65] by computing a single set of basis functions for one group of coordinates for one value of the other coordinates.[66, 37, 67, 68, 38, 69, 70] In this chapter we develop and apply a very different contraction strategy. It is related to the work of Davis and Heller[48] (DH), of Poirier and co-workers,[40, 55, 71, 52, 72] and of Tannor and co-workers.[53, 73] The key idea is that an efficient basis is one whose phase space representation covers the same region as the wavefunctions one wishes to compute. This idea motivated the early work of DH, and is clearly expressed in Ref. 74 where Poirier discusses the Wigner representation of a basis.

The simple idea of using basis functions (whose Wigner representation is) localized in phase space is intuitive and attractive. It should enable us to use knowledge extracted from classical mechanics to design an efficient basis. One expects that a basis covering (in the Wigner sense) a region slightly larger than the classical region of phase space should be sufficiently large for the purpose of computing accurate wavefunctions. For several decades scientists have pursued the hope that such a classically-motivated basis would be useful [48, 74, 40, 71, 55, 41, 42, 52, 53, 73, 72]. DH were the first to apply this idea in chemical physics.[48] They used a 1D von Neumann (vN) basis on a grid with each function corresponding to a phase space area of size h. Their approach worked surprisingly poorly. If the area per basis function is reduced and the size of the basis is increased, it is sometimes possible to obtain accurate results. However, in many cases as the basis size is increased (and the "area" per function is decreased), near linear dependence of the basis becomes so severe that it is not possible to compute accurate energy levels.

Poirier and co-workers introduced new ideas for mitigating the deficiencies of the DH

approach. In one set of papers,[40, 71, 55] they define orthonormal Weylets and show that it is possible to use a relatively small number of Weylets and compute accurate energies. There is no problem with near linear dependence because the basis is orthonormal. In another set of papers, they use a symmetrized Gaussian basis and solve a generalized eigenvalue problem.[52, 72] Also in this approach, there is no problem with near linear dependence. Dawes and Carrington used a simultaneous diagonalization (SD) algorithm to make 1D wavelet-like orthogonal basis functions and showed that for many dimensional problems it possible to calculate accurate energies by pruning the basis formed by making products of the 1D SD functions products.[41, 42] Shimshovitz and Tannor (ST) [53] introduced a "periodic von Neumann with biorthogonal exchange" (pvb) basis for solving the TISE. ST begin with a discrete variable representation [75, 34, 25] (DVR) of the Hamiltonian, transform to the pvb basis, prune the pvb basis, and solve a generalized eigenvalue problem.

Our chapter reports progress on two fronts. (1) We explain in detail when, and why discarding vN basis functions works, despite the fact that the corresponding (e.g. Hamiltonian) matrix elements are not small. (2) We show that an iterative eigensolver can be used to solve a vN matrix eigenvalue problem. To do this, it is essential to formulate the problem as a regular (i.e. not a generalized) matrix eigenvalue problem. Because the matrix eigenvalue problem we solve is not generalized (i.e. no overlap matrix on the right side multiplying the matrices of eigenvectors and eigenvalues), it is possible, to use an iterative eigensolver and hence avoid storing large matrices. Poirier and co-workers have shown that phase-space localized basis methods can be applied to polyatomics without iterative eigensolvers. Recently this has been achieved by using massive computers, as methods of direct linear algebra, which require storing matrices, are used to solve eigenproblems with matrices whose size is $\sim 10^5$.

[52, 72] In an older paper, using much less computer power, Poirier applied his ideas to compute levels of a 15D isotropic harmonic oscillator with unit frequency. [40] The percentage error criterion used in [40] and explained in Ref. 71 is $\delta_{wavelet} = [100(E_{eiv} - E_{exact})]/(10D)$, where D is the dimensionality and E_{eiv} is the computed eigenvalue. When $\delta_{wavelet} = 2$, absolute errors are large, e.g. when $D = 15$ and $E_{exact} = 7.5$ (the energy of the ground state) the absolute error is 3. Lombardini and Poirier have used a subspace iteration iterative method with their Weylets. [76] This is done for model problems by exploiting sparsity. Iterative eigensolvers obviate the need to store matrices, and thus greatly reduce the cost of computing energy levels of interest.[77]

4.4 Using a von Neumann basis

In this section we present and analyse several ways of using a von Neumann basis. Subsection 4.4.1 is devoted to the original DH approach. Rather than using the vN functions as basis functions they can be used to contract a DVR basis. [52] This can be thought of as a basis transformation. This idea is introduced in subsection 4.4.2. In subsection 4.4.2 we explain that some basis transformations yield a pruneable matrix and others do not. The eigenvalue problem is pruneable if rows of the matrix of eigenvectors can be discarded. In subsections 4.4.3 and 4.4.4, we compare the two projection strategies.

4.4.1 Projecting $\hat{H}$ into a vN basis

Start by representing

$$\hat{H}\psi_n(x) = \epsilon_n\psi_n(x) \ . \tag{4.2}$$

in a huge vN basis to obtain the eigenvalue problem

$$\mathbf{H_G W} = \mathbf{S_G W E} \ , \tag{4.3}$$

where $(\mathbf{H_G})_{m',m} = \langle g_{m'}|\hat{H}|g_m\rangle$, $(\mathbf{S_G})_{m',m} = \langle g_{m'}|g_m\rangle$, $m', m = 1, \cdots F$, and $g_{m(i,j)}(x) = \exp\left[-\alpha_i \left(x - x_i\right)^2 + i p_j \left(x - x_i\right)\right]$ is a vN Gaussian centered at (x_i, p_j) with width parameter α_i. In Eq. (4.3) $\mathbf{W}$ is a matrix containing the eigenvectors and $\mathbf{E}$ is a diagonal matrix whose nonzero elements are the eigenvalues. One hopes that it is possible discard some of the basis functions (prune the basis) without degrading the accuracy of the eigenvalues. DH replace Eq. (4.3) with

$$\mathbf{H^c_G W^c} = \mathbf{S^c_G W^c E^c} \ , \tag{4.4}$$

where, like $\mathbf{H_G}$ and $\mathbf{S_G}$, $(\mathbf{H^c_G})_{m',m} = \langle g_{m'}|\hat{H}|g_m\rangle$ and $(\mathbf{S^c_G})_{m',m} = \langle g_{m'}|g_m\rangle$, but with $m', m = 1, \cdots N_k$. Thus, N_k is the size of the chopped matrix.

4.4.2 Projecting H into a vN basis

Instead of using the g_m as basis functions, one can use them to contract some other basis.[53] To do this, begin by projecting the TISE into some real finite orthonormal basis (a discrete variable representation [75, 34, 25] basis is convenient) whose N functions are denoted $\phi_\alpha(x)$,

$$\mathbf{HU} = \mathbf{U\tilde{E}} \ . \tag{4.5}$$

The goal is now to find a basis of finite-dimensional *vectors* in which one can represent columns of $\mathbf{U}$. This is not the same as finding a basis of *functions* with which we can represent $\psi_n(x)$. We introduce $\mathbf{U} = \mathbf{GA}$, where $(\mathbf{G})_{\alpha,m} = \langle \phi_\alpha | g_m \rangle$ are elements of a square

transformation matrix. One obtains,

$$\mathbf{G}^\dagger\mathbf{H}\mathbf{G}\mathbf{A} = \mathbf{S}\mathbf{A}\tilde{\mathbf{E}} \ , \tag{4.6}$$

where $\mathbf{S} = \mathbf{G}^\dagger\mathbf{G}$. The $\mathbf{H}$ used in the original ST paper was the Fourier grid Hamiltonian[78] and their $\phi_\alpha(x)$ were periodic Fourier-Grid-Hamiltonian (FGH) functions, but other DVRs can also be used.[1, 73]

The matrices in Eq. (4.6) are as large as $\mathbf{H}$. To make the transformation useful one must prune the basis, i.e. reduce the number of vN functions from N to N_k. As explained by ST, if this is done by retaining only selected rows and columns of both $\mathbf{G}^\dagger\mathbf{H}\mathbf{G}$ and $\mathbf{S}$, eigenvalues of the pruned problem differ significantly from those of Eq. (4.6). [53] In terms of symbols, $\tilde{\tilde{\mathbf{E}}}$ differs significantly from $\tilde{\mathbf{E}}$, where $\mathbf{C}^\dagger\mathbf{G}^\dagger\mathbf{H}\mathbf{G}\mathbf{C}\mathbf{A}_\mathbf{c} = \mathbf{C}^\dagger\mathbf{S}\mathbf{C}\mathbf{A}_\mathbf{c}\tilde{\tilde{\mathbf{E}}}$, and $\mathbf{C}$ is a diagonal matrix with N_k diagonal elements equal to one and $N_d = N - N_k$ (the number of discarded basis functions) elements equal to zero. When a matrix is multiplied on the right by $\mathbf{C}$, some of its columns are set to zero.

In general, prune-ability can be achieved by replacing $\mathbf{G}$ with a matrix $\mathbf{T}$ and Eq. (4.6) with $\mathbf{T}^\dagger\mathbf{H}\mathbf{T}\mathbf{X} = \mathbf{T}^\dagger\mathbf{T}\mathbf{X}\tilde{\mathbf{E}}$, and choosing $\mathbf{T}$ so that $(\mathbf{T}^\dagger\mathbf{T})^{-\mathbf{1}}\mathbf{T}^\dagger\mathbf{H}\mathbf{T}$ (or $\mathbf{T}^\dagger\mathbf{H}\mathbf{T}(\mathbf{T}^\dagger\mathbf{T})^{-\mathbf{1}}$ or $(\mathbf{T}^\dagger\mathbf{T})^{-\mathbf{1/2}}\mathbf{T}^\dagger\mathbf{H}\mathbf{T}(\mathbf{T}^\dagger\mathbf{T})^{-\mathbf{1/2}}$) is nearly diagonal. There is another way. Choose a new basis and the corresponding transformation matrix $\mathbf{T}$ so that $\mathbf{U} = \mathbf{T}\mathbf{X}$, $\mathbf{T}^\dagger\mathbf{H}\mathbf{T}\mathbf{X} = \mathbf{S}_\mathbf{T}\mathbf{X}\tilde{\mathbf{E}}$, and $\mathbf{T}^\dagger\mathbf{H}\mathbf{T}^{-\dagger}\mathbf{Y} = \mathbf{Y}\tilde{\mathbf{E}}$, where $\mathbf{S}_\mathbf{T} = (\mathbf{T}^\dagger\mathbf{T})$ and $\mathbf{T}^{-\dagger} = (\mathbf{T}^\dagger)^{-\mathbf{1}}$, and choose $\mathbf{T}$ so that the desired portion of $\mathbf{Y} = \mathbf{T}^\dagger\mathbf{U}$ has rows that are tiny. When such a basis can be found, it is possible to remove rows and columns of $\mathbf{T}^\dagger\mathbf{H}\mathbf{T}^{-\dagger}$ without jeopardizing the accuracy of the desired eigenvalues. To explain why this is true, define $\mathbf{M} = \mathbf{T}^\dagger\mathbf{H}\mathbf{T}^{-\dagger}$, and $\tilde{\mathbf{M}}$ which is obtained by replacing the N_k elements, that correspond to retained basis functions, of each of the N_d columns of $\mathbf{M}$ that correspond to discarded basis functions, with zeros. If the retained

and discarded rows and columns are grouped together then the retained-discarded corner of $\tilde{\mathbf{M}}$ is zero, and therefore the desired eigenvalues and eigenvectors of $\tilde{\mathbf{M}}$ are exactly equal to eigenvalues and eigenvectors of the retained corner of $\tilde{\mathbf{M}}$ and are nearly equal to eigenvalues and eigenvectors of the retained-retained corner of $\mathbf{M}$.

One option is to choose $\mathbf{T} = \mathbf{G}^{-\dagger}$. This choice of $\mathbf{T}$ is equivalent to beginning with Eq. (4.6) and multiplying on the left by $\mathbf{S^{-1}}$, as $\mathbf{S^{-1}G}^{\dagger} = \mathbf{G^{-1}}$. One then obtains

$$\mathbf{G^{-1}HGA} = \mathbf{A}\tilde{\mathbf{E}} \ , \tag{4.7}$$

where $\mathbf{Y}$ in the previous paragraph is replaced by $\mathbf{A}$; $\mathbf{A} = \mathbf{G^{-1}U}$. If $A_{m,n}$ were small for some m, then it would be possible to discard rows and columns of $(\mathbf{G^{-1}})\mathbf{HG}$. Does one expect $A_{m,n}$ to be small for some m? The mth element of the nth column of $\mathbf{A}$ is small if the entries of large magnitude of the mth row of $\mathbf{G^{-1}}$ only occur in columns that correspond to entries of $\mathbf{U}_n$ ($\mathbf{U}_n$ is a column of $\mathbf{U}$) of small magnitude. However, in general, there is no reason to expect some rows of $\mathbf{G^{-1}}$ to have large magnitude elements only for α values for which $\mathbf{U}_{\alpha,n}$ is small. It is therefore not obvious that rows and columns can be removed from $(\mathbf{G^{-1}})\mathbf{HG}$.

Another option is to choose $\mathbf{T} = \mathbf{G}$ to obtain the eigenvalue problem $\mathbf{G}^{\dagger}\mathbf{HG}^{-\dagger}\mathbf{B} = \mathbf{B}\tilde{\mathbf{E}}$, where in this case $\mathbf{Y}$ is replaced by $\mathbf{B}$ and $\mathbf{B} = \mathbf{G}^{\dagger}\mathbf{U}$. If no rows and columns are removed, the eigenvalues are equal to those obtained from the pvb formulation of ST, but in the pvb basis one must solve a generalized eigenvalue problem. Is there reason to believe that rows of the desired portion of $\mathbf{B}$ may be small? When the ϕ_α basis is a DVR basis, the mth element of the nth column of $\mathbf{B}$ will be small if in the mth row of $\mathbf{G}^{\dagger}$ the only large magnitude elements correspond to $|g_m(x_\alpha)|$ values for which the magnitude of $\psi_n(x_\alpha)$ is small. There are such rows because the g_m functions and the wavefunctions are localized in position space.[73, 79]

The mth element of the nth column of $\mathbf{B}$ will be small whenever $\mathbf{G}_m^\dagger \mathbf{U}_n$ is small. This can happen even if in row $\mathbf{G}_m^\dagger$ of $\mathbf{G}^\dagger$ elements of large magnitude correspond to large elements $|\mathbf{U}_{\alpha,n}|$. It occurs, for example, when a vN Gaussian is highly oscillatory (i.e. large p_j) in a region in which $\psi_n(x_\alpha)$ is relatively flat. Some rows of the desired portion of $\mathbf{B}$ are small because both the vN Gaussians and the wavefunctions are localized in momentum space. For these reasons, and because $\mathbf{G}^\dagger\mathbf{H}\mathbf{G}^{-\dagger}\mathbf{B} = \mathbf{B}\tilde{\mathbf{E}}$ is not a generalized eigenvalue problem, it should be possible to remove columns and rows of $\mathbf{G}^\dagger\mathbf{H}\mathbf{G}^{-\dagger}$ without significantly altering the desired eigenvalues. The pruned eigenvalue problem obtained from $\mathbf{G}^\dagger\mathbf{H}\mathbf{G}^{-\dagger}\mathbf{B} = \mathbf{B}\tilde{\mathbf{E}}$ is

$$\mathbf{C}^\dagger\mathbf{G}^\dagger\mathbf{H}\mathbf{G}^{-\dagger}\mathbf{C}\mathbf{B}_\mathbf{c} = \mathbf{B}_\mathbf{c}\widetilde{\mathbf{E}}_\mathbf{c}^\mathbf{B}, \tag{4.8}$$

Note that pruning $\mathbf{G}^\dagger\mathbf{H}\mathbf{G}^{-\dagger}$ by removing rows of $\mathbf{G}^\dagger$ and pruning $\mathbf{G}^{-1}\mathbf{H}\mathbf{G}$ by removing rows of $\mathbf{G}^{-\dagger}$ correspond to removing different vN functions. The desired eigenvalues of Eq. (4.8) are close to those of the un-pruned problem. Eq. (4.8) is used in Section 4.5.

As explained after Eq. (4.7), one does not necessarily expect some rows of the desired portion of $\mathbf{A}$, where $\mathbf{G}^{-1}\mathbf{H}\mathbf{G}\mathbf{A} = \mathbf{A}\tilde{\mathbf{E}}$ to be small. Therefore, it is not clear that eigenvalues of the corresponding pruned problem,

$$\mathbf{C}^\mathbf{T}\mathbf{G}^{-1}\mathbf{H}\mathbf{G}\mathbf{C}\mathbf{A}_\mathbf{c} = \mathbf{A}_\mathbf{c}\widetilde{\mathbf{E}}_\mathbf{c}^\mathbf{A} \tag{4.9}$$

will be nearly equal to those of the un-pruned problem. To prune Eq. (4.8) (Eq. (4.9)) one must identify small rows of the desired portion of $\mathbf{B}$ ($\mathbf{A}$). The gap between small and not small is larger for $\mathbf{B}$ than for $\mathbf{A}$, however, similar results are obtained by pruning the basis vectors that correspond to the smallest rows of $\mathbf{A}$ and $\mathbf{B}$. They are similar because eigenvalues of the transpose of a matrix are equal to eigenvalues of the matrix and most of

the removed rows of $\mathbf{G^{-1}}$ correspond to removed rows of $\mathbf{G}^{-\dagger}$

All of the ideas of this subsection are built on the suggestion of ST that it is best to first project into a finite (DVR) basis and only afterwards to discard vectors that correspond to vN functions. A fundamental difference between our approach and ST's is that we formulate the solution as a regular eigenvalue problem, $\mathbf{MY} = \mathbf{Y\tilde{E}}$. This makes using iterative eigensolvers practical. Whenever rows of the desired portion of the matrix of eigenvectors are tiny, rows and columns of $\mathbf{M}$ can be discarded, regardless of the size of the elements. Tiny here refers to being orders of magnitude smaller than the kept rows of the matrix of eigenvectors. The approach of ST also works, although they (separately) prune two matrices and solve a generalized eigenvalue problem. Why does the ST approach work? ST solve $\mathbf{S^{-1}G^{\dagger}HGS^{-1}B^{ST}} = \mathbf{S^{-1}B^{ST}}\widetilde{\mathbf{E^{ST}}}$. Although when all matrices are $N \times N$, it is clear that $\widetilde{\mathbf{E^{ST}}} = \widetilde{\mathbf{E}}$, it is not obvious, after pruning to obtain $\mathbf{C^{T}S^{-1}G^{\dagger}HGS^{-1}CB_c^{ST}} = \mathbf{C^{T}S^{-1}CB_c^{ST}}\widetilde{\mathbf{E_c^{ST}}}$, that $\widetilde{\mathbf{E_c^{ST}}} \approx \widetilde{\mathbf{E_c^{B}}}$. It is true because (1) columns of $\mathbf{B^{ST}}$ are proportional to columns of $\mathbf{B}$ and therefore the desired portion of $\mathbf{B^{ST}}$ has $N - N_k$ rows with tiny elements; (2) when solving $\mathbf{S^{-1}G^{\dagger}HGS^{-1}B^{ST}} = \mathbf{S^{-1}B^{ST}}\widetilde{\mathbf{E^{ST}}}$ both $(\mathbf{B^{ST}})^{\dagger}\mathbf{S^{-1}G^{\dagger}HGS^{-1}B^{ST}} = \mathbf{\Lambda_1}$ and $(\mathbf{B^{ST}})^{\dagger}\mathbf{S^{-1}B^{ST}} = \mathbf{\Lambda_2}$ are diagonal, where $\widetilde{\mathbf{E^{ST}}} = \mathbf{\Lambda_1\Lambda_2}^{-1}$, and therefore replacing the elements of $\mathbf{S^{-1}G^{\dagger}HGS^{-1}}$ and $\mathbf{S^{-1}}$ whose row and column indices correspond to the $N - N_k$ discarded basis vectors, with zeros, has almost no effect on N_k eigenvalues. Note that this does not mean that elements replaced by zeros are small.

Another difference between the approach of Refs. 53 and 73 is the definition of $\mathbf{G}$. We define $(\mathbf{G})_{\alpha,m} = \langle\phi_\alpha|g_m\rangle$ and ST define $(\mathbf{G^{ST}})_{\alpha,m} = g_m(x_\alpha)$. $(\mathbf{G})_{\alpha,m} \neq (\mathbf{G^{ST}})_{\alpha,m}$ because DVR functions depend, in general, on quadrature weights and a weight function. [75, 34, 80, 25] If the weights are all equal the difference between $(\mathbf{G})$ and $(\mathbf{G^{ST}})$ is unimportant. In general, $(\mathbf{G})_{\alpha,m} = \sqrt{W_\alpha^{(N)}/w(x_\alpha)}g_m(x_\alpha)$, where $W_\alpha^{(N)}$ is a quadrature weight and $w(x)$ is

the weight function of the polynomials used to define the DVR. Defining $(\mathbf{G})_{\alpha,m}$ as we do, $\mathbf{G}^\dagger\mathbf{V}^{\mathbf{DVR}}\mathbf{G}$ is a quadrature approximation to $\langle g_{m'}|\hat{V}|g_m\rangle$. Including the weights decreases the size of the elements in the desired portion of $\mathbf{B}$ that correspond to vN functions one wishes to discard and therefore improves the quality of the pruned basis. It is possible to attain pruneability with *any* basis for which rows of $\mathbf{T}^\dagger$ are not nearly linearly dependent and for which multiplying rows of $\mathbf{T}^\dagger$ by columns of $\mathbf{U}$ yields small numbers. This will be the case for any DVR basis. There is no periodicity requirement.[1]

4.4.3 Comparison of projecting $\hat{H}$ and projecting H

Why does using a basis of non-orthogonal g_m functions to compute eigenvalues of $\hat{H}$ by solving Eq. (4.4) not work as well as solving $\mathbf{G}^\dagger\mathbf{H}\mathbf{G}^{-\dagger}\mathbf{B} = \mathbf{B}\tilde{\mathbf{E}}$? It is partly due to the fact that pruning $\mathbf{G}^\dagger\mathbf{H}\mathbf{G}^{-\dagger}$ introduces less error. When calculating eigenvalues of $\hat{H}$ one removes rows and columns of *two* matrices and when calculating eigenvalues of $\mathbf{H}$ one removes rows and columns of only *one* matrix.

The simplest way to prune Eq. (4.3) is to remove rows and columns of both $\mathbf{S_G}$ and $\mathbf{H_G}$. An eigenvalue problem of the form $\mathbf{MY} = \mathbf{Y\Lambda}$ is prune-able if basis functions are sorted by diagonal elements of $\mathbf{M}$ and off-diagonal elements of $\mathbf{M}$ are smaller further from the diagonal. One might imagine that the eigenvalue problem of Eq. (4.3) would be prune-able if the vNs were sorted by the energy of the phase space point at which they are localized and off-diagonal elements of both $\mathbf{H_G}$ and $\mathbf{S_G}$ were smaller further from the diagonal. $\mathbf{H_G}$ and $\mathbf{S_G}$ matrices with this property are nearly diagonal. However, even if $\mathbf{H_G}$ *and* $\mathbf{S_G}$ are nearly diagonal, $\mathbf{S_G^{-1}H_G}$ (and $\mathbf{S_G^{-1/2}H_GS_G^{-1/2}}$) are not and therefore pruning significantly degrades the quality of the eigenvalues.

To understand better why needing to prune two matrices causes error and to establish a

link between projecting $\hat{H}$ and projecting $\mathbf{H}$, it is helpful to think about moving $\mathbf{S_G}$ to the left before pruning. Eq. (4.4) can be derived from

$$\hat{H}|\psi_n\rangle = \epsilon_n|\psi_n\rangle \ , \tag{4.10}$$

in four steps. First, replace $|\psi_n\rangle$ with $\sum_m^F W_{mn}|g_m\rangle$ and multiply on the left by $\langle g_{m'}|$, $m' = 1, \cdots F$, to obtain Eq. (4.3). Second, define $\mathbf{\hat{Z}} = \mathbf{S_G W}$. Eq. (4.3) is equivalent to $\mathbf{H_G S_G^{-1} \hat{Z}} = \mathbf{\hat{Z} E}$. Third, remove $F - N_k$ rows and columns of the *product* $\mathbf{H_G S_G^{-1}} = \mathbf{H_G R_G}$ (where $\mathbf{R_G} = \mathbf{S_G^{-1}}$) to obtain the eigenvalue problem ${}^{\mathbf{r}}\mathbf{H_G}\ {}^{\mathbf{r}}\mathbf{R_G Z} = \mathbf{Z\tilde{E}}$, where ${}^{\mathbf{r}}\mathbf{H_G}$ and ${}^{\mathbf{r}}\mathbf{R_G}$ are rectangular matrices. Fourth, replace ${}^{\mathbf{r}}\mathbf{H_G}$ with the square matrix obtained from it by removing $F - N_k$ columns of ${}^{\mathbf{r}}\mathbf{H_G}$ and ${}^{\mathbf{r}}\mathbf{R_G}$ with the square matrix $\mathbf{S_G^c}$ made by removing rows and columns of $\mathbf{S_G}$ and *then* inverting. The fourth step degrades the accuracy of eigenvalues. It requires replacing ${}^{\mathbf{r}}\mathbf{R_G}$ with the inverse of the retained-retained corner of $\mathbf{S_G}$. When $\mathbf{S_G}$ is not nearly diagonal they may be quite different. Eq. (4.8) corresponds to not implementing the fourth step, but instead inserting DVR resolutions of the identity, with F terms, into $(\mathbf{H_G})_{m'm} = \langle g_{m'}|\hat{H}|g_m\rangle$ and $(\mathbf{S_G})_{m'm} = \langle g_{m'}|g_m\rangle$. $\mathbf{H_G}$ is then replaced with $\mathbf{G^\dagger H G}$ and $\mathbf{S_G}$ is replaced with $\mathbf{G^\dagger G}$. One can then exploit the fact that $\mathbf{G S^{-1}} = \mathbf{G^{-\dagger}}$. This approach has the advantage that it obviates the fourth step without needing to deal with the complete (with $m = 1, 2, \cdots F$) basis.

Starting with the $F \times F$ eigenvalue problem of the second step and introducing DVR resolutions of the identity, one obtains $\mathbf{G^\dagger H G S^{-1} B} = \mathbf{B\tilde{E}}$, where $\mathbf{S^{-1}} = \left(\mathbf{G^\dagger G}\right)^{\mathbf{-1}} = \mathbf{G^{-1} G^{-\dagger}}$. If the size of the eigenvalue problem is then reduced by implementing the third and fourth steps, one solves $\mathbf{C^T G^\dagger H G C (C^T S C)^{-1} \widehat{B_c}} = \mathbf{\widehat{B_c} \widehat{E_c^B}}$. The errors are large. They are large, not due to the discretization created by introducing the DVR resolutions of the identity, but because of the approximations inherent in the fourth step. This is confirmed by starting

with $\mathbf{G^\dagger HG(G^T G)^{-1}B = B\tilde{E}}$. in which all of the matrices are $F \times F$ and replacing $\mathbf{G}$ with a rectangular matrix made by from F vN functions and $F+1$ DVR functions. If the discretization were causing the problem, adding a DVR function would not increase errors. However, for the Morse potential of Refs. 53, 1, with 197 DVR ϕ_α functions and 196 vNs, the error in the ground state is 5×10^{-2} hartree. Using $\mathbf{G^\dagger HG^{-\dagger}B = B\tilde{E}}$, where all the matrices are 196×196 the error is 5×10^{-14} hartree. This is dramatic confirmation of the error introduced by pruning $\mathbf{G^\dagger HG}$ and $\mathbf{S}$ separately (as in the fourth step) rather than pruning one matrix ($\mathbf{G^\dagger HG^{-\dagger}}$). It is also true that the accuracy of the eigenvalues of the ST equation ($\mathbf{C^T S^{-1} G^\dagger HGS^{-1} CB_c^{ST} = C^T S^{-1} CB_c^{ST} \widetilde{E_c^{ST}}}$) is ruined by using $F+1$ DVR functions because when $\mathbf{G}$ is rectangular $\mathbf{\left(G^\dagger G\right)^{-1} \neq G^{-1} G^{-\dagger}}$. Implementing the fourth step outlined above introduces error that can be avoided by, instead, using an equation like $\mathbf{G^\dagger H(G^\dagger)^{-1} B = B\tilde{E}}$. This will be true not only with vN functions, but whenever phase-space localized basis functions are used to compute eigenvalues of $\hat{H}$. Of course, some sets of phase-space localized functions are better than others. A good set of functions reduces the error made in the fourth step. The more nearly diagonal $\mathbf{H_G}$ and $\mathbf{S_G}$, the smaller is the error.

4.4.4 Are rows of a matrix like B tiny even when no intermediate basis is used?

As explained in subsection 4.4.2, $\mathbf{G^\dagger HG^{-\dagger}}$ is prune-able because rows of the desired portion of $\mathbf{B}$ are tiny. In this subsection, we explain that a similar eigenvector matrix $\tilde{\mathbf{B}}$ for the eigenvalue problem obtained with $\hat{H}$, does not have tiny rows. The intermediate basis therefore facilitates pruning. The most obvious way to find an eigenvalue problem for which the desired part of the matrix of eigenvectors, like the desired portion of $\mathbf{B}$, has tiny rows,

but that is obtained without introducing a DVR intermediate basis, is to expand $\psi_n(x)$ in the basis,

$$|b_i\rangle = \sum_{m=1}^{N_k} |g_m\rangle \left(\mathbf{S_G^c}^{-1}\right)_{mi} \ , \tag{4.11}$$

where, $i = 1, 2, \cdots, N_k$, and then multiply the TISE on the left by $\langle g_k|$. The expansion coefficients, $\tilde{b}_{in}$,

$$|\psi_n\rangle = \sum_{i}^{N_k} |b_i\rangle \tilde{b}_{in} \tag{4.12}$$

satisfy

$$\sum_{i}^{N_k} \langle g_k|\hat{H}|b_i\rangle \tilde{b}_{in} = \sum_{i}^{N_k} \langle g_k|b_i\rangle \tilde{b}_{in} E_n \ . \tag{4.13}$$

Does the desired portion of $\tilde{\mathbf{B}}$, where $(\tilde{\mathbf{B}})_{in} = \tilde{b}_{in}$, have tiny rows? If it does then one expects to be able to prune the eigenvalue problem of Eq. (4.13). Compare Eq. (4.12) with the equation for $|\psi_n\rangle$ obtained by pre-multiplying $|\psi_n\rangle$ with a vN resolution of the identity.

$$|\psi_n\rangle = \sum_{i,m}^{F} |g_m\rangle \left(\mathbf{S_G^{-1}}\right)_{mi} \langle g_i|\psi_n\rangle \ , \tag{4.14}$$

where $(\mathbf{S_G})$ is the overlap matrix of a huge vN basis with F functions, $F > N_k$. The sum in Eq. (4.11) has fewer terms, and therefore it is not true that $\tilde{b}_{in} = \langle g_i|\psi_n\rangle$. Although the matrix whose elements are $\langle g_i|\psi_n\rangle$ will have small rows, one is not able to conclude that the matrix whose elements are $\tilde{b}_{in}$ also has small rows. Thus, the eigenvalue problem of Eq. (4.13) is not pruneable.

It is due to the fourth step of subsection 4.4.3 that, when using the vN functions as a basis (rather than using them to transform a matrix), the desired portion of the eigenvector matrix $\tilde{\mathbf{B}}$ does not have tiny rows. If $(\mathbf{S_G})$ were block diagonal then the inverse of the upper left $N_k \times N_k$ block of $(\mathbf{S_G})$ would equal the upper $N_k \times N_k$ block of ${}^{\mathbf{r}}\mathbf{R}_{\mathbf{G}}$, and the upper

limit of the sums in Eq. (4.14) could be reduced from F to N_k. This, in turn, would ensure that $\tilde{b}_{in} = \langle g_i|\psi_n\rangle$.

4.5 Application to H_2O

There are two key advantages of writing the eigenvalue problem as $\mathbf{C^T G^\dagger H G^{-\dagger} C B_c} = \mathbf{B_c C \widetilde{E^B_C}}$ or $\mathbf{C^T G^{-1} H G C A_c} = \mathbf{A_c \widetilde{E^A_C}}$ rather than
$\mathbf{C^T S^{-1} G^\dagger H G S^{-1} C^T B^{ST}_c} = \mathbf{C^T S^{-1} C B^{ST}_c \widetilde{E^{ST}_c}}$. First, iterative eigensolvers are much more costly for a generalized eigenvalue problem.[77] For a generalized eigenvalue problem, it is necessary to solve linear equations at each step of the iteration. If matrices are large, then the linear equations must also be solved with an iterative method. This means there are nested sets of matrix-vector products. If vN basis functions are to be useful for solving challenging vibrational problems, it is imperative that they be used in conjunction with iterative methods. Without iterative methods, it is necessary to store matrices. Second, although $\mathbf{S^{-1}}$ is easy to compute, $\mathbf{[C^T S^{-1} C]^{-1}}$ is not. This is owing to the fact that $\mathbf{S}$ is a direct product of matrices, and thus its inverse is a direct product of inverses of small matrices. To use the ST formulation with an iterative eigensolver, one would need to solve linear equations with (or invert) the matrix $\mathbf{[C^T S^{-1} C]}$.

We apply the ideas to compute vibrational energy levels of H_2O using Radau coordinates, [81, 82] r_1, r_2, θ, and the potential of Polyansky, Jensen, and Tennyson.[83] Before pruning, the basis is a direct product basis with functions $g_{i_1,j_1}(r_1) g_{i_2,j_2}(r_2) g_{i_3,j_3}(\theta)$ where, e.g., $g_{i_3,j_3}(\theta) = \exp\left[-\alpha_3^{i_3}\left(\theta - \theta^{i_3}\right) + i p_3^{i_3,j_3}\left(\theta - \theta^{i_3}\right)\right]$. For the kth coordinate there is an $N_k^i \times N_k^j$ grid of vNs. N_k^i is the number of position centers and N_k^j is the number of momentum centers. For r_k , $k = 1, 2$, $N_k^i = 5$ and $N_k^j = 6$. $r_k^{i_k} = 1 + i_k \mathrm{d}x - \mathrm{d}x/2$, $i_k = 1, 2, \cdots N_k^i$, where $\mathrm{d}x = (4.5 - 1)/N_k^i$ and 1 and 4.5 are the ends of the box in which

we build a sinc DVR,[56] with 30 functions. Atomic units are used in this chapter. $p_k^{j_k} = \left(j_k - N_k^j/2\right) \mathrm{d}p + \mathrm{d}p/2$, $j_k = 1, 2, \cdots N_k^j$, where $dp = h/dx$ which is equal to $2\pi/dx$ in atomic units. N_k^j is even in this chapter. The width parameter $\alpha_k^{i_k}$ is $\mathrm{d}p/(2\hbar \mathrm{d}x)$. [53, 52, 48] For the θ coordinate, $N_3^i = 8$ and $N_3^j = 6$. The θ vNs are built from a Legendre DVR with 48 functions. Although the Legendre functions are polynomials in $Z = \cos\theta$, we use vNs that are $g_{i_3,j_3}(\theta) = \exp\left[-\alpha_3^{i_3}\left(\theta - \theta^{i_3}\right) + ip_3^{i_3,j_3}\left(\theta - \theta^{i_3}\right)\right]$. The points θ^{i_3}, $i_3 = 1, 2, \cdots, N_3^i$, are $\theta^{i_3} = \left(\Theta^{i_3 * N_3^j - N_3^j/2} + \Theta^{i_3 * N_3^j - N_3^j/2 + 1}\right)/2$ where Θ^n is $\cos^{-1}(Z^n)$ with Z^n being a Legendre DVR point. Using vNs that depend on [73] $(\theta - \theta^{i_3})$ rather than $(Z - Z^{i_3})$ yields a more equally spaced vN grid. $p_3^{i_3,j_3} = \left(j_3 - N_3^{j_3}/2\right) \mathrm{d}p^{i_3} + \mathrm{d}p^{i_3}/2$, $j_3 = 1, 2, \cdots, N_3^{j_3}$, with $\mathrm{d}p^{i_3} = 2\pi/\mathrm{d}\theta^{i_3}$ where $\mathrm{d}\theta^{i_3} = \left(\theta^{i_3+1} - \theta^{i_3-1}\right)/2$ but at the edges we use $\mathrm{d}\theta^1 = \theta^2 - \theta^1$ and $\mathrm{d}\theta^{N_3^i} = \theta^{N_3^i} - \theta^{N_3^i - 1}$. For the θ coordinate, the width parameter depends on θ^i and is $\alpha^{i_3} = \mathrm{d}p^{i_3}/2\hbar\mathrm{d}\theta^{i_3}$. This helps ensure linear independence of the columns of $\mathbf{G}$. If the width parameter is independent of θ^{i_3}, the condition number of $\mathbf{G}$ may be large, and this would decrease the accuracy of the computed energies. Even with the width parameter we choose, poor conditioning may somewhat reduce the accuracy of energies computed with a Legendre DVR. When an equally spaced DVR is used, there is no such problem.

A simple Arnoldi eigensolver without implicit or explicit restarts is used.[77] It would be easy to reduce the computation time by using ARPACK.[33] The Lanczos algorithm is not an option because we need the eigenvalues of a non-symmetric matrix. To use the Arnoldi eigensolver we must evaluate matrix-vector products with both $\mathbf{C^T G^\dagger V G^{-\dagger} C}$ and $\mathbf{C^T G^\dagger K G^{-\dagger} C}$, where $\mathbf{H = K + V}$ is a DVR matrix. vNs are useful because the direct product basis can be pruned. Pruning is obviously good because it reduces the size of the basis and decreases (because it reduces the spectral range) the number of matrix-vector products required to obtain converged eigenvalues. However, pruning also complicates the

efficient evaluation of matrix-vector products. There is an ineluctable trade-off between reducing the size of the basis and increasing the complexity of the matrix-vector products. Iterative methods are not efficient if matrix-vector products are done by building the matrix and explicitly multiplying rows of the matrix with the vector. Instead, one must exploit either sparsity or structure of the matrix. When solving the Schrödinger equation it is common to exploit structure because often matrices are not sparse. To use a pruned VN basis, one must identify and exploit the structure of the pruned VN basis. We do this by using sequential summation with summation limits that depend on indices not being summed over.[84, 43, 19, 45, 85, 86] We also use mapping arrays.

The size of the full direct product basis is $N_1N_2N_3 = N_1^iN_1^jN_2^iN_2^jN_3^iN_3^j$. A basis function is $g_{n_1}(r_1)g_{n_2}(r_2)g_{n_3}(\theta)$. The single index n_k ($k = 1, 2, 3$), on a 1D vN represents values of i_k and j_k. The working basis is made by pruning this direct product basis. The basis is pruned as explained in Section 4.5.1. From the pruned basis we determine $n_1(m_1), n_2(m_1, m_2), n_3(m_1, m_2, m_3)$ and $M_1, M_2(m_1), M_3(m_1, m_2)$. $M_1, M_2(m_1), M_3(m_1, m_2)$ which are upper limits on sums (see below). When doing matrix-vector products we sum over consecutive values of m_1, which labels retained functions for r_1, over consecutive values of m_2, which labels retained functions for r_2, and over consecutive values of m_3, which labels retained functions for θ. We begin by building a set of retained n_1 values. n_1 values are in the list if they are in the pruned basis for at least one (n_2, n_3) pair. The retained n_1 values are labelled with consecutive m_1 values and this establishes a link $n_1(m_1)$. In a similar fashion we build a set, for a specific $n_1(m_1)$, that includes the n_2 values that are in the pruned basis for at least one value of n_3; this establishes $n_2(m_1, m_2)$. We then build a set, for specific $n_1(m_1)$ and $n_2(m_1, m_2)$ values, that includes the n_3 values that are in the pruned basis; this establishes $n_3(m_1, m_2, m_3)$. We store tables for n_1, n_2, and n_3. The number of elements in

the set of retained n_1 values is M_1. For each m_1 the number of possible m_2 is $M_2(m_1)$. $M_3(m_1, m_2)$ is, for each m_1, m_2 pair, the number of θ functions. Each retained basis vector is labelled by (m_1, m_2, m_3). So that the vectors we manipulate are labelled by a single index we define a final mapping array $t(n_1, n_2, n_3)$. Each value of t corresponds to a triple (m_1, m_2, m_3) and to a triple (n_1, n_2, n_3). t is a table with as many elements as the full direct product size $N_1 N_2 N_3$. Only triples (n_1, n_2, n_3) that correspond to retained basis functions are assigned a value of t. t is labelled in lexicographical order, i.e. $t(1,1,1) = 1, t(1,1,2) = 2, \cdots$.

Consider first the matrix-vector product in the pruned basis for the term with $\mathbf{V}$. It is

$$\mathbf{C^T G^\dagger V G^{-\dagger} C z_{n_1,n_2,n_3}} \ , \tag{4.15}$$

where $\mathbf{G}^\dagger = {}^{\mathbf{1}}\mathbf{G}^\dagger \otimes {}^{\mathbf{2}}\mathbf{G}^\dagger \otimes {}^{\mathbf{3}}\mathbf{G}^\dagger$. For the H_2O calculation, the condition numbers of ${}^{\mathbf{1}}\mathbf{G}$ (also ${}^{\mathbf{2}}\mathbf{G}$) and ${}^{\mathbf{3}}\mathbf{G}$ are on the order of 10^1 and 10^3 respectively. These matrices are well conditioned and their inverses are accurate, so $\mathbf{G}^{-\dagger} = {}^{\mathbf{1}}\mathbf{G}^{-\dagger} \otimes {}^{\mathbf{2}}\mathbf{G}^{-\dagger} \otimes {}^{\mathbf{3}}\mathbf{G}^{-\dagger}$ is accurate. They are certainly orders of magnitude smaller than the condition number of $\mathbf{S_G}$, required to obtain good accuracy with Eq. (4.4). It should also be noted that in the ST formulation, the matrix whose condition number may cause numerical problems is $\mathbf{C^T G^\dagger G C}$. Its condition number is roughly the square of that of ${}^{\mathbf{1}}\mathbf{G}$, required to use Eq. (4.8). The pruned matrix-vector product is

$$\sum_\alpha ({}^1\mathbf{G}^\dagger_{n_1',\alpha}) \sum_\beta ({}^2\mathbf{G}^\dagger)_{n_2',\beta} \sum_\gamma ({}^3\mathbf{G}^\dagger)_{n_3',\gamma} V_{\alpha,\beta,\gamma} \times \sum_{m_1=1}^{M_1} ({}^1\mathbf{G}^{-\dagger}_{\alpha,n_1}) \sum_{m_2=1}^{M_2(m_1)} ({}^2\mathbf{G}^{-\dagger})_{\beta,n_2} \sum_{m_3=1}^{M_3(m_1,m_2)} ({}^3\mathbf{G}^{-\dagger})_{\gamma,n_3} z_{t(n_1,n_2,n_3)} \tag{4.16}$$

where α, β, γ label DVR points for r_1, r_2, θ. All n_k values in the matrix-vector product equations, Eq. (4.16), Eq. (4.18), Eq. (4.20), are derived from the $n_1(m_1), n_2(m_1, m_2), n_3(m_1, m_2, m_3)$ tables. Doing the sums sequentially in this fashion significantly reduces the cost of the matrix-vector product. Similar ideas have been used before.[84, 43, 19, 45, 85, 86, 28, 29, 87] If Eq. (4.15) were implemented by building the matrix $\mathbf{C^T G^\dagger V G^{-\dagger} C}$ and multiplying its rows with the vector, the cost of the matrix-vector product would scale as N_k^2, where N_k is the number of retained 3D VNs. Sequential summation has been used with[84, 43, 19, 45, 85, 86, 28, 29, 87] and without[28, 29, 87, 88, 89, 90] constrained indices.

The matrix-vector product for the term with $\mathbf{K}$ is simpler because the KEO is factorizable. In Radau coordinates the KEO is[81, 82]

$$T = -\frac{\hbar^2}{2\mu_1}\frac{\partial^2}{\partial r_1^2} - \frac{\hbar^2}{2\mu_2}\frac{\partial^2}{\partial r_2^2} - \frac{\hbar^2}{2}\left(\frac{1}{\mu_1 r_1^2} + \frac{1}{\mu_2 r_2^2}\right)\frac{\partial}{\partial Z}\left(1 - Z^2\right)\frac{\partial}{\partial Z}, \tag{4.17}$$

where $Z = \cos\theta$, and $\mu_1 = \mu_2$ is the mass of hydrogen. For the r_2 term in the KEO, the matrix-vector product is

$$\sum_{m_1=1}^{M_1} \delta_{n_1', n_1} \sum_{m_2=1}^{M_2(m_1)} (^{\mathbf{2}}\mathbf{K_G})_{n_2', n_2} \sum_{m_3=1}^{M_3(m_1,m_2)} \delta_{n_3', n_3} z_{t(n_1,n_2,n_3)} \tag{4.18}$$

In this equation,

$$(^{\mathbf{2}}\mathbf{K_G})_{c_2', c_2} = \sum_{\gamma,\gamma'} {}^{\mathbf{2}}\mathbf{G}^\dagger_{n_2',\gamma}\, {}^{\mathbf{2}}\mathbf{K}_{\gamma',\gamma}\, {}^{\mathbf{2}}\mathbf{G}^{-\dagger}_{\gamma,n_2}, \tag{4.19}$$

with $^{\mathbf{2}}\mathbf{K}$ being a DVR matrix representing the second term in the KEO. For the r_1 term in

the KEO, the matrix-vector product is similar. For the θ term it is,

$$\sum_{m_1=1}^{M_1} ({}^{\mathbf{1}}\mathbf{F})_{n_1',n_1} \sum_{m_2=1}^{M_2(m_1)} \delta_{n_2',n_2} \sum_{m_3=1}^{M_3(m_1,m_2)} ({}^{\mathbf{3}}\mathbf{K_G})_{n_3',n_3} z_{t(n_1,n_2,n_3)} + \sum_{m_1=1}^{M_1} \delta_{n_1',n_1} \sum_{m_2=1}^{M_2(m_1)} ({}^{\mathbf{2}}\mathbf{F})_{n_2',n_2} \sum_{m_3=1}^{M_3(m_1,m_2)} ({}^{\mathbf{3}}\mathbf{K_G})_{n_3',n_3} z_{t(n_1,n_2,n_3)} \quad (4.20)$$

where

$$({}^{\mathbf{k}}\mathbf{F})_{n_k',n_k} = \frac{\hbar}{2\mu_k} \sum_{\alpha} {}^{\mathbf{k}}\mathbf{G}^{\dagger}_{n_k',\alpha} \frac{1}{(r_k^{\alpha})^2} ({}^{\mathbf{k}}\mathbf{G}^{-\dagger}_{\alpha,n_k}) \quad (4.21)$$

$$({}^{\mathbf{3}}\mathbf{K_G})_{n_3',n_3} = \sum_{\gamma,\gamma'} {}^{\mathbf{3}}\mathbf{G}^{\dagger}_{n_3',\gamma} {}^{\mathbf{3}}\mathbf{K}_{\gamma',\gamma} ({}^{\mathbf{3}}\mathbf{G}^{-\dagger}_{\gamma,n_3}) \quad (4.22)$$

with $\mathbf{K^3}$ being a DVR matrix representing $\frac{-\partial}{\partial Z}(1-Z^2)\frac{\partial}{\partial Z}$.

In the matrix-vector product for the term with $\mathbf{V}$, the sums over the DVR indices are not constrained and the DVR grid is large. This will make it hard, despite the prune-ability of the VN basis to compute the vibrational spectrum of a molecule with a general potential and having more than 5 atoms. The size of the product grid for a molecule with 5 atoms is roughly 10^9. One option is to convert the potential to sum of products (SOP) form.[91, 92, 93] There are competing methods that also exploit the SOP form.[94, 95] Another option is to use a constrained grid.[43, 96]

4.5.1 Results

Although the use of a vN basis is motivated by the idea that only vNs centered at points in the classically allowed region of phase space should be required to solve the Schrödinger equation, in practice one needs more. Even in 1D this is true. [79] If it were possible to do a calculation with a very large vN basis, one could identify the vNs that can be safely removed

from the basis by examining components of eigenvectors. In practice, one needs a strategy for adding vNs to build up the basis. Putting vNs in the classically allowed region gives a good starting basis. In Ref. 73 the authors add to the basis, vNs that are phase-space neighbors of vNs that are in the basis and which have large eigenvector components. We use a simpler method that might result in a basis that is larger than the one would obtain using the ST method. We start by keeping all the 3-D vNs that have a potential value (at the vN's center) below 5500 cm^{-1}. The 50 lowest eigenvalues/eigenvectors are then computed using the Arnoldi algorithm. If, for a given n, $c_g = \sum_{n=1}^{50} |B_{g,n}|$ is smaller than some threshold value, that determines the size of the final basis, the corresponding vN is deemed unimportant and removed from the basis. Denote the basis obtained after the vNs are removed the current basis. To the current basis, we add other vNs in a shell around it. To build the shell, we add, e.g. for θ, for each θ^{i_3} for which there are vNs with $p_3^{i_3,j_3}$, two new vNs with the same θ^{i_3}, one with $p_3^{i_3,j_3} = p_3^{i_3,j_3^{max}} + dp_3^{i_3}$ where $p_3^{i_3,j_3^{max}}$ is the largest $p_3^{i_3,j_3}$, and one with $-p_3^{i_3,j_3^{max}} - dp_3^{i_3}$. We also add four additional vNs, two with $\theta_{i_3}^{max} + d\theta_{i_3}$ and $p_3^{i_3+1,j_3} = \pm p_3^{i_3+1,j_3=N_3^j/2}$ and two with $\theta_{i_3}^{min} - d\theta^{N_3^{i_3}}$ and $p_3^{i_3-1,j_3} = \pm p^{i_3-1,j_3=N_3^j/2}$. To obtain real eigenvalues it is necessary to add/keep vNs in pairs with $\pm p^{ij}$. 3D vNs in the shell are made by taking all possible products of the added 1D vNs with themselves and with vNs in the current basis. The lowest 50 eigenvalues are then re-calculated and vNs with small c_g are removed to determine a new current basis. This process is repeated by adding and pruning new shells until eigenvalues of the desired accuracy are obtained. The number of basis functions added in a shell would be large for a molecule with more atoms. The Shimshovitz, Bacic, and Tannor scheme for adding basis functions [73] only adds vNs that are neighbours of vNs that make a significant contribution to the previously calculated eigenfunctions and therefore adds fewer vNs that are later removed using eigenvector coefficients.

The results in Table 4.1 demonstrate that when using Eq. (4.8), it is possible to significantly reduce the size of the vN basis. It is straightforward to compute exact vibrational levels of H_2O using a direct product DVR. These are used as reference energies to assess the accuracy of the pruned vN bases. The direct product DVR basis has 30 sinc DVR functions for r_1 and 30 sinc DVR for r_2 and 48 Legendre DVR for θ. Eigenvalues of the DVR matrix were computed with a Lanczos eigensolver using established ideas.[29] With only 7528 vN basis functions all errors are below 2.1cm^{-1}. The largest error with a pruned vN basis of size 9512 is 0.17cm^{-1}.

Table 4.1: The error of the lowest 100 calculated vibrational energies computed with Eq. (4.8) and two different pruned basis sets. Absolute error is relative to calculated energies E converged to less than 0.01cm^{-1}.

		Absolute Error (cm^{-1})	
n	E(cm^{-1})	N=7528	N=9512
0	4634.76	0.00	0.00
1	6229.42	0.00	0.00
2	7786.25	0.00	0.00
3	8291.87	0.00	0.00
4	8390.59	0.00	0.00
5	9301.60	0.01	0.00
6	9869.69	0.00	0.00
7	9966.12	0.00	0.00
8	10767.85	0.02	0.00
9	11409.94	0.01	0.00
10	11506.31	0.00	0.00
11	11836.90	0.00	0.00
12	11884.60	0.01	0.00
13	12079.43	0.01	0.00
14	12171.42	0.02	0.00
15	12908.59	0.02	0.00
16	13008.70	0.01	0.00
17	13396.48	0.00	0.00
18	13441.53	0.01	0.00
19	13486.11	0.06	0.00

Continued on next page

Table 4.1 – continued from previous page

n	E(cm^{-1})	N=7528	N=9512
20	13634.80	0.00	0.00
21	14354.87	0.10	0.02
22	14467.42	0.02	0.01
23	14679.25	0.42	0.00
24	14919.28	0.00	0.00
25	14963.22	0.02	0.00
26	15156.51	0.00	0.00
27	15235.55	0.07	0.04
28	15248.52	0.09	0.03
29	15503.27	0.02	0.00
30	15667.30	0.01	0.00
31	15702.48	0.14	0.00
32	15850.04	0.80	0.02
33	15872.14	0.02	0.01
34	16401.45	0.01	0.02
35	16447.29	0.05	0.01
36	16642.54	0.01	0.00
37	16774.37	0.05	0.04
38	16785.94	0.10	0.04
39	16959.16	0.34	0.00
40	17041.59	0.02	0.00
41	17139.45	0.19	0.00
42	17200.10	0.01	0.00
43	17203.70	0.08	0.02
44	17833.30	0.03	0.04
45	17887.17	0.13	0.02
46	18085.93	0.02	0.01
47	18229.26	0.64	0.01
48	18277.45	0.02	0.07
49	18287.47	0.11	0.05
50	18428.03	0.46	0.02
51	18438.30	0.44	0.05
52	18464.15	0.25	0.01
53	18466.30	0.07	0.04
54	18544.98	0.07	0.00
55	18701.56	0.00	0.00
56	18856.57	0.13	0.04
57	18954.19	0.15	0.04
58	19173.43	0.05	0.02
59	19182.55	0.34	0.02

Continued on next page

Table 4.1 – continued from previous page

n	E(cm^{-1})	N=7528	N=9512
60	19267.15	0.29	0.05
61	19400.59	2.08	0.03
62	19499.34	0.34	0.05
63	19553.81	1.52	0.04
64	19741.99	0.11	0.08
65	19753.54	0.08	0.07
66	19848.83	0.74	0.01
67	19980.41	0.25	0.00
68	19983.06	0.04	0.02
69	20010.59	0.14	0.04
70	20170.34	0.02	0.01
71	20377.45	0.10	0.05
72	20441.09	0.92	0.01
73	20467.93	0.14	0.05
74	20558.14	0.26	0.09
75	20667.40	0.24	0.02
76	20683.23	0.06	0.02
77	20743.35	1.00	0.06
78	20831.88	0.13	0.03
79	21162.87	0.13	0.07
80	21176.92	0.21	0.05
81	21343.24	0.89	0.04
82	21424.91	0.18	0.05
83	21457.63	0.01	0.02
84	21458.34	0.24	0.03
85	21532.67	0.38	0.17
86	21532.84	0.22	0.14
87	21601.81	0.02	0.01
88	21697.60	0.57	0.07
89	21797.03	0.59	0.13
90	21862.07	0.23	0.11
91	21948.37	0.22	0.08
92	21969.74	0.32	0.14
93	22024.77	0.88	0.08
94	22083.25	0.88	0.04
95	22095.43	0.04	0.04
96	22131.71	0.36	0.01
97	22163.24	0.08	0.05
98	22385.39	0.06	0.02
99	22521.26	0.53	0.03

4.6 Conclusion

In this chapter we demonstrate that an iterative eigensolver can be straightforwardly and efficiently used with a pruned vN (Gaussian) basis when the eigenvalue problem is formulated as in Eq. (4.8). We also explain in detail the importance of first projecting into a DVR basis and then using vNs to contract the DVR basis. This is the first time that vN basis functions have been used in conjunction with an iterative eigensolver. If vN basis functions are to be useful for studying polyatomic dynamics, it is imperative that the matrix equations be formulated as a regular (not a generalized) eigenvalue problem. To use iterative methods to solve a generalized eigenvalue problem, nested iterations are required. To use Eq. (4.8), one must evaluate matrix-vector products with $\mathbf{G}^{\dagger}\mathbf{H}\mathbf{G}^{-\dagger}$. In many dimensions, elements of $\mathbf{G}^{-\dagger}$ are simple products of elements of $\mathbf{G}^{-\dagger}$ matrices for a single coordinate. There is no need to invert a large matrix. The ability to use phase-space localized basis functions and an iterative eigensolver opens the door to studying larger polyatomic molecules. An example calculation of vibrational levels of H_2O shows clearly that it possible to significantly prune the vN basis without degrading the quality of the energies.

It is tempting to assume that the best way to make a prune-able phase-space localized basis is to make basis functions so that, when the basis functions are sorted by the energy of the phase-space point at which they are localized, elements of both $\mathbf{H}$ and $\mathbf{S}$ of the eigenvalue problem $\mathbf{HX} = \mathbf{SXE}$ are smaller further from the diagonal. However, even if $\mathbf{H}$ and $\mathbf{S}$ are nearly diagonal, $\mathbf{S^{-1}H}$ (and $\mathbf{S^{-1/2}HS^{-1/2}}$) may not be and therefore pruning may significantly degrade the quality of the eigenvalues. The key idea of ST is to start with a DVR matrix $\mathbf{H}$ and to use vNs that are linear combinations of the original set of DVR functions

to contract the DVR basis. This gives the eigenvalue problem, $\mathbf{G}^\dagger\mathbf{H}\mathbf{G}\mathbf{A} = \mathbf{S}\mathbf{A}\tilde{\mathbf{E}}$, which can be re-written as $\mathbf{G}^\dagger\mathbf{H}\mathbf{G}^{-\dagger}\mathbf{B} = \mathbf{B}\tilde{\mathbf{E}}$. Rows and columns of $\mathbf{G}^\dagger\mathbf{H}\mathbf{G}^{-\dagger}$ can be removed because the desired part of $\mathbf{B}$ has rows with tiny elements. Note that the elements in the rows and columns of $\mathbf{G}^\dagger\mathbf{H}\mathbf{G}^{-\dagger}$ that are removed are not small.

Iterative eigensolvers have been used with polynomial (including DVR) bases for years.[34, 36, 60, 61, 62, 63, 64, 35, 65, 66, 37, 67, 68, 38, 69, 70] They make it possible to compute vibrational levels of molecules with general potentials and as many as 6 atoms.[97, 98, 85] The multiconfiguration time-dependent Hartree method uses optimized 1D functions and is also able to solve the Schrödinger equation for general potentials when the number of atoms is 6 or even larger.[99] Are pruned vN basis methods competitive? Although the ideas of this chapter that make it possible to combine vN bases with iterative solvers are critical, significant problems remain. The success of pruning for H_2O, demonstrated by the results of Table 4.1 is impressive, but contraction schemes based on polynomial basis functions are better. Better pruning schemes might make the vN methods more competitive. The effectiveness of standard contraction methods, whether used with a direct eigensolver[34, 36, 60, 61, 62, 63, 64] or an iterative eigensolver,[65, 37, 67, 68, 67, 69, 70] is based, in contrast to vN contraction, on the quality of the zeroth-order approximation used to define the basis functions. A vN approach is not based on a zeroth-order approximation and might work well where standard contraction methods are poor. It might, for example, be better for multi-well potentials. We have shown that for H_2O, it is possible to make a vN basis from a direct product of sinc and Legendre DVR functions and then contract it with vNs. If this also works for problems with potentials which do not have SOP form,[100, 101] the vN approach will be important. However, to apply the vN approach of this chapter to multi-well problems, one must develop better ideas for doing potential matrix-vector products.

In this chapter we use a full direct product grid. It might be possible to use non-product quadratures.[43, 19, 19, 85, 86]

Chapter 5

Assessing the utility of phase-space-localized basis functions: exploiting direct product structure and a new basis function selection procedure

5.1 Introduction

The manuscript in this chapter is a slight change from the previous two manuscripts of the previous two chapters as it improves on the HP doubly dense functions outlined in Chapter 2. There is no longer an underlying set of basis functions that is being contracted using the PSL functions, but the PSL functions are being used directly. The Hamiltonian being

examined is a simplified version of the Eckart-Watson Hamiltonian instead of the general polar coordinates used in Manuscript 2. Improvements to the matrix elements in the HP doubly dense basis, and which basis functions are chosen is also presented.

The following content of this chapter is the manuscript published as Ref. 3.

5.2 Abstract

In this chapter we show that it is possible to use an iterative eigensolver in conjunction with Halverson and Poirier's symmetrized Gaussian (SG) basis [Thomas Halverson and Bill Poirier, The Journal of Chemical Physics, **137**, 224101 (2012)] to compute accurate vibrational energy levels of molecules with as many as five atoms. This is done, without storing and manipulating large matrices, by solving a regular eigenvalue problem that makes it possible to exploit direct-product structure. These ideas are combined with a new procedure for selecting which basis functions to use. The SG basis we work with is orders of magnitude smaller than the basis made by using a classical energy criterion. We find significant convergence errors in previous calculations with SG bases. For sum-of-product Hamiltonians, SG bases large enough to compute accurate levels are orders of magnitude larger than even simple pruned bases composed of products of harmonic oscillator functions.

5.3 Introduction

To calculate many accurate vibrational energy levels of a polyatomic molecule, one must represent the corresponding wavefunctions in a basis and use methods of numerical linear algebra to determine the basis function coefficients.[39, 58, 34, 15] For a molecule with D

vibrational coordinates, a wavefunction is often represented in a direct product basis,

$$\psi(\mathbf{x}) = \sum_{n_1=1}^{N_1} \sum_{n_2=1}^{N_2} ... \sum_{n_D=1}^{N_D} c_{n_1,n_2,...,n_D} \ {}^1\theta_{n_1}(x_1) \ {}^2\theta_{n_2}(x_2)...{}^D\theta_{n_D}(x_D) \ , \tag{5.1}$$

where ${}^c\theta(x_c)$ is a 1D basis function for coordinate c, with maximum indices $N_1, N_2, ..., N_D$. The coefficients are components of eigenvectors of a matrix that represents the Hamiltonian operator in the same basis. A direct product basis is convenient because it enables one to evaluate the matrix-vector products required to use an iterative eigensolver to compute eigenvalues and eigenvectors of the Hamiltonian matrix at a cost that scales as N^{D+1}, where N is a representative value of N_c , $c = 1, \cdots D$.[25, 28, 29, 30] The N^{D+1} scaling relation is most obvious if the Hamiltonian is a sum of products (SOP) but can also be achieved for a general potential by using quadrature.[25] A SOP potential energy surface (PES) also has the advantage that it permits one to calculate all matrix elements from products of 1D integrals.[31]

Despite the advantages of a direct product basis, the cost of using a direct product basis to compute the spectrum of a molecule with more than five atoms is prohibitive. Most important is the memory cost which scales as N^D, with $D = 3A - 6$, where A is the number of atoms, for a $J = 0$ calculation. It is therefore advantageous to reduce the size of the basis to solve the Schrödinger equation for molecules, especially when there are more than four atoms. [15] There are two established ways to reduce the basis size: 1) contract direct product bases for sub-problems by computing eigenfunctions of reduced-dimension Hamiltonians;[34, 35, 36, 37, 38] 2) prune a direct product basis by discarding some basis functions.[39, 16, 40, 41, 42] Contraction can be used with a general, i.e. not a SOP, PES. Pruning can be used with a general PES, if it is combined with a nondirect product quadrature or collocation.[43, 44, 45, 46] If the harmonic frequencies of all the

coordinates are similar then a product harmonic oscillator basis (HOB) can be effectively pruned by retaining only basis functions for which $n_1 + n_2 + ... + n_D \leq N$. This reduces the basis size from N^D to

$$\frac{(D+N+1)!}{D!(N+1)!} \ . \tag{5.2}$$

Much better, and more general, pruning conditions exist. One can, for example, discard functions for which $g_1(n_1)+g_2(n_2)+...+g_D(n_D) \leq N$, where g_c are general functions.[45, 72] In this chapter, we use a basis each of whose functions is a product of phase-space localized 1D functions. Conceptually, the basis we use can be thought of being obtained from a direct product basis by pruning, but in practice the direct product basis is never built. We compare the sizes of the phase-space localized (PSL) with the HOB obtained from Eq. (5.2).

5.4 Using PSL basis functions to compute vibrational levels

In chemical physics, phase-space localized basis functions were first used by Davis and Heller[48] (DH). They encountered significant problems and the ideas were abandoned until they were revived by Poirier et al. [40, 55, 71, 52, 72] and Tannor and co-workers.[53, 73] The use of PSL functions is motivated by the idea that a basis whose functions have Wigner representations with significant amplitude only in and close to the classically allowed region of phase space will be efficient.[74] The hope is that it should be possible to discard PSL functions with significant amplitude (in the Wigner sense) outside the classically allowed region. To achieve good accuracy, it will also be necessary to retain basis functions with amplitude in the tunnelling region, but the motivation is nonetheless classical. Davis and Heller[48] used equally spaced Gaussians (on a phase-space grid) and found that they work

poorly.

The PSL strategy we use to obtain accurate energy levels of a Hamiltonian operator begins with a small PSL basis and successively incorporates additional functions into the basis (see Section 5.6). To understand why and how PSL methods work, it is useful, instead, to imagine starting with a *direct product* PSL basis large enough that the desired energy levels are certainly accurate and then reducing its size. Begin therefore with a (non-orthogonal) direct product basis $g_n(\mathbf{x})$ and insert an approximate resolution of the identity into the Schrödinger equation to obtain,

$$\sum_{n'}^{f^i}\sum_{n}^{f^e}\langle g_{n''}|(\hat{H}-E_t)|g_{n'}\rangle(S^{-1})_{n',n}\langle g_n|\psi_t\rangle = 0 \ , \tag{5.3}$$

where $S_{n,n'} = \langle g_n|g_{n'}\rangle$. Increase the upper limits f^e and f^i until the desired energy levels are deemed sufficiently accurate, when $f^e = f^i = F$. The best PSL functions are those for which 1) F is not too large and 2) for the desired states, $\langle g_n|\psi_t\rangle$ is small for some n. Accurate energies are obtained from Eq. (5.3), when elements of the $F \times F$ $\mathbf{S^{-1}}$ matrix are sufficiently close to those of an even larger $\mathbf{S^{-1}}$. In a basis of Gaussians, F must be huge. The doubly dense symmetrized Gaussian (SG) functions of Halverson and Poirier (HP) do a good job of satisfying both 1) and 2). Matrix elements of $\mathbf{S^{-1}}$ converge more quickly as F is increased in the SG basis than in the standard Gaussian basis. Therefore, $F_{SG} < F_{Gauss}$. See HP for more detail.[52, 102, 76]

The accuracy of the eigenvalues obtained by retaining only a subset of the F PSL functions will be determined not only by the choice of the PSL functions, but also by the method used to truncate the matrix eigenvalue problem obtained from Eq. (5.3). F is the size of an imaginary direct product PSL basis that is certainly large enough to compute accurate energies. Some of the F PSL functions may not be necessary and the eigenvalue problem

can therefore be truncated. There are different ways to truncate. The most obvious is to start with $\mathbf{H_G W = SWE}$, set $f^e = f^i$, and then remove rows *and* columns of $\mathbf{H_G}$ *and* $\mathbf{S}$. $(H_G)_{n,n'} = \langle g_n|\hat{H}|g_{n'}\rangle$. This yields the generalized eigenvalue problem,

$$\mathbf{C^\dagger H_G C W_c = C^\dagger S C W_c E^g} \ . \tag{5.4}$$

$\mathbf{C}$ is a diagonal matrix with N_k diagonal elements equal to one and $N_d = N - N_k$ (the number of discarded basis functions) elements equal to zero. As explained in Refs. 1, 2, instead of starting with $\mathbf{H_G W = SWE}$, one can start with the regular eigenvalue problem $\mathbf{H_G S^{-1} \mathcal{B} = \mathcal{B} E}$, where $B_{n,t} = \langle g_n|\psi_t\rangle$. Rows and columns of $\mathbf{H_G S^{-1}}$ can then be removed, by taking $f^e \ll F$, *without decreasing* f^i , to obtain

$$\mathbf{C^\dagger H_G S^{-1} C B = B E^r} \ . \tag{5.5}$$

$\mathbf{E^g}$ is labelled by g because it is obtained from a generalized eigenvalue problem. $\mathbf{E^r}$ is labelled by r because it is obtained from a regular eigenvalue problem. It is also possible to convert Eq. (5.4) into a regular eigenvalue problem,

$$\mathbf{C^T H_G C \left(C^T S C\right)^{-1} B_{pa} = B_{pa} E^g} \ . \tag{5.6}$$

$\mathbf{E^r}$ is closer to $\mathbf{E}$ than is $\mathbf{E^g}$, because it is by introducing additional approximations into Eq. (5.5) that one obtains Eq. (5.6). The subscript *pa* indicates that a product approximation has been made. Chopping matrices with $\mathbf{C}$ would introduce no error if *both* $\mathbf{H_G}$ and $\mathbf{S}$ were block diagonal, with blocks being labelled by retained and discarded functions. [2] $\mathbf{E^g}$ is not as good as $\mathbf{E^r}$ because 1) $\mathbf{C^\dagger H_G S^{-1} C}$ is made without discarding columns of $\mathbf{H_G}$ and rows

of $\mathbf{S^{-1}}$; 2) $\mathbf{C^{\dagger}S^{-1}C} \neq \mathbf{(C^{\dagger}SC)^{-1}}$. A key advantage of Eq. (5.5), compared to Eq. (5.4) is that it obviates the need to invert $\mathbf{C^{\dagger}SC}$. A symmetric formulation is also possible, if one starts with $\mathbf{S^{-1/2}H_GS^{-1/2}}\mathcal{X} = \mathcal{X}\mathbf{E}$. Chopping the product of factors together gives

$$\mathbf{C^{T}S^{-1/2}H_GS^{-1/2}CX} = \mathbf{XE^{o}}. \tag{5.7}$$

Re-arranging Eq. (5.4) to make a symmetric regular eigenvalue problem gives

$$\left(\mathbf{C^{T}SC}\right)^{\mathbf{-1/2}} \left(\mathbf{C^{T}H_GC}\right) \left(\mathbf{C^{T}SC}\right)^{\mathbf{-1/2}} \mathbf{X_{pa}} = \mathbf{X_{pa}E^{g}} \ . \tag{5.8}$$

Eq. (5.4), Eq. (5.6), and Eq. (5.8) have the same eigenvalues.

More accurate energies are obtained by using Eq. (5.5). Increased accuracy is almost always associated with increased cost. Is it costly to use Eq. (5.5)? It might be costly to invert $\mathbf{S}$ and it might be costly to calculate the retained corner of $\mathbf{H_GS^{-1}}$ because of the large number (F) of columns of $\mathbf{H_G}$ and rows of $\mathbf{S^{-1}}$. Inverting $\mathbf{S}$ does look scary because the original PSL basis is huge. However, it is actually straightforward to obtain elements of $\mathbf{S^{-1}}$ because the original PSL basis is a direct product basis and therefore $\mathbf{S^{-1}} = \mathbf{S_1^{-1}} \otimes \mathbf{S_2^{-1}} \cdots \mathbf{S_D^{-1}}$, where $\mathbf{S_c^{-1}}$ is the inverse of a small matrix for coordinate x_c. [2] Note that, in contrast, it is costly to invert $\mathbf{C^{T}SC}$. [73, 57] When an iterative eigensolver is used and the PES is a SOP, the cost of calculating the retained corner of $\mathbf{H_GS^{-1}}$ is also not a problem, *because it is never computed*. Potential matrix-vector products are evaluated term by term by doing sums sequentially. If the PES is a SOP,

$$H = \sum_{\ell=1}^{t} \prod_{c=1}^{D} \hat{t}^{(c,\ell)}(x_c), \tag{5.9}$$

and

$$\mathbf{H_G S^{-1}} = \sum_{\ell=1}^{t} [\mathbf{t^{(1,\ell)} S_1^{-1}} \otimes \mathbf{t^{(2,\ell)} S_2^{-1}} \otimes \cdots \otimes \mathbf{t^{(D,\ell)} S_D^{-1}}] \ . \tag{5.10}$$

It is also possible to obviate both the inversion of $\mathbf{S}$ and the computation of the retained corner of $\mathbf{H_G S^{-1}}$ by using PSL functions to contract a discrete variable representation (DVR) [25] with N^{DVR} functions. The contraction was first proposed in Ref. 53. Those ideas have been applied in several papers. [53, 73, 103] In these papers it is necessary to invert $\mathbf{G^T G}$, where $\mathbf{G}$ is the $N^{DVR} \times f^e$ DVR-PSL transformation matrix. Instead, one can compute eigenvalues of

$$\mathbf{G^T H G (G^T G)^{-1}} = \mathbf{G^T H (G^T)^{-1}} \ . \tag{5.11}$$

where $\mathbf{H}$ is a DVR Hamiltonian matrix. [1, 2] As long as both the DVR and the PSL basis are direct product bases, $(\mathbf{G^T})^{-1}$ is easily obtained by exploiting the direct product structure. The eigenvalue problem is,

$$\mathbf{G^T H (G^T)^{-1} B_d} = \mathbf{B_d E^d} \ . \tag{5.12}$$

The matrix of eigenvalues, labelled by d for DVR, is equal to the eigenvalue matrix obtained from the equation of Shimshovitz and Tannor.[53] There is no need to introduce a "periodic von Neumann with biorthogonal exchange" (pvb) basis. There is no need for periodicity. [1, 2] The resolution of the identity $(\mathbf{G(G^T G)^{-1} G^T})$ one inserts to derive Eq. (5.11) is exact (because one is using PSL functions to contract a DVR basis). The only approximation one makes is discarding rows and columns of the product $\mathbf{G^T H (G^T)^{-1}}$.

In this chapter, we do not use a DVR, but instead use Eq. (5.5) with the SG basis of Poirier and co-workers. Using the SG basis with Eq. (5.5), rather than Eq. (5.4), has the advantage that it is somewhat more accurate. The SG eigenvalues we obtain from Eq. (5.7) are about as accurate as those obtained by using Poirier's Weylet basis. [40, 55, 71] Halverson

and Poirier introduced the SG basis because it is "much more convenient".[52] They use it with Eq. (5.4).

A crucial part of the strategy of using PSL functions is deciding *which* ones to put into the working basis. It is straightforward to build a basis that includes PSL functions whose phase space centres are in a classically allowed region of phase space. The idea that the classical region associated with energy E, denoted $\mathcal{R}_E$ by Poirier, must be important for computing states with energy less than E motivated the development of PSL basis methods. There is no doubt that PSL functions in $\mathcal{R}_E$ must be in the working basis. The problem is that wavefunctions of states with energy less than E have tails that extend beyond $\mathcal{R}_E$. It is therefore necessary also to include PSL functions with amplitude outside the classical region. The simplest way to ensure that such PSL functions are in the working basis is to use the functions in the region $\mathcal{R}_{E_{thres}}$, where $E_{thres} > E$. In this chapter we use a better criterion for determining which PSL to include in the working basis. The ideas are related to those of Refs. 73, 2.

There are three favourable properties of the approach of this chapter. First, it makes it possible to use iterative eigensolvers and thereby obviate the need to store (and compute) the Hamiltonian and overlap matrices. Note, however, that Poirier et al. have done impressive calculations using huge parallel computers and direct eigensolvers.[52, 71] Second, we obtain results about as accurate as those obtained with a Weylet basis but using a simpler SG basis. Third, we introduce a better way of choosing which product PSL functions to include in the final basis.

5.5 Advantage of truncating the product $\mathbf{H_G S^{-1}}$: 1D SG results

We use the doubly dense symmetrized Gaussian basis proposed in Refs. 76, 52. In atomic units ($\hbar = 1$) a 1D SG function is

$$d_n(x) = \exp\left[-\alpha\left(x - x_{n_x}\right)^2\right] \cos\left[p_{n_p}\left(x - x_{n_x} - \frac{dx}{2}\right)\right] , \tag{5.13}$$

where n is a composite index including n_x, n_p. x_{n_x} and p_{n_p} are the centres of the SG functions in phase-space with $x_{n_x} = n_x\sqrt{\pi} + \sqrt{\pi}/2$ and $p_{n_p} = n_p\sqrt{\pi} + \sqrt{\pi}/2$, both n_x, n_p are integers, and $n_p \geq 0$. This is the grid spacing used in Ref. 52 and with $\alpha = 1/2$ it generates a basis that is complete but not over-complete.

To assess the different truncated eigenproblems, we first use this basis to compute energy levels of

$$H = -\frac{1}{2}\frac{\mathrm{d}^2}{\mathrm{d}x^2} + \frac{1}{2}x^2 . \tag{5.14}$$

The original basis (whose size is F) is built from a 40×20 phase-space grid with $n_x = -20, -19. \cdots, 19, n_p = 0, 1, 2, \cdots 19$. It covers a square region of phase-space, $x \in [-20\sqrt{\pi}, 20\sqrt{\pi}]$, $p \in [-20\sqrt{\pi}, 20\sqrt{\pi}]$. All the matrix elements were calculated analytically and the matrices $\mathbf{H_G}$ and $\mathbf{S}$ were built. In this section, the functions included in the working basis are those whose centres are inside the region $\mathcal{R}_{E_{thres}}$, , i.e., those for which $\frac{p_{n_p}^2}{2} + \frac{x_{n_x}^2}{2} < E_{thres} = 55$. There are 56 retained basis functions.

In Figure 5.1, we compare Eq. (5.4) and Eq. (5.7) by plotting them together with eigenvalues of the full problem, $\mathbf{H_G W} = \mathbf{SWE}$. Eq. (5.4) is used in Refs. 52, 72, 48. It is clear that all 56 energies computed with the full 40×20 basis are accurate. The SG basis of HP

is designed to reduce the effect of the approximations required to get Eq. (5.8) (equivalent to Eq. (5.4)) from Eq. (5.7). The similarity of the two curves in Figure 5.1 confirms the advantages of the SG basis. Energies obtained from Eq. (5.7) are, however, always more accurate, see Figure 5.1. The accuracy difference is larger for smaller energies. The ground state energy computed with Eq. (5.7) has an extra digit of precision. Results obtained from Eq. (5.4) and Eq. (5.7) are less similar when the PSL functions are Gaussians. With SG functions, the difference between results obtained with Eq. (5.4) and Eq. (5.7), plotted in Figure 5.1, is similar to the difference between results obtained with Poirier's Weylet basis [40, 55, 71] and with HP's SG basis using Eq. (5.4). This difference has been noted by HP. [52] Energies obtained from Eq. (5.7) should be very close to those obtained with Weylets.

To use Eq. (5.7), which gives slightly better accuracy, it is necessary to compute the retained corner of $\mathbf{S^{-1/2} H_G S^{-1/2}}$, which requires summing over all 800 rows and columns of $\mathbf{H_G}$. In contrast, to use Eq. (5.4), one must only deal with 56×56 matrices. For a multidimensional problem, summing over all the SG functions in the original basis is not an option. However, for a multidimensional problem $\mathbf{S^{-1/2}}$ can be computed and stored by exploiting its direct product structure and if the PES is a SOP, matrix-vector products can be evaluated without calculating the retained corner of $\mathbf{S^{-1/2} H_G S^{-1/2}}$. Using Poirier's Weylet ideas, it is possible to implement Eq. (5.7) without summing over all the SG functions in the original basis.

In Figure 5.2 we compare Eq. (5.5) and Eq. (5.4). According to Ref. 2, the eigenvalues of Eq. (5.5) should be significantly more accurate than those of Eq. (5.4). This is indeed the case. There are two reasons. First, in Eq. (5.5) 800 columns of $\mathbf{H_G}$ and 800 rows of $\mathbf{S^{-1}}$ are retained. Second, $\mathbf{(C^T S C)^{-1}} \neq \mathbf{C^T (S)^{-1} C}$.

The eigenvalues of Eq. (5.5) are more accurate than those of Eq. (5.7) due to the fact that

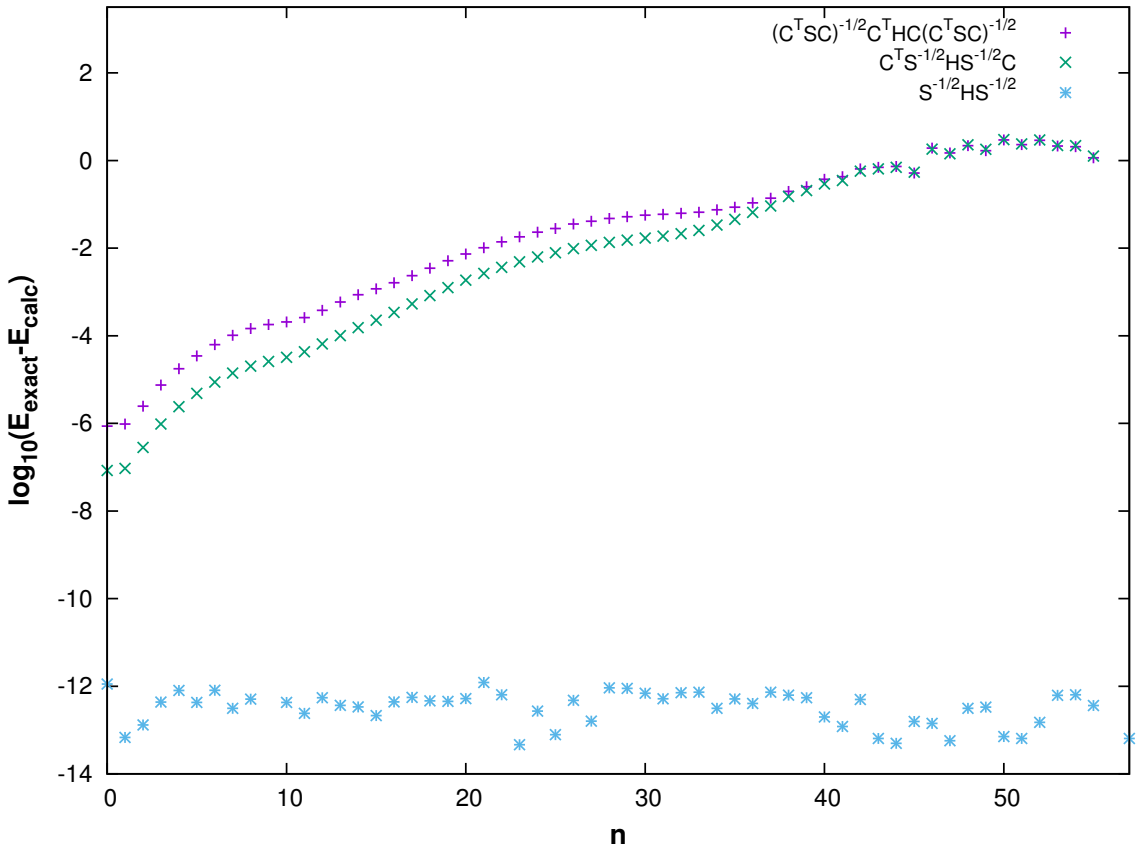

Figure 5.1: Comparison of the accuracy of Eq. (5.7) and Eq. (5.8) (or Eq. (5.4)) for the harmonic oscillator Hamiltonian. The starting basis of 800 SG functions is reduced to 56 basis functions. n on the x axis labels an eigenvalue.

$\mathbf{B}$ with elements $B_{n,t} = \langle g_n | \psi_t \rangle$ has columns with small components and the corresponding elements of $\mathbf{X} = \mathbf{S^{-1/2}B}$ are not as small. They are not as small because the small components of $\mathbf{B}$ get smeared out by $\mathbf{S^{-1/2}}$. This means that less error is introduced by chopping $\mathbf{H_G S^{-1}}$. We shall therefore use Eq. (5.5) for multidimensional calculations. For multidimensional problems $\mathbf{S^{-1}}$ will be computed and stored by exploiting direct product structure. For SOP PESs, we shall take advantage of direct product structure and not calculate the retained corner of $\mathbf{H_G S^{-1}}$.

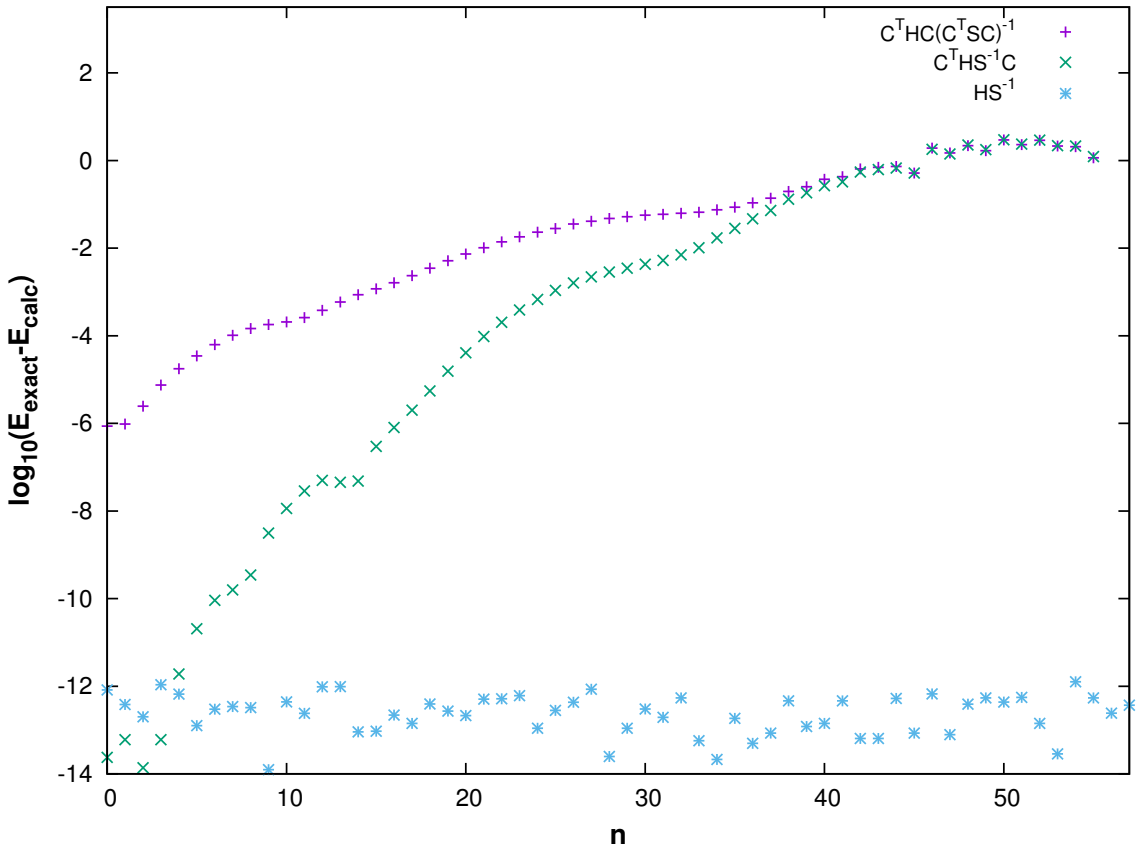

Figure 5.2: Comparison of the accuracy of Eq. (5.5) and Eq. (5.6) (or Eq. (5.4)) for the harmonic oscillator Hamiltonian. A starting basis with 800 SG functions is reduced to 56 basis functions. n on the x axis labels an eigenvalue.

5.6 Expanding a basis of PSL functions

One wishes to choose a working basis that includes only the PSL functions corresponding to large components of the columns of $\mathbf{B}$ associated with desired energies. It is not possible to solve the Schrödinger equation in the full basis (with F functions). Instead, one needs some means of determining which are the important functions. For the Hamiltonian,

$$H = -\frac{1}{2}\frac{\mathrm{d}^2}{\mathrm{d}x^2} + \frac{1}{2}x^2 + \frac{1}{10}x^3 + \frac{1}{100}x^4 \ , \tag{5.15}$$

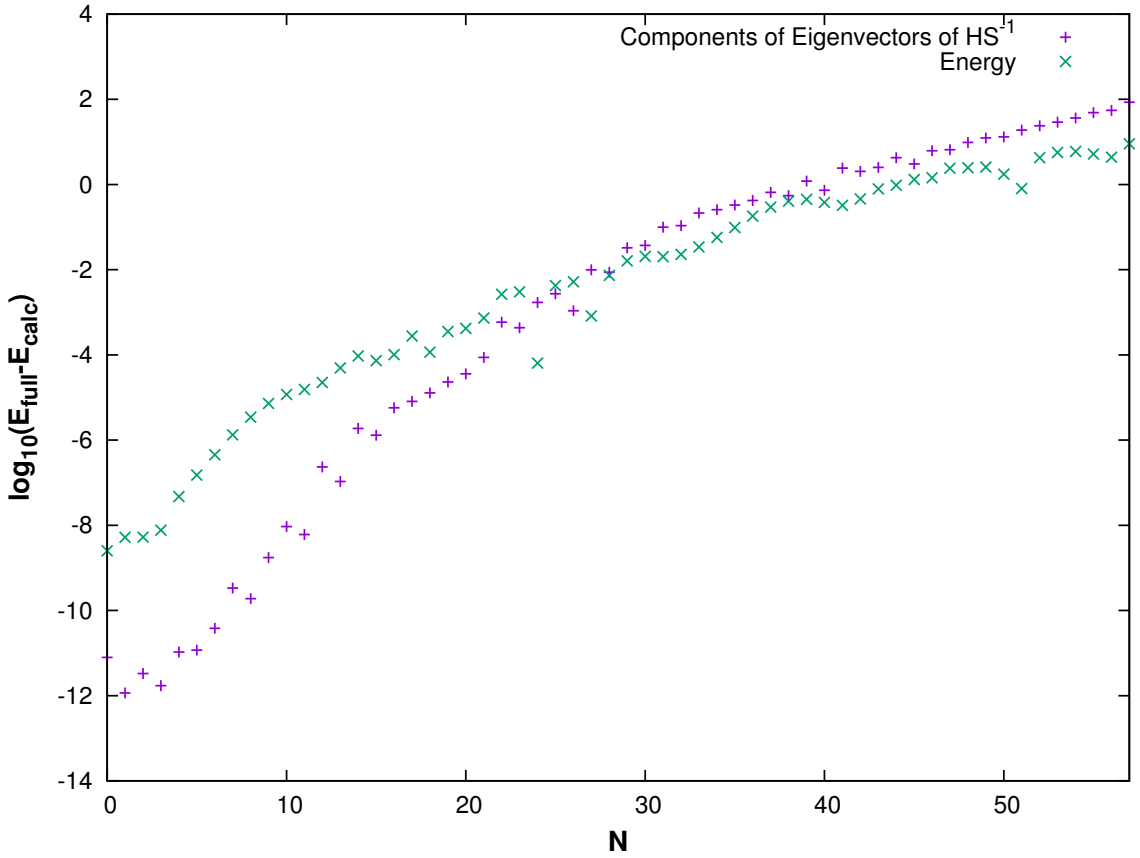

Figure 5.3: Comparison of the accuracy achieved by using a basis composed of the 56 functions whose classical energy is less than a threshold of 55, and a basis composed of the 56 functions for which components of eigenvectors of $\mathbf{HS^{-1}}$ are largest The latter basis is clearly better.

putting SG basis functions into $\mathcal{R}_{E_{thres}}$ works less well.

Clearly, it would be better to determine which PSL functions to include in the working basis by using elements of $\mathbf{B}$. There are several schemes for expanding a PSL basis so that it includes the important functions. [73, 2] The scheme we use in this chapter begins by identifying a small set of basis functions that are important and then adding new functions that are in some sense close to those deemed important. If $|B_{nm}|$ is tiny then removing the nth basis function will have almost no effect on the mth eigenvalue. [2] It is also true that

if $|B_{nm}|$ is large the nth basis function is important for calculating the mth eigenvalue. We, therefore, deem a basis function important if $c_n^{sum} = \sum_{m=1}^{10} |B_{nm}|$ is large. c_n^{sum} is the sum of the absolute values of the components of the 10 eigenvectors whose eigenvalues are smallest, for a given basis function n. If we retain the 56 basis functions with the largest values of c_n^{sum}, we obtain a working basis with which the first 25 eigenvalues are more accurate than those computed using the 56 functions that satisfy the $\mathcal{R}_{E_{thres}}$ criterion, see Figure 5.3. This establishes the advantage of using eigenvector components to determine which functions are included in the working basis to calculate the lowest energy eigenvalues. For typical spectroscopic problems, it is most important to calculate the lowest eigenvalues accurately. However, if one wishes to calculate a large number of eigenvalues to a fairly low accuracy level, a basis made with the $\mathcal{R}_{E_{thres}}$ criterion might be better.

For a real multi-dimensional problem, we want to build the working basis without knowing $\mathbf{B}$ and we therefore iteratively expand the basis by successively adding to the basis new functions, $d_{\mathbf{n}'}$, whose phase-space centres are close to those of functions $d_{\mathbf{n}}$ already in the basis and for which $c_{\mathbf{n}}^{sum}$ is large. For a multi-dimensional problem $\mathbf{n} = \{n_1, n_2, \cdots, n_D\}$. The strategy is based on the assumption that both wavefunctions and the basis functions are localized and smooth in phase space. To make the basis, we first create a starting basis and then add functions to it. Functions in the starting basis are those whose phase-space centres are in a region $\mathcal{R}_{E_{thres}}$ for a Hamiltonian that is the separable harmonic part of the full Hamiltonian and with a small E_{thres}. The classical energy that corresponds to a PSL function is a sum of positive terms, one for each of the $2D$ terms in the separable harmonic Hamiltonian. To build the starting basis one must, in principle, consider for possible inclusion all phase-space points in a huge direct product grid and for each of these points add up contributions from each of the $2D$ terms to obtain an energy, E_{sum}, and reject

those functions for which $E_{sum} > E_{thres}$. In practice, for a given point, there is no need to add contributions for all $2D$ terms because when $E_{sum} > E_{thres}$ there is no need to add contributions (all positive) from other terms. There is also no need to loop over all points on the huge direct product grid. Assume the top loops are over n_{x_1} and n_{p_1} and the bottom loops are over n_{x_D} and n_{p_D}. If, when considering for possible inclusion, the phase-space point $n_{x_1}, n_{p_1}, n_{x_2}, n_{p_2}, \cdots n_{x_D}, n_{p_D}$,after summing over terms for $c = 1, 2, 3 \quad$, $E_{sum} > E_{thres}$, then there is no need to execute the remaining loops, for $c = 4, 5, \cdots, D$. If nothing were done to avoid looping over all the points of the huge direct product basis and all the $2D$ terms, the cost of determining which PSL to include in the starting basis would scale exponentially with D. Halverson and Poirier[72] use a more sophisticated method, that defeats this exponential scaling, to define their final basis which is defined so that it contains all PSL functions with centres in $\mathcal{R}_{E_{thres}}$, for the full Hamiltonian. Determining only a starting basis is simpler.

To generate the basis we do a set of Arnoldi calculations with increasing basis sizes. The first Arnoldi calculation is done with the starting basis of the previous paragraph. $c_{\mathbf{n}}^{sum}$ values are calculated for each of the N_k functions in the starting basis. The $c_{\mathbf{n}}^{sum}$ are then sorted using the Quicksort algorithm. [104] We add to the basis neighbours of the PSL function with the largest $c_{\mathbf{n}}^{sum}$, then neighbours of the PSL function with the 2nd largest $c_{\mathbf{n}}^{sum}$, etc. When the size of the basis has been increased 5% we stop adding functions. For a given $\mathbf{n}$, corresponding to the phase space point (n_{x_c}, n_{p_c}), $c = 1, 2, ..., D$, the neighbours added are PSL functions with phase space points (n_{x_c}, n_{p_c}), which are 1) $n'_{x_c} = n_{x_c}$ and $n'_{p_c} = n'_{p_c} + 1$; 2) $n'_{x_c} = n_{x_c} - 1$ and $n'_{p_c} = 1$; 3) $n'_{x_c} = n_{x_c} + 1$ and $n_{p_c} = 1$. There are a total of $3D$ neighbours. The basis composed of the starting basis and the neighbours is the first expanded basis. It in turn is expanded to form the second expanded basis by doing another Arnoldi calculation and adding more neighbours. The process is repeated until we

deem energy levels converged. Each new basis is 5% larger than the previous basis. We maintain a list of functions in the basis with index m, and a list of $c_{\mathbf{n}}^{sum}$ values for functions in the basis for which we have not yet checked whether their neighbours should be included. The m corresponding to the largest $c_{\mathbf{n}}^{sum}$ values can be obtained from $\mathbf{n}$ using the mapping in the next section. Before adding a neighbour, we use the same mapping to determine whether it is already in the basis. The initial list of $c_{\mathbf{n}}^{sum}$ values includes all the functions in the starting basis. After adding neighbours for a particular basis function $\mathbf{n}$ to a basis, we remove that $c_{\mathbf{n}}^{sum}$ from the list of $c_{\mathbf{n}}^{sum}$ for not-yet-checked functions. $c_{\mathbf{n}}^{sum}$ is calculated only for functions in the not-yet-checked list. This saves computation time in later iterations due to the fact that many PSL functions have already had their phase-space neighbours added to the basis. It is perilous to determine whether an eigenvalue is converged by comparing values at different basis sizes because the plot of an eigenvalue as a function of basis size may have plateaus. One way to ensure that eigenvalues are converged is to add basis functions until the $c_{\mathbf{n}}^{sum}$ of all the basis functions are all less than a small cutoff value. When all $c_{\mathbf{n}}^{sum}$ in the not-yet-checked list are below the cutoff value, convergence is achieved. It might also be possible to use residuals to monitor convergence.

5.7 Computing a spectrum

Using the ideas of the previous sections, it is possible to sculpt a basis for a Hamiltonian. Unfortunately, even the basis that includes only the most important functions from a huge direct product basis is itself so large that most computers do not have enough memory to calculate eigenvalues of the basis representation of the Hamiltonian using methods of direct linear algebra. Phase-space basis methods that require inverting an overlap matrix for the retained PSL functions are similarly limited by the need to store and manipulate large

matrices. [73, 103] One option is to use massively parallel computers. [52, 102] Another is to use an iterative eigensolver. Iterative eigensolvers have been used to compute vibrational spectra for many years. [25, 15, 105, 106, 29, 107, 108, 109, 110] They have the obvious advantage that they obviate the need to store the Hamiltonian matrix. Nevertheless, they are only efficient if there is a good way of evaluating matrix-vector products. When the basis is a direct product, matrix-vector products can be efficiently evaluated by doing sums sequentially.[25, 29] To use this idea, there is no need to build a Hamiltonian matrix because matrices representing 1D factors are sequentially applied to vectors. These ideas cannot be used when the basis does not have product structure and a pruned basis built as explained in the previous section does not have product structure. Avila and Carrington have shown that, despite pruning, it is possible to efficiently evaluate matrix-vector products by doing sums sequentially, *if basis functions are retained by imposing a pruning condition that itself has structure.*[43, 19, 46] A basis chosen to include only the important PSL functions will, in general, not have exploitable structure. New ideas are therefore required to evaluate matrix-vector products, in order to make iterative eigensolvers useful.

The technique we use to evaluate matrix-vector products only works if the Hamiltonian is a SOP. Matrix-vector products are evaluated term by term and, for each term, factor by factor. We compute eigenvalues of $\mathbf{H_G S^{-1}}$ where $\mathbf{H_G} = \sum_\ell^{\mathbf{t}} \mathbf{H}_\ell$ and $\mathbf{S} = \mathbf{S_1} \otimes \mathbf{S_2} \otimes \cdots \mathbf{S_D}$. To explain the ideas we shall focus on a single term,

$$\mathbf{H}_\ell = \mathbf{H}_\mathbf{1}^\ell \otimes \mathbf{H}_\mathbf{2}^\ell \otimes \cdots \mathbf{H}_\mathbf{D}^\ell \ , \tag{5.16}$$

and therefore on $\mathbf{H}_\ell \mathbf{S^{-1}} = \mathbf{H}_\mathbf{1}^\ell \mathbf{S}_\mathbf{1}^{-\mathbf{1}} \otimes \mathbf{H}_\mathbf{2}^\ell \mathbf{S}_\mathbf{2}^{-\mathbf{1}} \otimes \cdots \otimes \mathbf{H}_\mathbf{D}^\ell \mathbf{S}_\mathbf{D}^{-\mathbf{1}} = {}^\mathbf{1}\mathbf{O}^\ell \otimes {}^\mathbf{2}\mathbf{O}^\ell \otimes \cdots \otimes {}^\mathbf{D}\mathbf{O}^\ell$. Note that many of the $\mathbf{H}_\mathbf{c}^\ell, c = 1, 2, \cdots D$ factors may be (1D) overlap matrices. If the PES is a Taylor Series then other $\mathbf{H}_\mathbf{c}^\ell$ are $\mathbf{x_c}^i, i = 1, 2, 3, 4$; others are $\mathbf{p_c}^2$ We shall drop the superscript

ℓ in the rest of this section. For one factor of one term, the matrix-vector product one must evaluate could be written

$$v_{n'_{x_1},n'_{p_1},...,n'_{x_c},n'_{p_c},..,n'_{p_D}} = \sum_{n_{p_c}=1}^{N_{p_c}} \sum_{n_{x_c}=1}^{N_{x_c}} {}^{\mathbf{c}}\mathbf{O}_{n'_c,n_c} z_{n'_{x_1},n'_{p_1},...,n'_{p_{c-1}},n_{x_c},n_{p_c},n'_{x_{c+1}},n'_{p_{c+1}},..,n'_{p_D}} \ , \tag{5.17}$$

where n_{x_c} and n_{p_c} are position and momentum labels for coordinate x_c, and n_c is a composite label that includes n_{x_c} and n_{p_c}. ${}^{\mathbf{c}}\mathbf{O}_{n'_c,n_c}$ depends on n_{x_c} and n_{p_c} and n'_{x_c} and n'_{p_c} because each 1D basis function has both position and momentum labels. The vectors are stored in a 1D array indexed by m and the matrix-vector product is

$$\begin{aligned} v(m'(n'_{x_1}, n'_{p_1}, ..., n'_{x_c}, n'_{p_c}, .., n'_{p_D})) = \\ \sum_{np_c=1}^{Np} \sum_{nx_c=1}^{Nx} {}^{\mathbf{c}}\mathbf{O}_{n'_c,n_c} z(m(n'_{x_1}, n'_{p_1}, .., n'_{p_{c-1}}, n_{x_c}, n_{p_c}, n'_{x_{c+1}}, .., n'_{p_D})) \ , \end{aligned} \tag{5.18}$$

The sums must be done for $m' = 1, 2, \cdots, N_k$. Knowing a value of m' one finds values of $n'_{x_1}, n'_{p_1}, ..., , n'_{x_c}, n'_{p_c}, ..., n'_{p_D}$ from a $N_k \times 2D$ table that is stored. The table is denoted A. Its m'th row contains the $2D$ $n'_{x_1}, n'_{p_1}, ..., n'_{x_c}, n'_{p_c}, ..., n'_{p_D}$ labels for the m'th basis function. Note that we are not, as is often the case when evaluating matrix-vector products in a pruned basis, transforming the input vector into the output vector, index by index sequentially, with $D + 1$ nested loops. When indices are transformed sequentially, the transformed and untransformed indices are separately constrained. In this case, the length of intermediate vectors increases and then decreases. [43, 84] Instead, for each factor, the vector on the LHS of Eq. (5.18) has only as many elements as there are retained basis functions. This is similar to the strategy of Ref. 111.

It remains to explain how knowing $n'_{x1}, n'_{p1}, ..., n'_{x_{c-1}}, n'_{p_{c-1}}, n_{x_c}, n_{p_c}, n'_{x_{c+1}}, n'_{p_{c+1}} ..., n'_{p_D}$ one

finds m, which labels the input vector. In principle this could be done by storing a D dimensional array with $(N_x N_p)^D$ elements, whose value is m, if the corresponding function is in the basis, and 0, if the corresponding function is not in the basis. Of course, this is impossible because the array is huge. It is also not necessary because many of the elements of the array would be zero. Instead, we use a recursive mapping. It is determined by making a list of retained $n_{x_1}, n_{p_1}, ..., , n_{x_c}, n_{p_c}, ..., n_{p_D}$ functions and labelling them with $m = 1, 2, \cdots N_k$. It works regardless of the order of the retained basis functions. The idea is illustrated by giving here an example with two coordinates and four indices $n_{x_1}, n_{p_1}, n_{x_2}, n_{p_2}$ which for simplicity will be written t_1, t_2, t_3, t_4. If there are four indices, we store four matrices, $\mathbf{T_1}, \mathbf{T_2}, \mathbf{T_3}, \mathbf{T_4}$ which are initialized as zero matrices. Non-zero elements of $\mathbf{T_1}, \mathbf{T_2}, \mathbf{T_3}, \mathbf{T_4}$ are determined as follows. The smallest value of m for which $t_1 = k_1$ (regardless of t_2, t_3, t_4) is denoted m_{k_1} and is stored in $T_1(1, k_1)$. The subscript on T indicates that it is for t_1. The smallest value of m for which $t_1 = k_1$ and $t_2 = k_2$ (regardless of t_3, t_4) is labelled as m_{k_1,k_2} and stored in $T_2(m_{k_1}, k_2)$. The smallest value of m for which $t_1 = k_1$, $t_2 = k_2$ and $t_3 = k_3$ (regardless of t_4) is labelled as m_{k_1,k_2,k_3} and stored in $T_3(m_{k_1,k_2}, k_3)$. The value of m for which $t_1 = k_1$, $t_2 = k_2$, $t_3 = k_3$, and $t_4 = k_4$ is labelled as m_{k_1,k_2,k_3,k_4} and is stored in $T_4(m_{k_1,k_2,k_3}, k_4)$. This mapping can be extended to many more dimensions by simply adding more $\mathbf{T_i}$ matrices.

The memory cost of this mapping is relatively low. Assuming that we use the same N_x and N_p for all coordinates, the $\mathbf{T}$ matrix for a coordinate index has $(N_k+1)N_x$ elements and the $\mathbf{T}$ matrix for a momentum index has $(N_k+1)N_p$ elements. Each $\mathbf{T}$ matrix has N_k+1 and not N_k rows because this reduces the number of if statements required. We add a zeroth row with elements $T_c\,(0, k_c)$=0. so that when $m_{k_1,...k_{c-1}} = T_{c-1}\left(m_{k_1,...k_{c-2}}, k_{c-1}\right) = 0$, i.e. the basis function with labels $k_1, ..., k_{c-1}, k_c$ is not in the retained basis, $T_c\left(m_{k_1,...k_{c-1}}, k_c\right) = T\,(0, k_c) = 0$ and does not need to be set to zero by using if statements. Only one if statement, after all

D T_c matrices have been used, is necessary to determine if a basis function is in the retained basis. Namely, if $m_{k_1,...,k_D} = 0$ then the basis function with indices $k_1, ...k_D$ is not in the retained basis. The total memory cost is therefore $(N_k + 1)D(N_x + N_p)$. If N_x and N_p were different for different coordinates, it would be $(N_k + 1)\sum_c (N_{x_c} + N_{p_c})$.

We actually do not sum over n_{x_c}, as indicated in Eq. (5.18). For a set of labels on the output vector, i.e., $n'_{x_1}, n'_{p_1}, ..., , n'_{x_c}, n'_{p_c}, , ..., n'_{p_D}$, which corresponds to m', we need to sum not over *all* n_{x_c} values, but only over all possible n_{x_c} values. This is done by using another mapping. The matrix-vector product is,

$$v(m'(n'_{x_1}, n'_{p_1}, ..., n'_{x_c}, n'_{p_c}, ..., n'_{p_D})) = \sum_{l_{x_c}=1}^{U_{x_c}(m')} \sum_{n_{p_c}=1}^{U_{p_c}(m'')} {}^{\mathbf{c}}\mathbf{O}_{n'_c,n_c} z(m(n'_{x_1}, n'_{p_1}, ..., n'_{p_{c-1}}, n_{x_c}, n_{p_c}, n'_{x_{c+1}}, ..., n'_{p_D})) \ , \tag{5.19}$$

The reason we sum over l_{x_c}, rather than n_{x_c}, is that basis functions with $2D-2$ indices $n'_{x_1}, n'_{p_1}, ..., n'_{p_{c-1}}, n'_{x_{c+1}}, ..., n'_{p_D}$ do not exist for some n_{x_c}. If we sum over l_{x_c}, we can sum over consecutive values. Due to the method used to add basis function neighbours in Section 5.6, there are no holes in the n_{p_c} index list and therefore no need for an l_{p_c} index. For any n_{x_c}; $n_{p_c} = 1$ is always added first; $n_{p_c} = 2$ is always added second; etc. To use Eq. (5.19) one must find n_{x_c} from l_{x_c}.

We make two matrices, $\mathbf{M_{x_c}}$ and $\mathbf{M_{p_c}}$, defined so that a row contains position indices of basis functions that have indices $n'_{x_1}, n'_{p_1}, ..., n'_{p_{c-1}}, n'_{x_{c+1}}, ..., n'_{p_D}$. From the position index stored in $\mathbf{M_{p_c}}$, we find n_{x_c} using Table *A*. In Eq. (5.19), $U_{x_c}(m')$, $m' = 1, \cdots, N_k$, is the number of different n_{x_c} values that occur in the basis, for particular values of $n'_{x_1}, n'_{p_1}, ..., n'_{p_{c-1}}, n'_{x_{c+1}}, ..., n'_{p_D}$, regardless of the value of n_{p_c}. The functions with the smallest n_{x_c} are labelled by $l_{x_c} = 1$; the functions with the second smallest n_{x_c} are labelled

Table 5.1: An example retained basis set table A_e of indices.

m	n_{x_1}	n_{p_1}	n_{x_2}	n_{p_2}
1	2	1	2	1
2	1	1	2	2
3	1	1	2	1
4	1	1	4	1
5	1	1	4	2
6	1	1	2	3

by $l_{x_c} = 2$; etc. $M_{x_c}(m', l_{x_c})$ is the position, denoted m'', in A of the basis function with l_{x_c}, $n_{p_c} = 1$ and $(n'_{x_1}, n'_{p_1}, ..., n'_{p_c-1}, n'_{x_{c+1}}, ..., n'_{p_D})$. m' labels the component of the output vector being computed. $n_{p_c} = 1$ is used because the basis function with $n_{p_c} = 1$ is always retained. $M_{x_c}(m', l_{x_c})$ is stored as a $N_k \times N_{x_c}$ matrix. $U_{p_c}(m'')$ is the number of n_{p_c} values for a given set of $2D-1$ indices, $(n'_{x_1}, n'_{p_1}, ..., n'_{p_c-1}, n_{x_c}, n'_{x_{c+1}}, ..., n'_{p_D})$. $U_{p_c}(m'')$ is a vector of length N_k. $\mathbf{M_{p_c}}$ is stored as a $N_k \times N_{p_c}$ matrix and $M_{p_c}(m'', n_{p_c}) = p$ is the position in A of the basis function with l_{x_c}, n_{p_c} and $(n'_{x_1}, n'_{p_1}, ..., n'_{p_c-1}, n'_{p_{c+1}}, ..., n'_{p_D})$. From the position, n_{x_c} can be obtained from the mth row of table A.

An example should make this easier to follow. A 2D problem with 6 basis functions has the $A = A_e$ table shown in Table 5.1. If $c = 2$, so that the sum is over l_{x_2} and p_{x_2}, and we are computing the component $m' = 6$ with indices $(n_{x_1}, n_{p_1}, n_{x_2}, n_{p_2}) = (1, 1, 2, 3)$, then $U_{x_2}(6) = 2$ and the two possible n_{x_2} values are $2, 4$ ($n_{x_1} = n_{p_1} = 1$). $l_{x_2} = 1$ corresponds to $n_{x_2} = 2$ and $l_{x_2} = 2$ corresponds to $n_{x_2} = 4$. With $l_{x_2} = 1$ (or $n_{x_2} = 2$) and $n_{p_2} = 1$, the position in A_e is 3 so $m'' = M_{x_2}(6, 1) = 3$. This is the basis function with indices $(1, 1, 2, 1)$. $U_{p_2}(3) = 3$ because there are three possible n_{p_2} values: $1, 2, 3$. The rightmost sum in Eq. (5.19) is therefore over $n_{p_2} = 1, 2, 3$. The corresponding m positions in z contributing to the sum are $M_{p_2}(3, 1) = 3, M_{p_2}(3, 2) = 2, M_{p_2}(3, 3) = 6$. With $l_{x_2} = 2$ ($n_{x_2} = 4$), $M_{x_2}(6, 2) = 4$, and $U_{p_2}(4) = 2$ because there are two possible values of n_{p_2} (they are 1 and 2). The m values to be summed are therefore $M_{p_2}(4, 1) = 4, M_{x_2}(4, 2) = 5$. Note that

the double sum corresponds to adding contributions from m in the order $3, 2, 6, 4, 5$. As is necessary, position $m = 1$ of z does not contribute.

5.8 Test calculations: P_2O, CH_2O, CH_2NH

We use the ideas of sections 5.4, 5.5 , 5.6, and 5.7 to compute vibrational energy levels of three realistic (but SOP) Hamiltonians: a P_2O Hamiltonian (with the PES of Pouchan *et al*[112]), a CH_2O Hamiltonian (using a refitted potential based on Ref. 113), and a CH_2NH Hamiltonian (using the potential of Pouchan and Zaki[114], as interpreted in Ref. 102). These calculations enable us to test the efficiency of the method. Testing with molecules having three, four, and five atoms, we shall show how the method scales in practice, when spectroscopic accuracy is required.

We present only results with the SG PSL basis of Halverson and Poirier (HP). Although we use the same SG basis as HP, our calculations differ from theirs. 1) We compute eigenvalues of the product $\mathbf{H_G S^{-1}}$; the number of columns of $\mathbf{H_G}$ (and the number of rows of $\mathbf{S^{-1}}$) is larger than the number of rows of $\mathbf{H_G}$ (and the number of columns of $\mathbf{S^{-1}}$). 2) We use a different approach to selecting SG PSL functions to retain. 3) To make it possible to retain a huge number of SG PSL functions, we use an iterative eigensolver. We do not report results obtained with a Gaussian basis. The SG results are systematically better because the SG functions have phase-space boxes that are smaller, with size (in 1D) $h/2$, than the Gaussian phase space boxes which (in 1D) have size h. As explained by HP, smaller phase space boxes enables one to cover the important region of phase space with less waste. All matrix elements are calculated exactly. The SG basis could also be used to contract a direct product DVR, as was done previously with a Gaussian basis. [53, 1, 2, 53, 73] Using the DVR obviates the need to use a SOP PES, but for a SOP PES there is no reason not to use

the SG basis directly. With a Gaussian basis, it is better to use it to contract a DVR because without a DVR the number of columns of $\mathbf{H_G}$ (and the number of rows of $\mathbf{S^{-1}}$) required to get converged eigenvalues is huge.

5.8.1 Choosing the 1D basis sets

We need to specify exterior and interior 1D bases, i.e. choose f^i and f^e (see Eq. (5.3)). There are $\mathcal{N}_e$ 1D exterior basis functions; $\mathcal{N}_e = \mathcal{N}_x^e \mathcal{N}_p^e$, where $\mathcal{N}_x^e$ is the number of exterior position labels and $\mathcal{N}_p^e$ is the number of exterior momentum labels. There are $\mathcal{N}_i$ 1D interior basis functions; $\mathcal{N}_i = \mathcal{N}_x^i N_p^i$, where $\mathcal{N}_x^i$ is the number of interior position labels and $\mathcal{N}_p^i$ is the number of interior momentum labels. Products of the 1D basis functions are the multi-dimensional basis functions. $\mathcal{N}_e^D$ is the number of rows of $\mathbf{H_G}$ (and columns of $\mathbf{S^{-1}}$) in Eq. (5.5). $\mathcal{N}_i^D$ is the number of columns of $\mathbf{H_G}$ (and rows of $\mathbf{S^{-1}}$ in Eq. (5.5). We choose a large $\mathcal{N}_i$. This does not significantly increase the cost of the calculation because $\mathbf{H_G}$ is a sum of direct products and $\mathbf{S}$ is also a direct product. The size of $\mathbf{S^{-1}}$ is $\mathcal{N}_i^D \times \mathcal{N}_i^D$, but we only invert $\mathcal{N}_i \times \mathcal{N}_i$ matrices. To ensure accurate levels we take $\mathcal{N}_x^i = 40, \mathcal{N}_p^i = 20$ which corresponds to a grid of points at $(\sqrt{\pi}(n_x - 20) - \sqrt{\pi}/2, \sqrt{\pi}(n_p - 1) + \sqrt{\pi}/2)$ where $n_x = 1, \cdots, 40, n_p = 1, \cdots, 20$. This may be larger than necessary. We choose $\mathcal{N}_x^e = 12$ and $\mathcal{N}_p^e = 6$. This corresponds to grid points at $(\sqrt{\pi}(n_x - 6) - \sqrt{\pi}/2, \sqrt{\pi}(n_p - 1) + \sqrt{\pi}/2)$ where $n_x = 1, \ldots, 12, n_p = 1, \cdots, 6$. These values are chosen because $\mathcal{N}_i = 12, \mathcal{N}_j = 6$ is the smallest direct product (in phase-space) basis with which one can calculate the lowest 6 energy levels of the Harmonic oscillator to machine precision. With this 1D basis, we are certain that it is possible to calculate accurate levels of the multi-dimensional Hamiltonians, if enough multi-dimensional basis functions are retained. We choose $\mathcal{N}_e < \mathcal{N}_i$ because decreasing $\mathcal{N}_e$ reduces the size of the M and T mappings and decreases the size of all the

$^{\mathbf{c}}\mathbf{O}$ matrices. The maximum indices N_{x_c}, N_{p_c} are equal for all c in our calculations, and $N_{x_c} = \mathcal{N}_x^e = 12$ and $N_{p_c} = \mathcal{N}_x^e = 6$.

Before launching the iterative eigensolver we compute a set of 72×800 matrices. The same 1D basis is used for all coordinates and we therefore only need to compute matrices for $x_1, x_1^2, x_1^3, x_1^4, -\frac{\partial^2}{\partial x_1^2}$. We also need a 800×72 matrix $\mathbf{S_1^{-1}}$ (the same for all coordinates). It is obtained from elements of the inverse of the 800×800 matrix $\mathbf{S_1}$.

5.8.2 Results

ARPACK with the reverse communication driver dnaupd is used to perform all calculations. The number of columns (NCV) is taken to be three times the size of the number of eigenvalues (NEV) calculated, for each molecule studied. The default stopping criteria of machine precision is used for the calculations.[33] Although RULE [115] could also be used, ARPACK is more robust.

Levels of P_2O are reported in columns 4 and 5 of Table 5.2. The levels published by HP (columns 2 and 3) are about as accurate as those we compute with both having an error of less than 0.1cm^{-1}. [102] However, we attain similar accuracy with a PSL basis whose size is two orders of magnitude smaller. Our basis is much smaller because we do not chop the $\mathbf{S}$ and $\mathbf{H_G}$ matrices separately (we use Eq. (5.5) and Eq. (5.7)) and because we use a different procedure for determining which basis functions to retain. It is our basis function selection method (section 5.6) that is the most important. Using our basis selection method, but chopping $\mathbf{S}$ and $\mathbf{H_G}$ separately (i.e. Eq. (5.4)), rather than using Eq. (5.5) increases the size of the SG basis required to obtain levels within 0.1cm^{-1} of numerically exact levels, by more than a factor of two. The eigenvalues of Eq. (5.7) are close to those of Eq. (5.4) because the eigenvalues of Eq. (5.7) are close to those of Eq. (5.8) (see section 5.6) and the eigenvalues of

Eq. (5.4)) are equal to those of Eq. (5.8). The advantage of Eq. (5.5) is therefore significant, but much less important than the advantage of the new basis function selection procedure.

Although with Eq. (5.7) one requires requires a larger basis to achieve the same accuracy (compare columns 4 and 5), Eq. (5.7) has the significant advantage that it is a symmetric eigenproblem and therefore the Lanczos algorithm can be applied. Owing to the fact that the memory cost of the Lanczos algorithm is much less (only two vectors of length N_k must be stored) than that of ARPACK (which requires many vectors), Eq. (5.7) could be used with a much larger basis. When using Lanczos, the c_m^{sum} values would be calculated from eigenvectors computed by doing a second set of Lanczos iterations, [65, 116] with no additional memory requirements. Implemented in this fashion, the memory cost is dominated by the mappings. There would also be additional computation required to force the Hamiltonian matrix to be Hermitian.[111]

It is encouraging that it is possible to significantly decrease the size of the SG basis. However, even our SG basis is much larger than the HOB basis built using Eq. (5.2) with $N = 17$, which is good enough to converge all the levels in the table to three decimal places, It is surely possible to reduce the size of the HOB further by using a better pruning condition. $\sum_c g_c(x_c) \leq N$ with carefully chosen $g_c(x_c)$ would be much better. Even $\alpha_1 n_1 + \alpha_2 n_2 + \alpha_3 n_3$ with $\alpha_c \neq 1$ would be better. Even with $n_1 + n_2 + n_3 \leq N$, the HOB is about an order of magnitude smaller than our best SG basis (and three orders of magnitude smaller than the HP SG basis).

Of course, it is important to test Eq. (5.5) on a problem with a larger D. We therefore also did calculations on CH_2O. This enables us to examine how the cost of the method scales with basis size. We first did calculations on the PES of Romanowski et al.[117] Although the Romanowski PES is usable with a pruned harmonic oscillator basis, it has holes (i.e.

Table 5.2: The lowest 26 vibrational levels (with respect to the zero point energy) of P_2O.

State	Ref. 102		Eq. (5.5)	Eq. (5.7)	HOB
Basis size	201414	405521	4995	11033	1140
v_1	197.481	197.474	197.479	197.481	197.479
$2v_1$	395.464	395.452	395.461	395.465	395.463
$3v_1$	593.930	593.914	593.928	593.935	593.929
v_2	643.912	643.968	643.900	643.900	643.897
$4v_1$	792.858	792.838	792.858	792.867	792.858
$v_1 + v_2$	839.844	839.893	839.827	839.832	839.826
$5v_1$	992.228	992.205	992.227	992.241	992.228
$2v_1 + v_2$	1036.272	1036.316	1036.251	1036.261	1036.252
$6v1$	1192.018	1191.991	1192.022	1192.037	1192.018
$3v_1 + v_2$	1233.174	1233.213	1233.158	1233.170	1233.154
v_3	1265.393	1265.411	1265.308	1265.308	1265.295
$2v_2$	1290.641	1290.537	1290.610	1290.623	1290.599
$7v_1$	1392.207	1392.176	1392.221	1392.236	1392.206
$4v_1 + v_2$	1430.530	1430.563	1430.515	1430.529	1430.509
$v_1 + v_3$	1460.187	1460.196	1460.092	1460.100	1460.082
$v_1 + 2v_2$	1485.176	1485.071	1485.141	1485.170	1485.134
$8v_1$	1592.771	1592.738	1592.787	1592.813	1592.770
$5v_1 + v_2$	1628.317	1628.344	1628.296	1628.319	1628.294
$2v_1 + v_3$	1655.502	1655.507	1655.402	1655.419	1655.396
$2v_1 + 2v_2$	1680.214	1680.110	1680.180	1680.220	1680.172
$9v_1$	1793.689	1793.652	1793.704	1793.745	1793.687
$6v_1 + v_2$	1826.512	1826.532	1826.507	1826.524	1826.488
$3v_1 + v_3$	1851.319	1851.321	1851.237	1851.249	1851.213
$3v_1 + 2v_2$	1875.735	1875.631	1875.719	1875.769	1875.692
$v_2 + v_3$	1897.546	1897.512	1897.449	1897.447	1897.421
$3v_2$	1936.341	1936.288	1936.284	1936.299	1936.260

spurious minima) that make it impossible to converge energy levels using SG functions. Instead, we used a PES obtained from the PES of Ref. 113 by calculating derivatives with respect to normal coordinates to make a Taylor series approximation. [118] Many energy levels converged with the Taylor series PES. The lowest thirty energy levels, computed with the same methods as for P_2O, are shown in Table 5.3. These levels are low enough that they are probably not shifted by holes in the PES. For CH_2O, the HOB, pruned with $n_1 + n_2 + n_3 + n_4 + n_5 + n_6 \leq 15$, which is large enough to converge all the energies in the table to the number of digits shown, is about 14 times smaller than the best SG basis. To some extent the size of the SG basis is inflated by the holes still present in the re-fitted PES. This is due to the fact that our basis function selection algorithm has a propensity to add SG functions in holes. However, even if these SG functions are removed from the basis, the SG basis is still about an order of magnitude larger than the HOB basis.

To further test Eq. (5.5) and assess the utility of PSL bases, we have also computed energy levels of CH_2NH, for which $D = 9$. In this case, a direct product harmonic basis is large enough that the memory cost of a simple direct product Lanczos calculation is prohibitive. It is for such problems that one needs new ideas. We use the potential of Ref. 114, as interpreted by HP in Ref. 102. The sums over indices are constrained and there are factorial terms in front of the sums. [102]. In Ref. 102, HP use their SG basis to compute vibrational levels. Our results are summarized in Table 5.4. We see no evidence that our basis functions are sampling holes. To converge the first 10 levels to within about 1 cm^{-1} we require about 26×10^6 SG functions. It is impossible to compare our results with those of HP for two reasons: 1) their convergence errors are much larger than 1 cm^{-1}; 2) two of the their force constants are not the values reported in the table of Ref. 114.[119] Energy levels computed with the largest basis in Ref. 102 are reported in column 4. These energies were generously

Table 5.3: The lowest 30 calculated vibrational energies of CH_2O. Levels computed with Eq. (5.5) are compared to those computed with a pruned harmonic basis.

State	Eq. (5.5)	HOB
Basis size	713883	54264
1	5781.022	5781.019
2	6937.357	6937.344
3	7030.013	7030.001
4	7283.862	7283.837
5	7530.419	7530.383
6	8088.318	8088.248
7	8196.896	8196.848
8	8274.013	8273.950
9	8437.703	8437.642
10	8503.379	8503.319
11	8569.769	8569.707
12	8617.996	8617.937
13	8677.273	8677.166
14	8781.941	8781.841
15	8784.038	8783.958
16	9025.296	9025.137
17	9226.167	9225.849
18	9262.918	9262.840
19	9355.044	9354.847
20	9448.225	9448.042
21	9507.199	9506.904
22	9583.644	9583.429
23	9637.372	9637.242
24	9696.828	9696.623
25	9701.028	9700.894
26	9744.542	9744.372
27	9791.924	9791.786
28	9817.159	9816.758
29	9854.375	9854.175
30	9934.984	9934.785

provided by the authors. Our best SG basis, with which one *can* compute accurate levels, is more than two orders of magnitude larger than the very simple HOB basis built from the pruning condition $\sum_c n_c \leq N$. Much better HOB bases could be devised. It appears that if one wishes accurate levels, the SG basis, which is the best known PSL basis, is not competitive for molecules like CH_2NH and CH_2O.

It might be true, that if one were satisfied with less accurate levels and needed more of them that the SG basis would be competitive. However, the levels reported in Ref. 102 have large convergence errors. The two largest bases used by HP have 212197 and 409581 functions. It is dangerous to assume that the difference between energies computed with two SG bases is a good measure of convergence error. [52, 102, 72] One might conclude from Table IV of Ref. 102, that the convergence error of the first $frequency$ (i.e. difference between the first level and the zpe(zero point energy)) is about 5 cm^{-1}. Reported energy level differences for the first 10 frequencies are all less than about 43 cm^{-1}. According to Table V of Ref. 102, there are 11 states for which the difference between levels computed with the two largest HP bases is less than 1 cm^{-1}. HP underestimate their convergence error. With 409'581 functions their lowest frequency is 1212.581 cm^{-1}. The converged value (on their PES) is 1105.56cm^{-1}, see column 5 of Table 5.4. Therefore, the true error is not about 5 but about 100cm^{-1}. Errors in the first 10 levels (not frequencies) are about 1000cm^{-1}; see Table 5.4. HP's ZPE is 1105 cm^{-1} larger than the harmonic ZPE. It seems that it is misleading to assess convergence by comparing two SG bases whose size differs by only a factor of 2.

Table 5.4: The lowest 10 vibrational energies of CH_2NH, computed with an SG basis and Eq. (5.5) compared to those computed with a pruned harmonic basis. Energies in columns two and three are computed from the PES obtained by using the force constants of Ref. 114 and constraining the sums in the Taylor Series (see Ref. 102). Energies in the fifth column are those obtained using PES of HP.

State	Eq. (5.5)	HOB	Ref. 102	HOB
Force constants	Pouchan et. al values		HP values	
Basis size	$26,366,233$	$48,620$	$409,581$	$48,620$
1	8852.295	8852.071	9983.564	8851.921
2	9958.153	9957.626	11196.144	9957.479
3	9968.981	9968.488	11205.075	9984.451
4	10054.049	10053.418	11261.246	10036.156
5	10250.342	10249.690	11485.806	10249.544
6	10347.336	10346.757	11537.412	10346.601
7	10522.775	10522.042	11873.982	10521.900
8	11075.542	11074.420	12418.345	11077.042
9	11078.118	11077.183	12475.341	11090.375
10	11100.351	11099.336	12482.965	11142.427

5.9 Conclusion

We have shown that it is possible to use an iterative eigensolver in conjunction with Halverson and Poirier's symmetrized Gaussian basis to compute accurate vibrational energy levels of molecules with as many as five atoms, without using massive parallelization and storing and manipulating huge matrices. This is done by solving a regular (rather than a generalized) eigenvalue problem. The regular eigenvalue problem has several advantages. First, the direct product structure of a basis, with size F, of products of 1D SG functions is exploited to exactly compute elements of the associated $F \times F$ matrix $\mathbf{S^{-1}}$. Other methods require manipulating $\mathbf{C^T S C}$, which is more costly because it has no structure.[73, 52, 72, 103] Second, if the Hamiltonian is a sum of products, the fact that $\mathbf{H_G}$ is a sum of direct products makes it possible to use iterative eigensolvers to solve the Schrödinger equation. This obviates the need to store and compute with $\mathbf{C^T S C}$ and $\mathbf{C^T H_G C}$. Although the size of $\mathbf{C^T S C}$

and $\mathbf{C^T H_G C}$ is *much* smaller than F, for a challenging problem it will also be large. Third, solutions of the regular eigenvalue problem are more accurate than solutions of the generalized eigenvalue problem of the same size. These ideas are made much more powerful by combining them with a new procedure for selecting which basis functions to retain. We do this with a basis building method that uses elements of the eigenvectors of $\mathbf{C^T H_G S^{-1} C}$ to identify basis functions whose neighbours are incorporated into the basis. The resulting basis is orders of magnitude smaller than the basis made by using the classical energy criterion. Nonetheless, the success of this chapter is built on the ingenious SG functions of HP.

Although the improvements suggested in this chapter make it possible to use phase-space localized functions to solve a 9D Schrödinger equation, it seems that PSL functions offer no advantages, if one wishes to compute low-lying vibrational energy levels of a molecule whose PES has a single minimum. Simple and naive bases made by pruning direct product harmonic bases make it possible to calculate the lowest energy levels with orders of magnitude fewer basis functions. Bases of this type also have the advantage that it is possible to use them in conjunction with nondirect product quadratures to compute levels when the Hamiltonian is not a SOP. It might be possible that PSL are advantageous when one wishes a very large number of vibrational levels. However, we have demonstrated that one must be careful about assessing convergence errors. PSL functions, and particularly HP's SG basis might be useful for molecules whose PESs have several wells. For such molecules it is hard or impossible to find good zeroth order models that can be used to choose basis functions. The PSL function idea has the advantage that it should work equally well for single-well and multi-well PESs. PSL methods may therefore have a competitive advantage for non-SOP Hamiltonians. However, to apply PSL methods to a Hamiltonian that is not a SOP new ideas are required to obviate the need to store the potential on a direct product grid.

Chapter 6

Summary and Conclusions

6.1 Summary

This thesis has made progress in the use of PSL basis functions on multiple fronts. It was first shown that these basis functions can be used to contract other DVR basis functions which are more useful in general polar coordinates. We then made progress in the theoretical understanding of why the original vN functions of Davis and Heller failed to converge. This was due to the necessity of projecting on to a grid (most conveniently a DVR) and inverting the resulting overlap matrix before pruning basis functions. Using a grid removed the issue of needing an huge number of basis functions to obtain a pruneable basis.

Progress has also been made in the dimensionality of the systems one could study using PSL functions. This was done by converting the symmetric generalized eigenproblem into an non-generalized asymmetric eigenproblem. This reformulation permitted the use of iterative methods and accurate results could be obtained for a 9D system. Redefining how the DD matrix elements were calculated also allowed more accurate results to be obtained. A final improvement was to choose basis functions iteratively from progressively larger calculations

as outlined in manuscript 3. This allowed the calculation of accurate eigenvalues with two orders of magnitude fewer basis functions than had previously been possible using a classical energy criterium.

6.2 Future Work

Manuscript 3 has clearly shown that PSL functions are not competitive for calculating accurate vibrational energies of single well problems. It is certainly possible that PSL functions will be of benefit to the studies of multi-well systems. It is not generally possible to have potentials for multi-well systems in the sum-of-products form assumed in this paper. Therefore, it is necessary to develop methods to calculate spectra using a general potential. This can possibly be done using collocation, or by utilizing the localized nature of the basis functions to use fewer quadrature points. For the latter, a method to perform matrix-vector products will need to be developed.

In a broader sense, it is clear that there is now a path to using any set of non-orthogonal basis functions assuming a well-conditioned overlap matrix can be formed. One simply has to project the basis onto a grid. Also, the basis expansion method can be applied to other types of basis functions assuming an order of importance can be imposed *a priori*. This has been tested on harmonic oscillator basis functions with some success.

Bibliography

[1] James Brown and Tucker Carrington. Comment on "Phase-Space Approach to Solving the Time-Independent Schrödinger Equation". *Phys. Rev. Lett.*, 114:058901, Feb 2015.

[2] James Brown and Tucker Carrington. Using an iterative eigensolver to compute vibrational energies with phase-spaced localized basis functions. *The Journal of Chemical Physics*, 143(4):–, 2015.

[3] James Brown and Tucker Carrington. Assessing the utility of phase-space-localized basis functions: Exploiting direct product structure and a new basis function selection procedure. *The Journal of Chemical Physics*, 144(24), 2016.

[4] Attila G. Csaszar, Csaba Fabri, Tamas Szidarovszky, Edit Matyus, Tibor Furtenbacher, and Gabor Czako. The fourth age of quantum chemistry: molecules in motion. *Phys. Chem. Chem. Phys.*, 14:1085–1106, 2012.

[5] M. Born and R. Oppenheimer. Zur Quantentheorie der Molekeln. *Annalen der Physik*, 389(20):457–484, 1927.

[6] J. N. Murrell, S. Carter, S. C. Farantos, P. Huxley, and A. J. C. Varandas. *Molecular Potential Energy Surfaces*. Wiley, New York, 1984.

[7] Graham Richards. Third Age of quantum chemistry. *Nature*, 278(5704):507, 1979.

[8] Henry F. Schaefer. Methylene: A Paradigm for Computational Quantum Chemistry. *Science*, 231(4742):1100–1107, 1986.

[9] Gabor Czako, Alexey L. Kaledin, and Joel M. Bowman. A practical method to avoid zero-point leak in molecular dynamics calculations: Application to the water dimer. *The Journal of Chemical Physics*, 132(16):164103, 2010.

[10] R.P. Bell. *The Tunnel Effect in Chemistry*. Chapman and Hall, London, 1980.

[11] David M. Dennison and G. E. Uhlenbeck. The Two-Minima Problem and the Ammonia Molecule. *Phys. Rev.*, 41:313–321, Aug 1932.

[12] Boris Podolsky. Quantum-Mechanically Correct Form of Hamiltonian Function for Conservative Systems. *Phys. Rev.*, 32:812–816, Nov 1928.

[13] James K.G. Watson. Simplification of the molecular vibration-rotation Hamiltonian. *Molecular Physics*, 15(5):479–490, 1968.

[14] Carl Eckart. Some Studies Concerning Rotating Axes and Polyatomic Molecules. *Phys. Rev.*, 47:552–558, Apr 1935.

[15] Joel M Bowman, Tucker Carrington, Jr., and Hans-Dieter Meyer. Variational quantum approaches for computing vibrational energies of polyatomic molecules. *Molecular Physics*, 106(16-18):2145–2182, 2008.

[16] Stuart Carter, Susan J. Culik, and Joel M. Bowman. Vibrational self-consistent field method for many-mode systems: A new approach and application to the vibrations of CO adsorbed on Cu(100). *The Journal of Chemical Physics*, 107(24):10458–10469, 1997.

[17] Stuart Carter, Joel M. Bowman, and Nicholas C. Handy. Extensions and tests of multimode: a code to obtain accurate vibration/rotation energies of many-mode molecules. *Theoretical Chemistry Accounts: Theory, Computation, and Modeling (Theoretica Chimica Acta)*, 100:191–198, 1998.

[18] Edit Matyus, Gabor Czako, Brian T. Sutcliffe, and Attila G. Csaszar. Vibrational energy levels with arbitrary potentials using the Eckart-Watson Hamiltonians and the discrete variable representation. *The Journal of Chemical Physics*, 127(8):084102, 2007.

[19] Gustavo Avila and Tucker Carrington, Jr. Using nonproduct quadrature grids to solve the vibrational Schrödinger equation in 12D. *The Journal of Chemical Physics*, 134(5):054126, 2011.

[20] Stuart Carter and Joel M. Bowman. The adiabatic rotation approximation for rovibrational energies of many-mode systems: Description and tests of the method. *The Journal of Chemical Physics*, 108(11):4397–4404, 1998.

[21] Celine Leonard, Nicholas C Handy, Stuart Carter, and Joel M Bowman. The vibrational levels of ammonia. *Spectrochimica Acta Part A: Molecular and Biomolecular Spectroscopy*, 58(4):825 – 838, 2002.

[22] Xiao-Gang Wang and Tucker Carrington, Jr. A simple method for deriving kinetic energy operators. *The Journal of Chemical Physics*, 113(17):7097–7101, 2000.

[23] Weitao Yang and Andrew C. Peet. The collocation method for bound solutions of the Schrödinger equation. *Chemical Physics Letters*, 153(1):98 – 104, 1988.

[24] Sergei Manzhos, Koichi Yamashita, and Tucker Carrington Jr. On the advantages of a

rectangular matrix collocation equation for computing vibrational spectra from small basis sets. *Chemical Physics Letters*, 511(46):434 – 439, 2011.

[25] John C. Light and Tucker Carrington, Jr. *Discrete-Variable Representations and their Utilization*, pages 263–310. John Wiley & Sons, Inc., 2000.

[26] Hua Wei and Tucker Carrington, Jr. The discrete variable representation of a triatomic Hamiltonian in bond length–bond angle coordinates. *The Journal of Chemical Physics*, 97(5):3029–3037, 1992.

[27] Julin Echave and David C. Clary. Potential optimized discrete variable representation. *Chemical Physics Letters*, 190(34):225 – 230, 1992.

[28] U. Manthe and H. Koppel. New method for calculating wave packet dynamics: Strongly coupled surfaces and the adiabatic basis. *The Journal of Chemical Physics*, 93(1):345–356, 1990.

[29] Matthew J. Bramley and Tucker Carrington, Jr. A general discrete variable method to calculate vibrational energy levels of three- and four-atom molecules. *The Journal of Chemical Physics*, 99(11):8519–8541, 1993.

[30] Matthew J. Bramley, John W. Tromp, Tucker Carrington, Jr., and Gregory C. Corey. Efficient calculation of highly excited vibrational energy levels of floppy molecules: The band origins of H_3^+ up to 35 000 cm^{-1}. *The Journal of Chemical Physics*, 100(9):6175–6194, 1994.

[31] Daniel A. Jelski, Randall H. Haley, and Joel M. Bowman. New vibrational self-consistent field program for large molecules. *Journal of Computational Chemistry*, 17(14):1645–1652, 1996.

[32] Cornelius Lanczos. An Iteration Method for the Solution of the Eigenvalue Problem of Linear Differential and Integral Operators. *Journal of Research of the National Bureau of Standards*, 45(4), 1950.

[33] R. B. Lehoucq, D. C. Sorensen, and C. Yang. *ARPACK Users Guide: Solution of Large-Scale Eigenvalue Problems with Implicitly Restarted Arnoldi Methods*. SIAM, Philadelphia, 1998.

[34] Z Bacic and JC Light. Theoretical methods for rovibrational states of floppy molecules. *Annual Review Of Physical Chemistry*, 40:469–498, 1989.

[35] S. Carter and N.C. Handy. A variational method for the determination of the vibrational (J = 0) energy levels of acetylene, using a Hamiltonian in internal coordinates . *Computer Physics Communications*, 51(12):49 – 58, 1988.

[36] James R. Henderson and Jonathan Tennyson. All the vibrational bound states of H_3^+. *Chemical Physics Letters*, 173(2):133 – 138, 1990.

[37] Xiao-Gang Wang and Tucker Carrington. New ideas for using contracted basis functions with a lanczos eigensolver for computing vibrational spectra of molecules with four or more atoms. *The Journal of Chemical Physics*, 117(15):6923–6934, 2002.

[38] Hua-Gen Yu. Two-layer Lanczos iteration approach to molecular spectroscopic calculation. *The Journal of Chemical Physics*, 117(18):8190–8196, 2002.

[39] S. Carter and N.C. Handy. The variational method for the calculation of RO-vibrational energy levels . *Computer Physics Reports*, 5(3):117 – 171, 1986.

[40] Bill Poirier. Using wavelets to extend quantum dynamics calculations to ten or more

degrees of freedom. *Journal of Theoretical and Computational Chemistry*, 02(01):65–72, 2003.

[41] Richard Dawes and Tucker Carrington. How to choose one-dimensional basis functions so that a very efficient multidimensional basis may be extracted from a direct product of the one-dimensional functions: Energy levels of coupled systems with as many as 16 coordinates. *The Journal of Chemical Physics*, 122(13):–, 2005.

[42] Richard Dawes and Tucker Carrington. Using simultaneous diagonalization and trace minimization to make an efficient and simple multidimensional basis for solving the vibrational Schrödinger equation. *The Journal of Chemical Physics*, 124(5):–, 2006.

[43] Gustavo Avila and Tucker Carrington. Nonproduct quadrature grids for solving the vibrational Schrödinger equation. *The Journal of Chemical Physics*, 131(17), 2009.

[44] David Lauvergnat and Andre Nauts. Torsional energy levels of nitric acid in reduced and full dimensionality with ElVibRot and Tnum. *Phys. Chem. Chem. Phys.*, 12:8405–8412, 2010.

[45] Gustavo Avila and Tucker Carrington. Using a pruned basis, a non-product quadrature grid, and the exact Watson normal-coordinate kinetic energy operator to solve the vibrational Schrödinger equation for C_2H_4. *The Journal of Chemical Physics*, 135(6), 2011.

[46] Gustavo Avila and Tucker Carrington. A multi-dimensional Smolyak collocation method in curvilinear coordinates for computing vibrational spectra. *The Journal of Chemical Physics*, 143(21), 2015.

[47] I. P. Hamilton and J. C. Light. On distributed Gaussian bases for simple model multidimensional vibrational problems. *The Journal of Chemical Physics*, 84(1):306–317, 1986.

[48] Michael J. Davis and Eric J. Heller. Semiclassical Gaussian basis set method for molecular vibrational wave functions. *The Journal of Chemical Physics*, 71(8):3383–3395, 1979.

[49] Sophya Garashchuk and John C. Light. Quasirandom distributed Gaussian bases for bound problems. *The Journal of Chemical Physics*, 114(9):3929–3939, 2001.

[50] W. van Dijk, J. Brown, and K. Spyksma. Efficiency and accuracy of numerical solutions to the time-dependent Schrödinger equation. *Phys. Rev. E*, 84(5, Part 2), NOV 17 2011.

[51] E. Wigner. On the quantum correction for thermodynamic equilibrium. *Phys. Rev.*, 40:749–759, Jun 1932.

[52] Thomas Halverson and Bill Poirier. Accurate quantum dynamics calculations using symmetrized Gaussians on a doubly dense Von Neumann lattice. *The Journal of Chemical Physics*, 137(22):–, 2012.

[53] Asaf Shimshovitz and David J. Tannor. Phase-Space Approach to Solving the Time-Independent Schrödinger Equation. *Phys. Rev. Lett.*, 109:070402, Aug 2012.

[54] A. M. Perelomov. On the completeness of a system of coherent states. *Theoretical and Mathematical Physics*, 6(2):156–164, 1971.

[55] Bill Poirier and A. Salam. Quantum dynamics calculations using symmetrized, orthogonal Weyl-Heisenberg wavelets with a phase space truncation scheme. II. Construction and optimization. *The Journal of Chemical Physics*, 121(4):1690–1703, 2004.

[56] Daniel T. Colbert and William H. Miller. A novel discrete variable representation for quantum mechanical reactive scattering via the S-matrix Kohn method. *The Journal of Chemical Physics*, 96(3):1982–1991, 1992.

[57] David J. Tannor, Norio Takemoto, and Asaf Shimshovitz. *Phase Space Approach to Solving the Schrdinger Equation: Thinking Inside the Box*, pages 1–34. John Wiley & Sons, Inc., 2014.

[58] Jonathan Tennyson. The calculation of the vibration-rotation energies of triatomic molecules using scattering coordinates. *Computer Physics Reports*, 4(1):1 – 36, 1986.

[59] Edwin L. Sibert. Variational and perturbative descriptions of highly vibrationally excited molecules. *International Reviews in Physical Chemistry*, 9(1):1–27, 1990.

[60] Joel M. Bowman and Bela Gazdy. A truncation/recoupling method for basis set calculations of eigenvalues and eigenvectors. *The Journal of Chemical Physics*, 94(1):454–460, 1991.

[61] Yanhui Qiu, John Z. H. Zhang, and Zlatko Bacic. Six-dimensional quantum calculations of vibration-rotation-tunneling levels of ν_1 and ν_2 HCl-stretching excited $(HCl)_2$. *The Journal of Chemical Physics*, 108(12):4804–4816, 1998.

[62] Mirjana Mladenović. Discrete variable approaches to tetratomic molecules: Part I: DVR(6) and DVR(3)+DGB methods . *Spectrochimica Acta Part A: Molecular and Biomolecular Spectroscopy*, 58(4):795 – 807, 2002.

[63] Mirjana Mladenović. Discrete variable approaches to tetratomic molecules: Part II: application to $\{H_2O_2\}$ and $\{H_2CO\}$. *Spectrochimica Acta Part A: Molecular and Biomolecular Spectroscopy*, 58(4):809 – 824, 2002.

[64] David Luckhaus. 6D vibrational quantum dynamics: Generalized coordinate discrete variable representation and (a)diabatic contraction. *The Journal of Chemical Physics*, 113(4):1329–1347, 2000.

[65] Matthew J. Bramley and Tucker Carrington. Calculation of triatomic vibrational eigenstates: Product or contracted basis sets, Lanczos or conventional eigensolvers? What is the most efficient combination? *The Journal of Chemical Physics*, 101(10):8494–8507, 1994.

[66] Jacek Koput, Stuart Carter, and Nicholas C. Handy. Ab initio prediction of the vibrational-rotational energy levels of hydrogen peroxide and its isotopomers. *The Journal of Chemical Physics*, 115(18):8345–8350, 2001.

[67] Hua-Gen Yu. An exact variational method to calculate vibrational energies of five atom molecules beyond the normal mode approach. *The Journal of Chemical Physics*, 117(5):2030–2037, 2002.

[68] Xiao-Gang Wang and Tucker Carrington, Jr. Contracted basis lanczos methods for computing numerically exact rovibrational levels of methane. *The Journal of Chemical Physics*, 121(7):2937–2954, 2004.

[69] Jean Christophe Tremblay and Tucker Carrington. Calculating vibrational energies and wave functions of vinylidene using a contracted basis with a locally reorthogonalized coupled two-term Lanczos eigensolver. *The Journal of Chemical Physics*, 125(9):–, 2006.

[70] Hee-Seung Lee and John C. Light. Molecular vibrations: Iterative solution with energy selected bases. *The Journal of Chemical Physics*, 118(8):3458–3469, 2003.

[71] Bill Poirier and A. Salam. Quantum dynamics calculations using symmetrized, orthogonal Weyl-Heisenberg wavelets with a phase space truncation scheme. III. Representations and calculations. *The Journal of Chemical Physics*, 121(4):1704–1724, 2004.

[72] Thomas Halverson and Bill Poirier. Large scale exact quantum dynamics calculations: Ten thousand quantum states of acetonitrile. *Chemical Physics Letters*, 624(0):37 – 42, 2015.

[73] Asaf Shimshovitz, Zlatko Bacic, and David J. Tannor. The von Neumann basis in non-Cartesian coordinates: Application to floppy triatomic molecules. *The Journal of Chemical Physics*, 141(23):–, 2014.

[74] Bill Poirier. Algebraically self-consistent quasiclassical approximation on phase space. *Foundations of Physics*, 30(8):1191–1226, 2000.

[75] J. C. Light, I. P. Hamilton, and J. V. Lill. Generalized discrete variable approximation in quantum mechanics. *The Journal of Chemical Physics*, 82(3):1400–1409, 1985.

[76] Richard Lombardini and Bill Poirier. Improving the accuracy of Weyl-Heisenberg wavelet and symmetrized Gaussian representations using customized phase-space-region operators. *Phys. Rev. E*, 74:036705, Sep 2006.

[77] Z Bai, J Demmel, J Dongarra, A Ruhe, H van der Vorst, and editors. *Templates for the solution of Algebraic Eigenvalue Problems: A Practical Guide*. SIAM, Philadelphia, 2000.

[78] C. Clay Marston and Gabriel G. Balint-Kurti. The Fourier grid Hamiltonian method

for bound state eigenvalues and eigenfunctions. *The Journal of Chemical Physics*, 91(6):3571–3576, 1989.

[79] David J. Tannor, Norio Takemoto, and Asaf Shimshovitz. *Phase Space Approach to Solving the Schrödinger Equation: Thinking Inside the Box*, pages 1–34. John Wiley & Sons, Inc., 2014.

[80] Hua Wei and Tucker Carrington. Discrete variable representations of complicated kinetic energy operators. *The Journal of Chemical Physics*, 101(2):1343–1360, 1994.

[81] Felix T. Smith. Modified heliocentric coordinates for particle dynamics. *Phys. Rev. Lett.*, 45:1157–1160, Oct 1980.

[82] Bruce R. Johnson and William P. Reinhardt. Adiabatic separations of stretching and bending vibrations: Application to H_2O. *The Journal of Chemical Physics*, 85(8):4538–4556, 1986.

[83] Oleg L. Polyansky, Per Jensen, and Jonathan Tennyson. The potential energy surface of H_2 ^{1}6O. *The Journal of Chemical Physics*, 105(15):6490–6497, 1996.

[84] Xiao-Gang Wang, , and Tucker Carrington, Jr. The utility of constraining basis function indices when using the Lanczos algorithm to calculate vibrational energy levels. *The Journal of Physical Chemistry A*, 105(12):2575–2581, 2001.

[85] Gustavo Avila and Tucker Carrington. Solving the vibrational Schrödinger equation using bases pruned to include strongly coupled functions and compatible quadratures. *The Journal of Chemical Physics*, 137(17):–, 2012.

[86] Gustavo Avila and Tucker Carrington. Solving the Schrödinger equation using Smolyak interpolants. *The Journal of Chemical Physics*, 139(13):–, 2013.

[87] Rongqing Chen, Guobin Ma, and Hua Guo. Full-dimensional quantum calculation of the vibrational energy levels of hydrogen peroxide (HOOH) . *Chemical Physics Letters*, 320(56):567 – 574, 2000.

[88] Xiao-Gang Wang and Tucker Carrington, Jr. A finite basis representation Lanczos calculation of the bend energy levels of methane. *Journal of Chemical Physics*, 118(15):6946, 2003.

[89] Richard Dawes, Xiao-Gang Wang, Ahren W. Jasper, and Tucker Carrington, Jr. Nitrous oxide dimer: A new potential energy surface and rovibrational spectrum of the nonpolar isomer. *The Journal of Chemical Physics*, 133(13):134304, 2010.

[90] Pranab Sarkar, Nicolas Poulin, and Carrington Tucker Jr. Calculating rovibrational energy levels of a triatomic molecule with a simple Lanczos method. *The Journal of Chemical Physics*, 110(21):10269–10274, 1999.

[91] A. Jaeckle and H.D. Meyer. Product representation of potential energy surfaces. *The Journal of Chemical Physics*, 104(20):7974–7984, 1996.

[92] Sergei Manzhos and Tucker Carrington. Using redundant coordinates to represent potential energy surfaces with lower-dimensional functions. *The Journal of Chemical Physics*, 127(1):–, 2007.

[93] Sergei Manzhos and Tucker Carrington. Using neural networks, optimized coordinates, and high-dimensional model representations to obtain a vinyl bromide potential surface. *The Journal of Chemical Physics*, 129(22):–, 2008.

[94] M.H. Beck, A. Jckle, G.A. Worth, and H.-D. Meyer. The multiconfiguration time-dependent Hartree (MCTDH) method: a highly efficient algorithm for propagating wavepackets . *Physics Reports*, 324(1):1 – 105, 2000.

[95] Arnaud Leclerc and Tucker Carrington. Calculating vibrational spectra with sum of product basis functions without storing full-dimensional vectors or matrices. *The Journal of Chemical Physics*, 140(17), 2014.

[96] David Lauvergnat and Andre Nauts. Quantum dynamics with sparse grids: A combination of Smolyak scheme and cubature. Application to methanol in full dimensionality . *Spectrochimica Acta Part A: Molecular and Biomolecular Spectroscopy*, 119(0):18 – 25, 2014. Frontiers in molecular vibrational calculations and computational spectroscopy.

[97] Xiao-Gang Wang and Tucker Carrington, Jr. Vibrational energy levels of CH_5^+. *The Journal of Chemical Physics*, 129(23):234102, 2008.

[98] Hua-Gen Yu. Full-dimensional quantum calculations of vibrational spectra of six-atom molecules. I. Theory and numerical results. *The Journal of Chemical Physics*, 120(5):2270–2284, 2004.

[99] Oriol Vendrell, Fabien Gatti, and Hans-Dieter Meyer. Strong isotope effects in the infrared spectrum of the Zundel cation. *Angewandte Chemie*, 121(2):358–361, 2009.

[100] Xiao-Gang Wang, Tucker Carrington, Jr., Richard Dawes, and Ahren W. Jasper. The vibration-rotation-tunneling spectrum of the polar and T-shaped-N-in isomers of $(NNO)_2$. *Journal of Molecular Spectroscopy*, 268(12):53 – 65, 2011.

[101] David J. Nesbitt. High-resolution infrared spectroscopy of weakly bound molecular complexes. *Chemical Reviews*, 88(6):843–870, 1988.

[102] Thomas Halverson and Bill Poirier. Calculation of exact vibrational spectra for P_2O and CH_2NH using a phase space wavelet basis. *The Journal of Chemical Physics*, 140(20):–, 2014.

[103] Shai Machnes, Elie Assemat, Henrik R. Larsson, and David J. Tannor. Quantum dynamics in phase space using projected von Neumann bases. *The Journal of Physical Chemistry A*, 120(19):3296–3308, 2016.

[104] C. A. R. Hoare. Algorithm 64: Quicksort. *Commun. ACM*, 4(7):321–, 1961.

[105] Shi-Wei Huang and Tucker Carrington, Jr. A comparison of filter diagonalisation methods with the Lanczos method for calculating vibrational energy levels. *Chemical Physics Letters*, 312(24):311 – 318, 1999.

[106] Pierre-Nicholas Roy and Tucker Carrington. An evaluation of methods designed to calculate energy levels in a selected range and application to a (one–dimensional) Morse oscillator and (threedimensional) HCN/HNC. *The Journal of Chemical Physics*, 103(13):5600–5612, 1995.

[107] Vladimir A. Mandelshtam and Howard S. Taylor. A low-storage filter diagonalization method for quantum eigenenergy calculation or for spectral analysis of time signals. *The Journal of Chemical Physics*, 106(12):5085–5090, 1997.

[108] Christophe Iung and Claude Leforestier. Accurate determination of a potential energy surface for CD_3H. *The Journal of Chemical Physics*, 90(6):3198–3203, 1989.

[109] Hua-Gen Yu and Sean C. Smith. The calculation of vibrational eigenstates by min-res filter diagonalization. *Berichte der Bunsengesellschaft fr physikalische Chemie*, 101(3):400–406, 1997.

[110] Rongqing Chen and Hua Guo. Discrete energy representation and generalized propagation of physical systems. *The Journal of Chemical Physics*, 108(15):6068–6077, 1998.

[111] Jason Cooper and Tucker Carrington. Computing vibrational energy levels by using mappings to fully exploit the structure of a pruned product basis. *The Journal of Chemical Physics*, 130(21), 2009.

[112] Claude Pouchan, Maroane Aouni, and Didier Bgu. Ab initio determination of the anharmonic vibrational spectra of P_2O in the region 200-2000 cm^{-1} . *Chemical Physics Letters*, 334(46):352 – 356, 2001.

[113] J.M.L. Martin, T.J. Lee, and P.R. Taylor. An accurate ab initio quartic force field for formaldehyde and its isotopomers. *Journal of Molecular Spectroscopy*, 160(1):105 – 116, 1993.

[114] Claude Pouchan and Khalil Zaki. Ab initio configuration interaction determination of the overtone vibrations of methyleneimine in the region 2800-3200cm^{-1}. *The Journal of Chemical Physics*, 107(2):342–345, 1997.

[115] Jean Christophe Tremblay and Tucker Carrington. A refined unsymmetric Lanczos eigensolver for computing accurate eigentriplets of a real unsymmetric matrix. *Electronic Transactions on Numerical Analysis*, 28:95–113, 2007.

[116] Xiao-Gang Wang and Tucker Carrington. A contracted basis-Lanczos calculation of vibrational levels of methane: Solving the Schrödinger equation in nine dimensions. *The Journal of Chemical Physics*, 119(1):101–117, 2003.

[117] Hubert Romanowski, Joel M. Bowman, and Lawrence B. Harding. Vibrational energy levels of formaldehyde. *The Journal of Chemical Physics*, 82(9):4155–4165, 1985.

[118] February 2012. The derivatives were calculated for us by Gustavo Avila.

[119] Tom Halverson and Bill Poirier. (private communication).